# Modular Degradable Hydrogels Based on Thiol-reactive Oxanorbornadiene Linkers

Cody J. Higginson, Seung Yeon Kim, Miguel Peláez-Fernández, Alberto Fernández-Nieves, M.G. Finn*

**Supporting Information**

Table of Contents



Supporting time-lapse videos S1 and S2: available online at http://pubs.acs.org.

## I. General

### Materials and Methods

Reagents and solvents were purchased from commercial sources and used as received, unless otherwise stated. When dry solvents were required, solvents were passed through activated alumina columns on a MBraun solvent purification system (MB-SPS), and collected in oven-dried glassware prior to use. Water was purified on a Millipore Milli-Q Advantage A10 system. Dimethyl acetylenedicarboxylate (DMAD) was purified prior to use by passing a 50% (v/v) solution in DCM through a column of normal phase silica gel (60 mesh), eluting with DCM and condensing under reduced pressure. Unless otherwise stated, the reactions were performed under inert atmosphere in capped reaction vessels. 4-arm thiol-terminated poly(ethylene glycol), (4-PEG-SH), was obtained from JenKem Technologies, USA and stored in a glove box purged with nitrogen. Thiol content was periodically assessed by Ellman's assay. As received, thiol content was ~85% of the expected value. Flash chromatography was performed on 60-mesh silica. Analytical TLC was performed on aluminum-backed plates and visualized by exposure to UV light and/or staining with aqueous potassium permanganate (2% $KMnO_4$ + 5% $K_2CO_3$) or ninhydrin stain. Preparative TLC was performed on glass-backed silica gel plates of 1 mm thickness, and visualized with UV light. Dye-containing materials were protected from light by wrapping the reaction and storage vessels in aluminum foil.

### Instrumentation

NMR spectra were obtained on Brüker AMX-400, and DRX-500 instruments in deuterated solvents (Cambridge Isotope Laboratories, Inc.) and referenced to the signals of residual protium in the NMR solvent. Spectra were processed in MestReNova-LITE software (Mestrelab Research). Routine mass spectra were obtained on an Advion Compact Mass Spectrometer (G1946D) ESI-MSD instrument, using direct sample injection followed with 9:1 CH3CN:H2O containing 0.1% formic acid as mobile phase. High-resolution mass spectrometry was performed on an Agilent 6230 ESI-TOF LC/MS instrument (G6230B) operating at 4 GHz with internal reference. LC was performed on an Agilent 1260 HPLC with a mobile phase gradient from 0-90% acetonitrile/water containing 0.1% formic acid on a Zorbax Extend-C18 Rapid Resolution HT (2.1 x 50mm, 1.8μm). Melting points were

measured in a Fisher-Johns melting point apparatus and are corrected. IR spectra were recorded on a Nicolet 6700 FTIR spectrophotometer with Smart Performer single-bounce ATR module in thin films or in solids dispersed on a diamond crystal. Absorbance spectra were recorded on an Evolution 220 UV-Vis spectrophotometer (ThermoFisher). Absorbance and fluorescence spectra were also collected on a VarioskanFlash plate reader (ThermoFisher). Rheological measurements were obtained on a Physica MCR 501 rheometer (Anton Paar), equipped with a peltier plate and an evaporation blocker hood. Measurements were taken using a truncated cone-plate geometry (part no. 47709, serial no. 11810), and gels were prepared *in situ* and trimmed prior to doing any measurements. Gel permeation chromatography (GPC) analysis was performed in DMF containing 0.1% LiBr additive at 1 mL/min flow rate (LC-20AD pump) on a Shimadzu GPC setup equipped with two Phenomenex Phenogel 10 μm linear columns (300 x 7.8 mm), autosampler (SIL-20A) and column oven (CTO-20A) set at 40 °C. Detection was achieved using a diode array detector (SPD-M20A), and RI detector (RID-10A), and instrument was calibrated with EasiVial poly(methyl methacrylate) standards (Agilent). Time-lapse photography was collected using Chronolapse software (v.1.0.4) and Creative Labs webcam (model VF0070), and photos were compiled using iMovie software (2009, v8.0.6). Still photographs were collected using built-in cameras on iPhone 3gs and 5c models.

## II. Synthetic Procedures

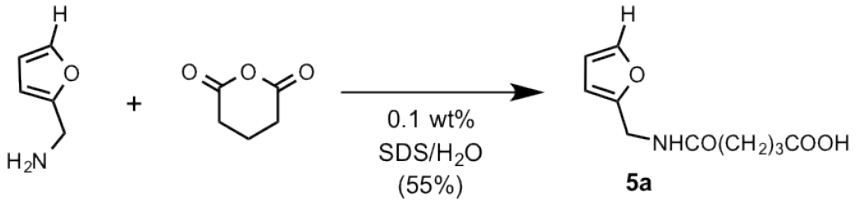


**N-glutaroylfurfurylamine, 5a**. Glutaric anhydride (2.4 g, 21.2 mmol, 1.18 equiv) was added portion-wise over 10 min to a solution of furfurylamine (1.74 g, 17.9 mmol) in 0.1 wt.% aqueous sodium dodecyl sulfonate (60 mL). The resulting solution was placed at 4 °C overnight. The colorless crystals of the product were filtered, washed with cold water (60 mL), and dried under vacuum, providing 1.67 g (45%) of **5a** as colorless crystals.

Additional **5a** was recovered by EtOAc extraction (3×15 mL) of the filtrate. The residue obtained from the combined organic extracts was dissolved in $H_2O$ (5 mL), filtered, and kept at 4 °C overnight. The colorless crystals of **5a** (0.39 g) were combined with the main batch (55% total yield). $R_f$ 0.56 (10% MeOH/EtOAc). $^1$H NMR (500 MHz, $CD_3OD$) δ 7.41 (dd, J = 1.8, 0.7 Hz, 1H), 6.33 (dd, J = 3.2, 1.9 Hz, 1H), 6.23 (dd, J = 3.2, 0.7 Hz, 1H), 4.34 (s, 1H), 2.32 (t, J = 7.4 Hz, 1H), 2.26 (t, J = 7.5 Hz, 1H), 1.89 (p, J = 7.5 Hz, 1H). 13C NMR (126 MHz, $CD_3OD$) δ 176.93, 175.31, 153.24, 143.42, 111.47, 108.17, 49.66, 49.49, 49.43, 49.32, 49.26, 49.15, 48.98, 48.81, 48.64, 37.24, 36.07, 34.15, 22.35. mp: 83-85 °C. ESI-MS: $[C_{10}H_{13}NO_4+H]^+$ 212.1.

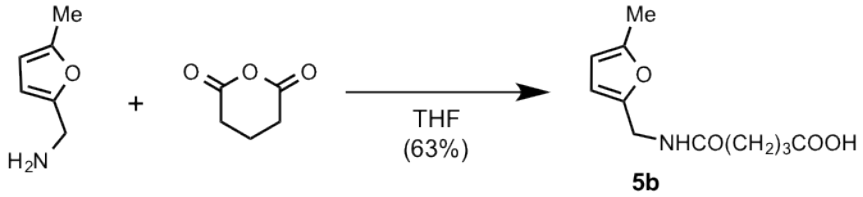

**5b**

**5-methyl-N-glutaroylfurfurylamine, 5b.** Glutaric anhydride (299 mg, 2.6 mmol, 1.18 equiv) was added portion-wise over 10 min to a solution of 5-methylfurfurylamine (247 mg, 2.22 mmol, 1 eqiv) in dry THF (7.4 mL). The resulting solution was stirred at room temperature under argon for 3 hours, and then condensed in vacuum. The residue was taken up in 10 mL ethyl acetate (EtOAc) and washed with water (10 mL) and 1 M HCl (2x10 mL). The aqueous layers were back extracted once with 20 mL EtOAc, and the combined organic layers were dried over anhydrous sodium sulfate ($Na_2SO_4$), filtered and condensed in vacuum. The organic crude was further purified by flash column chromatography on silica gel, eluting with a gradient from EtOAc through 10% MeOH/EtOAc to yield an off-white crystalline solid (318 mg, 63% yield). $R_f$ 0.59 (10% MeOH/EtOAc). $^1$H NMR (500 MHz, $CDCl_3$) δ 10.65 (brs, 1H), 6.08 (d, J = 3.0 Hz, 1H), 6.04 (s, 1H), 5.90 – 5.83 (m, 1H), 4.36 (d, J = 5.4 Hz, 2H), 2.41 (t, J = 7.1 Hz, 2H), 2.29 (t, J = 7.4 Hz, 2H), 2.25 (s, 3H), 1.96 (p, J = 7.2 Hz, 2H). $^{13}$C NMR (126 MHz, $CDCl_3$) δ 178.14, 172.49, 152.21, 149.25, 108.64, 106.49, 77.48, 77.23, 76.97, 36.91, 35.35, 33.18, 33.08, 20.82, 13.70. ESI-MS: $[C_{11}H_{15}NO_4+H^+]$ = 226.1.

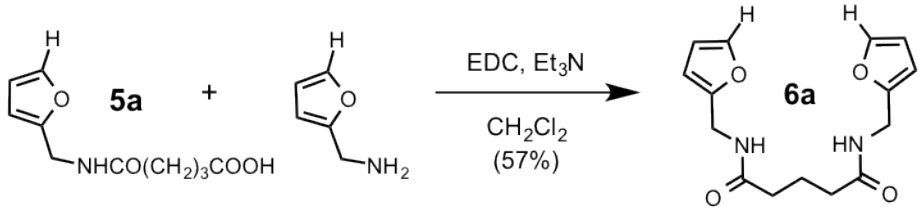


***N*¹,*N*⁵-bis(furan-2-ylmethyl)glutaramide**, **6a.** Compound **5a** (750 mg, 3.551 mmol, 1 equiv), EDC•HCl (816.8 mg, 4.261 mmol, 1.2 equiv), and triethylamine (1.48 mL, 10.65 mmol, 3 equiv) were dissolved in dichloromethane (50 mL) at room temperature and stirred for 10 minutes prior to addition of furfurylamine (345 μL, 3.906 mmol, 1.1 eq) and 30 mg dimethylaminopyridine. The resulting mixture was stirred at room temperature overnight to yield a pale yellow suspension. The precipitate of the desired product was collected by filtration, washing with dichloromethane (459 mg). Additional product was recovered from the filtrate was condensed and taken up in 35 mL ethyl acetate and washed with 2 x 35 mL 0.1 N HCl and 1 x 35 mL saturated $NaHCO_3$ . The organic layer was dried over $Na_2SO_4$, filtered and condensed in vacuum. The crude product obtained in the organic layer was further purified by flash chromatography on $SiO_2$ gel, eluting with a gradient from ethyl acetate through 10% methanol in ethyl acetate to yield a white crystalline solid (129 mg), which was combined with the previously collected precipitate (57% total). $R_f$ 0.74 (10% MeOH/EtOAc with 0.1% acetic acid). $^1$H NMR (500 MHz, DMSO-d6) δ 8.29 (t, J = 5.6 Hz, 2H), 7.53 (dd, J = 1.8, 0.8 Hz, 2H), 6.36 (dd, J = 3.1, 1.9 Hz, 2H), 6.20 (dd, 3.1, 0.8 Hz, 2H), 4.23 (d, J = 5.7 Hz, 4H), 2.10 (t, J = 7.5 Hz, 4H), 1.72 (p, J = 7.6 Hz, 2H). $^{13}$C NMR (126 MHz, DMSO) δ 172.18, 152.57, 142.26, 110.73, 106.99, 40.01, 39.93, 39.84, 39.76, 39.68, 39.60, 39.51, 39.42, 39.34, 39.18, 39.01, 35.65, 34.82, 21.66. mp: 154-156 °C. LC-HRMS: [$C_{15}H_{18}N_2O_4$+$H^+$] calc: 291.1339, obs: 291.1341. rt: 4.941 min (0-90% MeCN/$H_2O$).

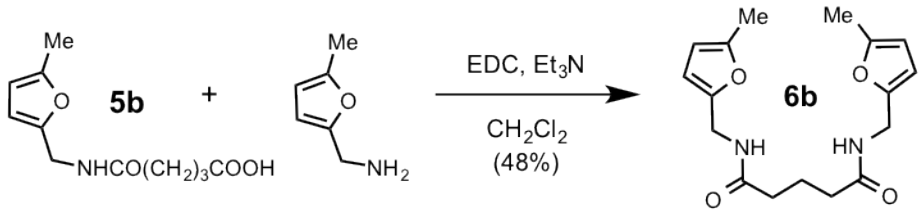

***N*¹,*N*⁵-bis((5-methylfuran-2-yl)methyl)glutaramide, 6b.** Compound **5b** (634 mg, 2.816 mmols, 1 equiv), EDC•HCl (648 mg, 3.38 mmol, 1.2 equiv), and triethylamine (1.48 mL, 10.65 mmol, 2.5 equiv) were dissolved in dichloromethane (19 mL) at room temperature and stirred for 10 minutes prior to addition of 5-methylfurfurylamine (345 µL, 3.10 mmol, 1.1 eq) and 30 mg dimethylaminopyridine. The resulting mixture was stirred at room temperature for 20 hours. The reaction mixture was condensed and partitioned between ethyl acetate (30 mL) and water (30 mL). Organic layer was washed with 1 x 20 mL saturated $NaHCO_3$ and 1 x 20 mL 1 M HCl. The organic layer was dried over anhydrous sodium sulfate, filtered and condensed in vacuum. Solid residue dissolved in chloroform with heating and allowed to stand to form crystals which were collected by vacuum filtration, washing with chilled chloroform (432 mg, 48%). $R_f$ 0.74 (5% MeOH/EtOAc). $^1$H NMR (500 MHz, $CD_3OD$) δ 6.08 (d, J = 2.7 Hz, 2H), 6.01 – 5.84 (d, J = 2.6 Hz, 2H), 4.27 (s, 4H), 2.29 – 2.16 (m, 10H), 1.90 (p, J = 7.5 Hz, 2H). $^{13}$C NMR (126 MHz, $CD_3OD$) δ 175.25, 153.00, 151.31, 109.07, 107.31, 49.66, 49.49, 49.32, 49.27, 49.15, 48.98, 48.81, 48.64, 37.41, 36.26, 23.28, 13.48. ESI-MS: [$C_{17}H_{22}N_2O_4$+$H^+$] = 319.2.

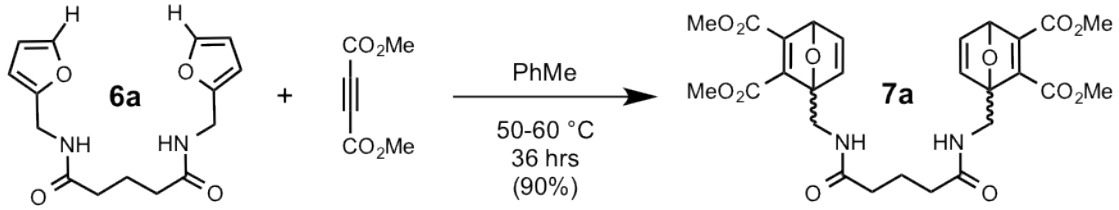


**Tetramethyl 1,1'-((glutaroylbis(azanediyl))bis(methylene))bis(7-oxabicyclo[2.2.1] hepta-2,5-diene-2,3-dicarboxylate), 7a.** Bis-furan **6a** (152 mg, 0.532 mmol, 1 equiv) and dimethyl acetylenedicarboxylate (163 µL, 1.33 mmol, 2.5 equiv) were combined with 600 µL toluene in a sealed vial purged with argon and heated directly on a hotplate set at 60 °C for 36 hours. The resulting slurry was suspended in diethyl ether and triturated. The resulting pale precipitate was collected by vacuum filtration and the filter cake was dried in high vacuum to yield a white solid comprised of an inseparable mixture of Bis-OND diastereomers (275 mg, 90%). $R_f$ 0.67 (10% MeOH/EtOAc). $^1$H NMR (500 MHz, $CDCl_3$) δ 7.21 (dd, J = 5.2, 1.9 Hz, 2H), 7.04 (d, J = 5.2 Hz, 2H), 6.36 (brs, 1H), 6.28 (brs, 1H), 5.64 (t, J = 1.9 Hz, 2H), 4.21 – 4.08 (m, 2H), 4.03 – 3.97 (m, 2H), 3.83 (app. d, J = 2.1 Hz, 6H), 3.78 (app. d, J = 1.4 Hz, 6H), 2.18 (t, J = 6.9 Hz, 4H), 1.95 (p, J = 6.9 Hz, 2H). $^{13}$C NMR (126 MHz,

$CD_3OD$) δ 172.84, 172.72, 164.12, 164.09, 162.77, 162.75, 153.80, 153.78, 153.07, 152.98, 145.41, 143.63, 143.53, 97.30, 97.21, 83.79, 83.76, 77.48, 77.23, 76.98, 52.78, 52.77, 52.59, 52.58, 37.71, 37.68, 34.93, 34.80, 21.82, 21.80. FT-IR ($cm^{-1}$): 3307, 2954, 1711, 1643, 1531, 1432, 1236, 1201, 1121. mp: 163-167 °C. LC-HRMS: [$C_{27}H_{30}N_2O_{12}$+$H^+$] calc: 575.1872, obs: 575.1885. rt: 5.620 min (0-90% MeCN/$H_2O$).

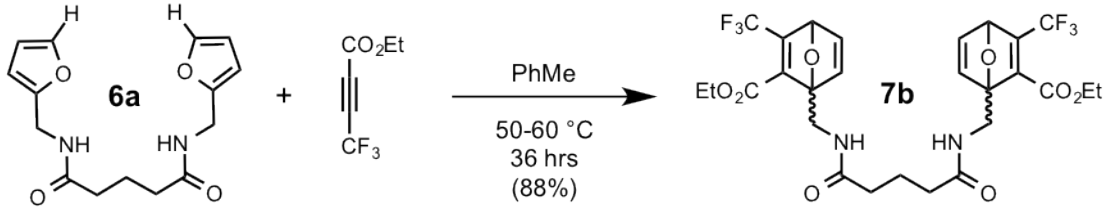


**Diethyl 1,1'-((glutaroylbis(azanediyl))bis(methylene))bis(3-(trifluoromethyl)-7-oxabicyclo[2.2.1]hepta-2,5-diene-2-carboxylate), 7b.** Bis-furan **6a** (50 mg, 0.172 mmol, 1 equiv) and ethyl 4,4,4-trifluoro-2-butynoate (59 µL, 0.413 mmol, 2.4 equiv) were combined with 500 µL toluene in a sealed vial purged with argon, and heated directly on a hotplate set at 60 °C for 40 hours. The resulting slurry was suspended in diethyl ether and triturated. The resulting pale precipitate was collected by vacuum filtration and the filter cake was washed with ether and dried in high vacuum to yield an off-white solid comprised of an inseparable mixture of Bis-OND isomers (94.5 mg, 88%). $R_f$ 0.47 (10% MeOH/$CH_2Cl_2$). $^1$H NMR (500 MHz, $CDCl_3$) δ 7.19 (dd, J = 5.1, 1.6 Hz, 2H), 7.11 (dd, J = 5.1, 1.7 Hz, 2H), 6.33 – 6.15 (m, 2H), 5.58 (s, 2H), 4.42 – 4.19 (m, 4H), 4.19 – 4.00 (m, 4H), 2.17 (t, J = 6.7 Hz, 4H), 1.94 (p, J = 6.5 Hz, 2H), 1.31 (t, J = 7.1 Hz, 6H). $^{13}$C NMR (126 MHz, $CD_3OD$) δ 172.77, 172.74, 162.49, 162.42, 151.74, 151.64, 151.45, 151.34, 151.25, 151.21, 151.17, 151.13, 144.70, 144.67, 144.21, 144.18, 124.79, 122.64, 120.50, 118.36, 97.30, 97.22, 82.66, 82.64, 82.62, 77.48, 77.23, 76.98, 62.35, 37.72, 37.68, 34.95, 22.03, 21.96, 14.05. $^{19}$F NMR (471 MHz, CDCl3) δ -62.80, -64.04, -64.13. FT-IR ($cm^{-1}$): 3303, 3083, 2961, 1720, 1640, 1549, 1302, 1267, 1134, 701. mp: 166-169 °C. LC-HRMS: [$C_{27}H_{28}F_6N_2O_{14}$+$H^+$] calc: 623.1823, obs: 623.1847. rt: 8.124 min (0-90% MeCN/$H_2O$).

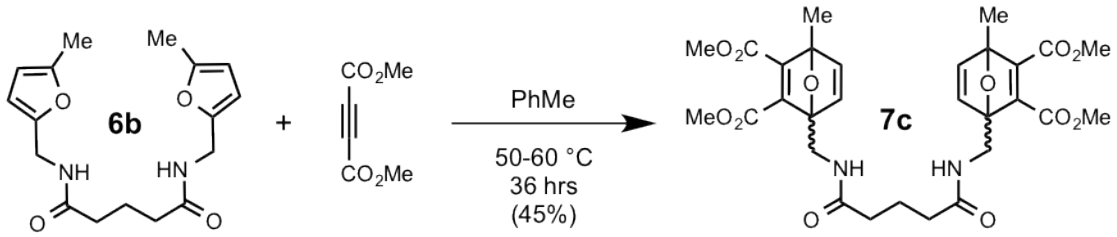


**Tetramethyl 4,4'-((glutaroylbis(azanediyl))bis(methylene))bis(1-methyl-7-oxabicyclo[2.2.1]hepta-2,5-diene-2,3-dicarboxylate), 7c.** Bis-furan **6b** (102.5 mg, 0.322 mmol, 1 equiv) and dimethyl acetylenedicarboxylate (98.1 µL, 0.805 mmol, 2.5 equiv) were combined with 1 mL toluene in a sealed vial purged with argon, and heated directly on a hotplate set at 60 °C for 36 hours. The resulting slurry was suspended in diethyl ether and triturated. The resulting syrup was loaded onto a packed silica gel column and eluted with a gradient from hexane through 3% MeOH/EtOAc to yield an off-white glassy residue comprised of an inseparable mixture of Bis-OND isomers (86.4 mg, 45%). $R_f$ 0.45 (2% MeOH/EtOAc). $^1$H NMR (500 MHz, $CDCl_3$) δ 7.07 (d, J = 5.1 Hz, 1H), 7.00 (d, J = 5.1 Hz, 1H), 6.95 – 6.94 (m, 2H), 6.55 (t, J = 5.9 Hz, 1H), 6.36 (t, J = 5.8 Hz, 1H), 4.34 (dd, J = 14.7, 7.0 Hz, 1H), 4.09 (dd, J = 14.7, 5.9 Hz, 1H), 4.01 (dd, J = 14.7, 6.0 Hz, 1H), 3.83 (d, J = 5.2 Hz, 1H), 3.80 – 3.74 (m, 11H), 2.18 (t, J = 6.8 Hz, 4H), 1.93 (p, J = 6.8 Hz, 2H), 1.76 (app. d, J = 5.9 Hz, 6H). $^{13}$C NMR (126 MHz, $CD_3OD$) δ 172.99, 172.83, 164.38, 164.27, 163.66, 163.37, 157.20, 156.62, 152.01, 151.36, 147.83, 147.59, 145.57, 144.96, 95.32, 95.20, 92.75, 92.71, 77.48, 77.23, 76.98, 52.64, 52.62, 52.53, 52.51, 37.93, 37.84, 35.05, 34.88, 22.33, 22.11, 15.39, 15.31. FT-IR ($cm^{-1}$): 3375, 2954, 1713, 1650, 1537, 1436, 1248, 1142. LC-HRMS: [$C_{29}H_{34}N_2O_{14}$+$H^+$] calc: 603.2185, obs: 603.2199. rt: 6.341 min (0-90% MeCN/$H_2O$).

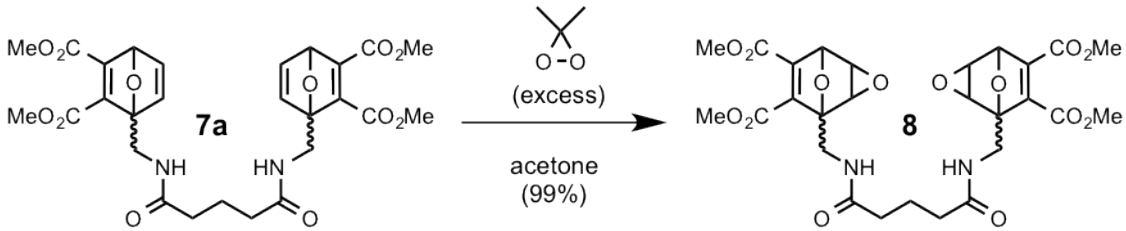


**Tetramethyl 1,1'-((glutaroylbis(azanediyl))bis(methylene))bis(3,8-dioxatricyclo[3.2.1.0$^{2,4}$]oct-6-ene-6,7-dicarboxylate), 8.** Bis-OND **7a** (52 mg, 0.091 mmol, 1 equiv) was dissolved in 3.36 mL of a freshly prepared ~0.07 M solution of dimethyldioxirane in

acetone. The reaction mixture was stirred at room temperature overnight, and then condensed in vacuo to yield an off-white solid (54.3mg, 99%). No further purification was necessary. $R_f$ 0.38 (10% MeOH/EtOAc). $^1$H NMR (500 MHz, $CDCl_3$) δ 6.85 – 6.80 (m, 2H), 5.01 (app. d, J = 12.2 Hz, 2H), 4.10 (dd, J = 14.9, 6.3 Hz, 1H), 3.93 – 3.92 (m, 2H), 3.84 – 3.71 (m, 17H), 2.34 – 2.11 (m, 4H), 1.94 (p, J = 6.5 Hz, 2H). $^{13}$C NMR (126 MHz, $CD_3OD$) δ 173.48, 173.31, 163.37, 163.15, 162.03, 161.95, 149.93, 149.86, 147.07, 146.89, 91.45, 91.10, 78.42, 78.40, 57.53, 56.93, 56.66, 53.10, 53.05, 52.83, 36.96, 36.87, 34.28, 34.16, 21.67, 21.34. FT-IR ($cm^{-1}$): 3367, 2955, 1713, 1666, 1530, 1433, 1238, 731. mp: 125-130 °C. LC-HRMS: [$C_{27}H_{30}N_2O_{14}$+$H^+$] calc: 607.1770, obs: 607.1779. rt: 5.072 min (0-90% MeCN/$H_2O$).

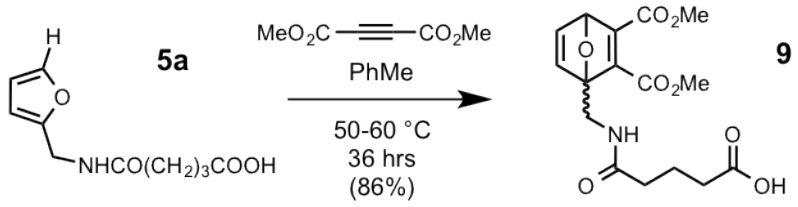


**5-(((2,3-bis(methoxycarbonyl)-7-oxabicyclo[2.2.1]hepta-2,5-dien-1-yl)methyl) amino)-5-oxopentanoic acid, 9.** Furan **5a** (999 mg, 4.73 mmol, 1 equiv) was combined with dimethyl acetylenedicarboxylate (814 µL, 6.622 mmols, 1.4 equiv) and 1 mL toluene in a sealed vial and heated directly on a hot plate at 60 °C while stirring for 5 hours. The reaction mixture was then diluted with 15 mL diethyl ether and triturated to yield an off-white precipitate that was collected by vacuum filtration and dried to constant mass under high vacuum (1.434 g, 86%). $R_f$ 0.57 (10% MeOH/EtOAc with 0.5% AcOH). $^1$H NMR (500 MHz, DMSO-$d_6$) δ 8.04 (s, 1H), 7.30 (dd, J = 5.1, 1.7 Hz, 1H), 7.10 (d, J = 5.2 Hz, 1H), 5.69 (d, J = 1.8 Hz, 1H), 3.93 (dd, J = 14.8, 6.6 Hz, 1H), 3.78 (dd, J = 14.9, 5.3 Hz, 1H), 3.71 (app. d, J = 4.2 Hz, 6H), 2.19 (t, J = 7.4 Hz, 2H), 2.10 (t, J = 7.4 Hz, 2H), 1.68 (p, J = 7.5 Hz, 2H). $^{13}$C NMR (126 MHz, DMSO-$d_6$) δ 175.06, 172.81, 164.75, 163.22, 154.85, 152.78, 146.11, 144.37, 83.78, 53.10, 40.86, 40.69, 40.53, 40.36, 40.20, 40.03, 39.86, 37.40, 34.96, 33.86, 21.46. FT-IR ($cm^{-1}$): 3354, 2955, 1709, 1635, 1544, 1435, 1236. ESI-MS: [$C_{16}H_{19}NO_8$+$H^+$] = 354.1.

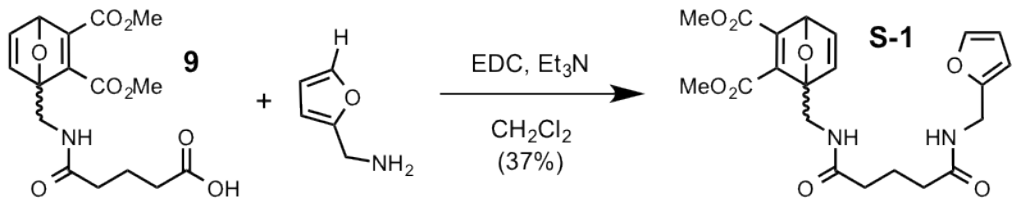


**Dimethyl 1-((5-((furan-2-ylmethyl)amino)-5-oxopentanamido)methyl)-7-oxabicyclo [2.2.1]hepta-2,5-diene-2,3-dicarboxylate, S-1.** OND **9** (199 mg, 0.563 mmol, 1.2 equiv) was dissolved in 3 mL $CH_2Cl_2$ and dicyclohexylcarbodiimide (136 mg, 0.788 mmols, 1.4 equiv) was added. The resulting solution was stirred at 4 °C for 15 minutes prior to addition of 41 µL (0.469 mmol, 1 eq) furfurylamine. The reaction mixture was allowed to reach room temperature and stirred for 6 hours before filtration and removal of solvent under reduced pressure. The crude was taken up in 10 mL ethyl acetate and washed with 1 x 10 mL 1 M HCl and 1 x 10 mL saturated $NaHCO_3$. The organic layer was dried over sodium sulfate, filtered and condensed in vacuum. The organic crude was further purified by silica gel column chromatography, eluting with a gradient from hexanes to 5% MeOH/EtOAc to yield a white solid (76 mg, 37%). $R_f$ 0.63 (10% MeOH/EtOAc with 0.5% AcOH). $^1$H NMR (500 MHz, $CDCl_3$) δ 7.33 – 7.30 (m, 1H), 7.19 (dd, J = 5.2, 1.9 Hz, 1H), 6.98 (d, J = 5.3 Hz, 1H), 6.59 (s, 1H), 6.28 (dd, J = 3.0, 1.9 Hz, 1H), 6.18 (t, J = 2.7 Hz, 1H), 6.16 – 6.09 (m, 1H), 5.59 (d, J = 1.9 Hz, 1H), 4.47 – 4.29 (m, 2H), 4.23 (dd, J = 14.8, 7.0 Hz, 1H), 3.87 (dd, J = 14.8, 4.9 Hz, 1H), 3.80 (s, 3H), 3.75 (s, 3H), 2.25– 2.18 (m, 4H), 1.98 – 1.86 (m, 2H). $^{13}$C NMR (126 MHz, $CDCl_3$) δ 172.68, 172.62, 164.14, 162.66, 153.82, 153.14, 151.79, 145.55, 143.06, 142.14, 110.62, 110.60, 107.35, 97.23, 83.79, 77.48, 77.23, 76.98, 52.80, 52.56, 37.66, 36.46, 35.00, 34.98, 21.75. ESI-MS: [$C_{21}H_{24}N_2O_8$+$H^+$] = 433.2.

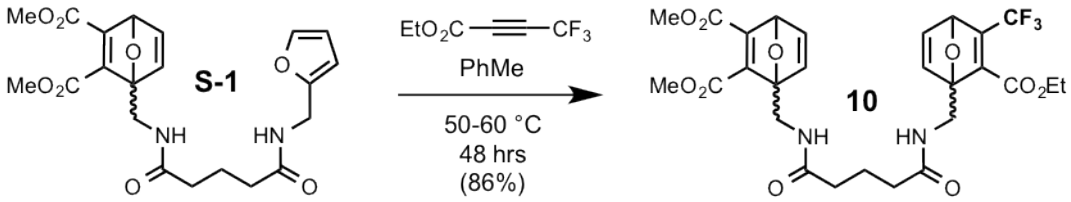


**Dimethyl 1-((5-(((2-(ethoxycarbonyl)-3-(trifluoromethyl)-7-oxabicyclo[2.2.1]hepta-2,5-dien-1-yl)methyl)amino)-5-oxopentanamido)methyl)-7-oxabicyclo[2.2.1]hepta-2,5-diene-2,3-dicarboxylate, 10.** Asymmetric OND-furan **S-1** (75.5 mg, 0.175 mmol, 1.0 equiv) was combined with ethyl 4,4,4-trifluoro-2-butynoate (32.5 µL, 0.228 mmols, 1.3

equiv), and 500 µL toluene in a sealed vial under argon. The mixture was heated directly on a hot plate at 60 °C for 48 hours. After cooling to room temperature, 3.5 mL diethyl ether was added to yield a pale yellow precipitate, which was collected by vacuum filtration. The solid was further purified by flash column chromatography on silica gel, eluting with a gradient from hexanes through 5% MeOH/EtOAc to yield a pale yellow solid (90 mg, 86%). $R_f$ 0.38 (EtOAc). $^1$H NMR (500 MHz, $CDCl_3$) δ 7.21 (dd, J = 5.2, 1.8 Hz, 1H), 7.19 – 7.13 (m, 1H), 7.11 (dd, J = 5.2, 1.5 Hz, 1H), 7.03 (dd, J = 5.2, 3.6 Hz, 1H), 6.36 – 6.35 (m, 1H), 6.22 – 6.18 (m, 1H), 5.63 (d, J = 1.8 Hz, 1H), 5.57 (br s, 1), 4.35 – 4.20 (m, 2H), 4.18 – 3.95 (m, 4H), 3.82 (m, 3H), 3.77 (s, 3H), 2.23 – 2.10 (m, 4H), 1.93 (p, J = 6.7 Hz, 2H), 1.31 (t, J = 7.1 Hz, 3H). $^{13}$C NMR (126 MHz, $CDCl_3$) δ 172.84, 172.80, 172.74, 172.69, 164.15, 164.05, 162.80, 162.71, 162.44, 162.37, 153.77, 153.64, 153.12, 153.07, 151.67, 151.58, 151.37, 151.29, 151.25, 151.24, 151.21, 151.19, 145.48, 145.42, 144.61, 144.32, 144.25, 143.53, 143.45, 124.78, 122.64, 120.50, 118.36, 97.34, 97.24, 97.22, 97.18, 83.80, 83.78, 82.65, 82.63, 82.61, 82.59, 77.48, 77.23, 76.97, 62.30, 52.81, 52.79, 52.60, 52.59, 37.78, 37.73, 37.63, 34.96, 34.91, 34.87, 21.95, 21.89, 14.06, 14.04. FT-IR (cm$^{-1}$): 3300, 2954, 1716, 1640, 1547, 1436, 1296, 1265, 1122, 702. mp: 93-97 °C. LC-HRMS: [$C_{27}H_{29}F_3N_2O_{10}$+H$^+$] calc: 599.1847, obs: 599.1889. rt: 6.950 min (0-90% MeCN/$H_2O$).

**Scheme S1.** Synthesis of Tris-OND electrophile **11**.

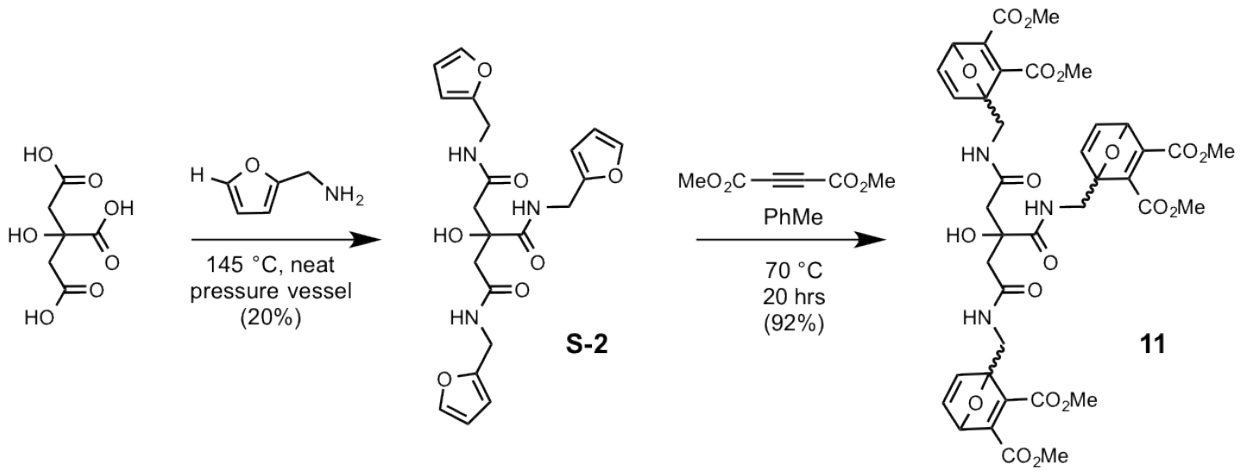

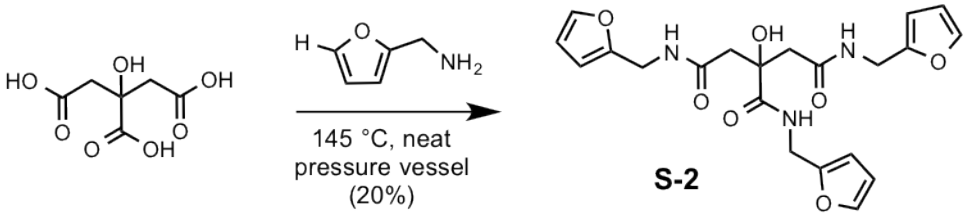


***N*¹,*N*²,*N*³-tris(furan-2-ylmethyl)-2-hydroxypropane-1,2,3-tricarboxamide, S-2.** Thermal amidation reactions presented here for the preparation of **S-2** and **S-4** are *unoptimized* and were performed using a modified procedure that has been previously described elsewhere.[1] Briefly, citric acid (1.00 g, 4.76 mmol, 1 equiv) combined with 1.282 mL furfurylamine (14.51 mmol, 3.05 equiv) in a 25 mL pressure vessel and 500 mg 4 Å molecular sieves and a stir bar were added. The solution was heated at 145 °C under argon for 3 hours, and then cooled to room temperature. The crude was dissolved in $CH_2Cl_2$ and purified by flash chromatography on silica gel, eluting with a gradient from hexanes through 5% MeOH/EtOAc to yield a pale yellow solid (398 mg, 20%). $R_f$ 0.34 (EtOAc). $^1$H NMR (500 MHz, $CDCl_3$) δ 7.40 (t, J = 5.5 Hz, 1H), 7.33 – 7.31 (m, 1H), 7.31 – 7.28 (m, 1H), 7.12 (br s, 2H), 6.63 (s, 1H), 6.29 (dd, J = 3.1, 1.9 Hz, 1H), 6.27 (dd, J = 3.0, 1.9 Hz, 2H), 6.18 (d, J = 2.7 Hz, 3H), 4.39 (dd, J = 15.5, 5.7 Hz, 2H), 4.32 (dd, J = 15.1, 5.5 Hz, 4H), 2.75 (d, J = 14.7 Hz, 2H), 2.59 (d, J = 14.7 Hz, 2H). $^{13}$C NMR (126 MHz, $CDCl_3$) δ 173.79, 170.59, 151.13, 150.95, 142.47, 142.40, 110.67, 110.63, 107.67, 107.59, 77.48, 77.23, 76.98, 75.67, 42.83, 36.67, 36.57. FT-IR ($cm^{-1}$): 3295, 3115, 2926, 1644, 1526, 1192, 1013. LC-HRMS: [$C_{21}H_{23}N_3O_7$+$H^+$] calc: 430.1609, obs: 430.1615. rt: 6.141 min (0-90% MeCN/$H_2O$).

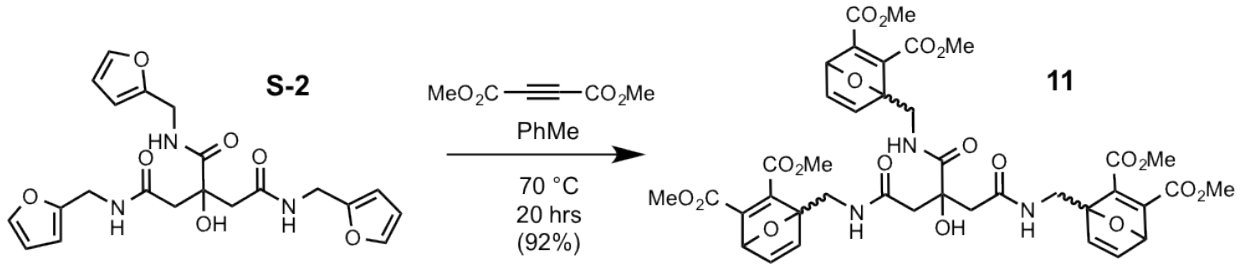


**Tetramethyl 1,1'-(((2-(2-(((2,3-bis(methoxycarbonyl)-7-oxabicyclo[2.2.1]hepta-2,5-dien-1-yl)methyl)amino)-2-oxoethyl)-2-hydroxysuccinyl)bis(azanediyl))bis(methylene))bis(7'-oxabicyclo[2.2.1]hepta-2,5-diene-2,3-dicarboxylate), 11.** Tris-

1 Krysmann, M.; Kelarakis, A.; Dalla, P.; Giannelis, E. *J. Am. Chem. Soc.* **2012**, 134, 747-750.

furan **S-2** (100.2 mg, 0.233 mmol, 1.0 equiv) was combined with dimethyl acetylenedicarboxylate (115 µL, 0.9334 mmols, 4 equiv) and 100 µL toluene in a sealed vial. The vial was purged with argon and heated directly on a hot plate at 70 °C for 20 hours. The reaction was then cooled to room temperature and purified by flash chromatography on silica gel, eluting with a gradient from ethyl acetate through 10% MeOH/EtOAc to yield a pale foaming solid (184.5 mg, 92%). $R_f$ 0.10 (EtOAc). $^1$H NMR (500 MHz, $CDCl_3$) δ 7.42 – 7.38 (m, 1H), 7.17 – 7.16 (m, 3H), 7.04 – 6.88 (m, 5H), 6.30 (dd, J = 9.2, 3.4 Hz, 1H), 5.59 (dd, J = 4.3, 1.8 Hz, 3H), 4.19 – 3.89 (m, 6H), 3.78 – 3.74 (overlapping singlets, 18H), 2.75 – 2.59 (m, 2H), 2.57 – 2.50 (m, 2H). $^{13}$C NMR (126 MHz, $CDCl_3$) δ 173.95, 173.90, 173.88, 173.84, 170.84, 170.81, 170.78, 170.73, 170.72, 164.05, 164.01, 163.99, 163.98, 162.89, 162.88, 162.83, 162.82, 153.48, 153.46, 153.40, 153.28, 153.24, 153.18, 153.13, 145.36, 145.31, 143.31, 143.22, 143.17, 143.15, 96.85, 96.84, 96.75, 96.74, 96.72, 83.87, 83.85, 83.81, 77.48, 77.23, 76.98, 75.27, 75.24, 75.22, 75.19, 52.68, 52.48, 42.70, 42.60, 42.54, 37.83, 37.76, 37.66. FT-IR ($cm^{-1}$): 3368, 2954, 1711, 1692, 1526, 1435, 1232, 712. LC-HRMS: [$C_{39}H_{41}N_3O_{19}$+$H^+$] calc: 856.2407, obs: 856.2428. rt: 6.727 min (0-90% MeCN/$H_2O$).

**Scheme S2.** Synthesis of Tetra-OND electrophile **12**.

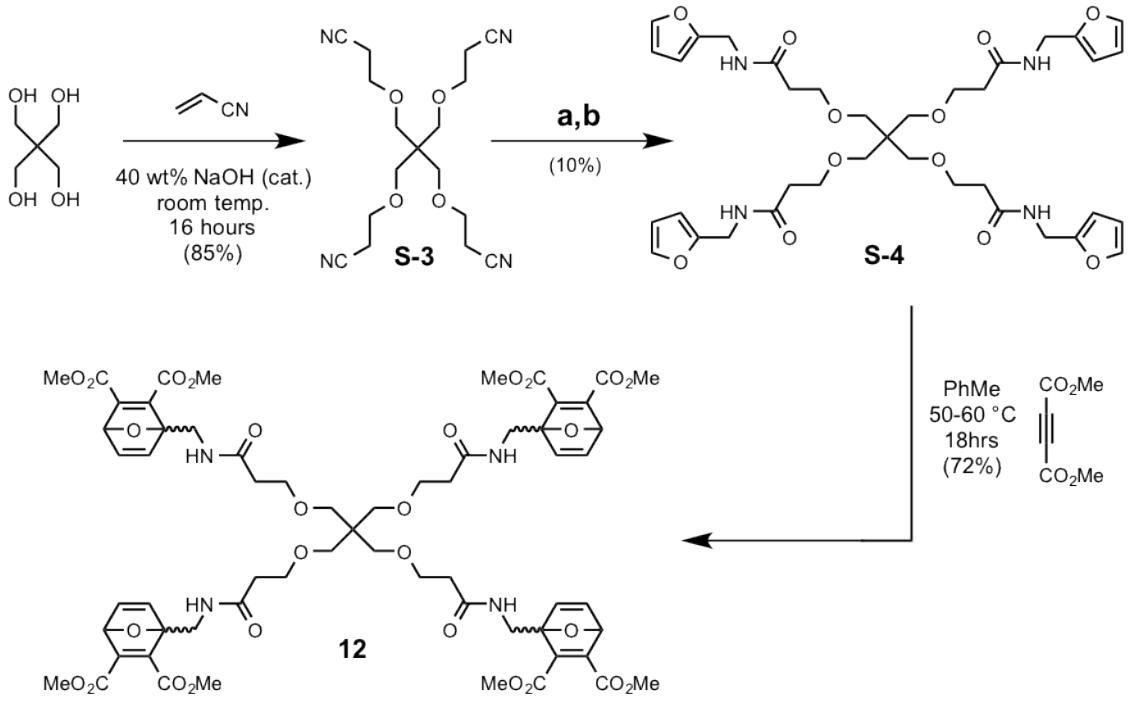

(a) conc. HCl, reflux, 4 hrs followed by extraction. (b) 1 equiv. furfurylamine, 145 °C, neat, pressure vessel, followed by flash chromatography.

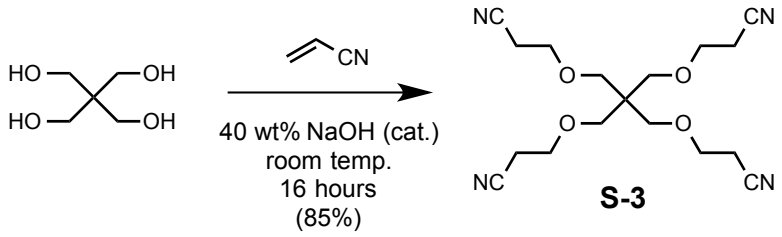


**3,3'-((2,2-bis((2-cyanoethoxy)methyl)propane-1,3-diyl)bis(oxy))dipropanenitrile, S-3.** Tetra-nitrile **S-3** was prepared using a previously described protocol.[2] Briefly, pentaerythriotol (1.00g, 7.34 mmol, 1 equiv.) was combined with acrylonitrile (2.175 mL, 33.03 mmols, 4.5 equiv.) at room temperature and 100 µL of 40 wt% aqueous sodium hydroxide was added. The mixture was stirred under nitrogen at room temperature for 24 hours. The crude was taken up in 20 mL 1N HCl and 20 mL ethyl acetate. The aqueous layer was extracted with a second volume of ethyl acetate, and the combined organic layers were washed once with brine, dried over anhydrous sodium sulfate, filtered and condensed under reduced pressure to yield a colorless oil that solidified on storage to a white solid (2.1794 g, 85%). Spectra are consistent with previously reported data. $R_f$ 0.16 (50% EtOAC/Hexane). $^1$H NMR (500 MHz, $CDCl_3$) δ 3.48 (t, J = 6.1 Hz, 3H), 3.30 (s, 3H), 2.45 (t, J = 6.1 Hz, 3H). $^{13}$C NMR (126 MHz, $CDCl_3$) δ 118.03, 77.49, 77.23, 76.97, 68.22, 65.25, 45.08, 18.19.

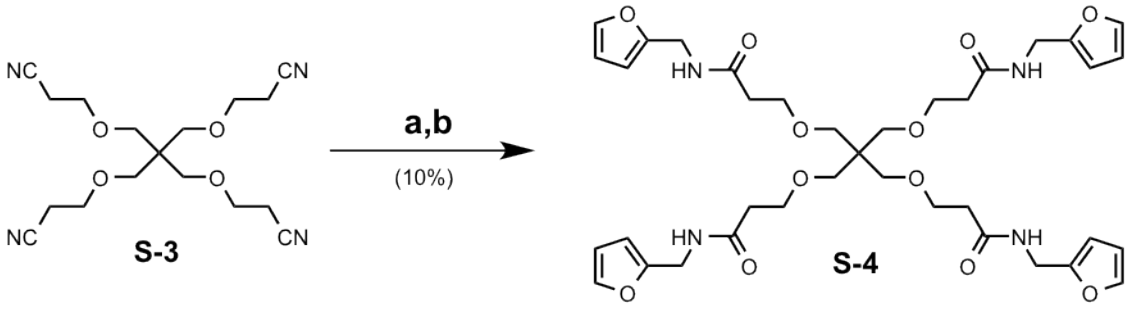


(a) conc. HCl, reflux, 4 hrs. (b) 1 equiv. furfurylamine, 145 °C, neat, pressure vessel.

2 Weizman, H.; Ardon, O.; Mester, B.; Libman, J.; Dwir, O.; Hadar, Y.; Chen, Y.; Shanzer, A. *J. Am. Chem. Soc.* **1996**, 118, 12368-12375.

**3,3'-((2,2-bis((3-((furan-2-ylmethyl)amino)-3-oxopropoxy)methyl)propane-1,3-diyl)bis(oxy))bis(*N*-(furan-2-ylmethyl)propanamide), S-4.** Tetra-furan **S-4** was prepared from the crude tetra-carboxylate formed by a previously described hydrolysis of tetra-nitrile **S-3**.[2] Briefly, the tetra-nitrile (1.5141 g, 4.35 mmols) was dissolved in 3 mL concentrated HCl and refluxed at 100 °C under nitrogen for 4 hours. The crude was suspended in 50 mL ethyl acetate and washed with 20 mL of water. The water layer was extracted with 4 x 20 mL EtOAc, and the organic layers were dried over anhydrous sodium sulfate and condensed at reduced pressure to yield a colorless viscous syrup (1.5 g, 81%). No further purification was performed, and consumption of nitrile was confirmed by FT-IR and $^{13}$C NMR. A portion of this syrup (492 mg, ~1.16 mmols) was combined with 430.2 µL furfurylamine (4.87 mmols, 4.2 equiv), 100 mg 4 Å molecular sieves and a stir bar in a sealed tube and heated at 145 °C for 4 hours, then cooled to room temperature. The brown syrup was partitioned between 20 mL $CH_2Cl_2$ and 20 mL saturated sodium bicarbonate. The organic layer was washed with 20 mL 1 M HCl, and 20 mL brine before being dried over anhydrous sodium sulfate, filtering and condensing in vacuum. The organic crude was further purified by flash chromatography on silica gel, eluting with a gradient from ethyl acetate through 10% MeOH/EtOAc to yield a white solid (77 mg, 10%). $R_f$ 0.44 (10% MeOH/EtOAc). $^1$H NMR (500 MHz, $CDCl_3$) δ 7.37 – 7.28 (m, 4H), 6.96 – 6.77 (m, 4H), 6.34 – 6.25 (m, 4H), 6.19 (d, J = 3.1 Hz, 4H), 4.39 (d, J = 5.6 Hz, 8H), 3.55 (t, J = 5.7 Hz, 8H), 3.17 (s, 8H), 2.36 (t, J = 5.7 Hz, 8H). $^{13}$C NMR (126 MHz, $CDCl_3$) δ 171.55, 151.71, 142.22, 110.67, 107.59, 77.48, 77.23, 76.98, 68.93, 67.30, 45.33, 36.76, 36.55. ESI-MS: [$C_{37}H_{48}N_4O_{12}$+$H^+$] = 740.0

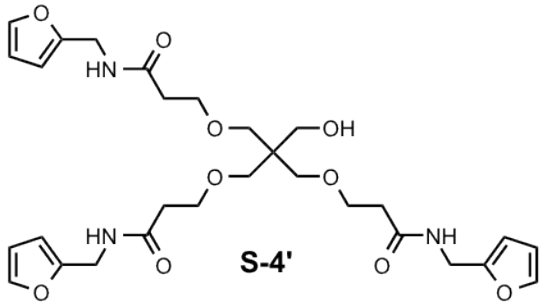

**S-4'**

**3,3'-((2-((3-((furan-2-ylmethyl)amino)-3-oxopropoxy)methyl)-2-(hydroxymethyl)propane-1,3-diyl)bis(oxy))bis(*N*-(furan-2-ylmethyl)propanamide), S-4'.** In addition to the desired product, tris-furan **S-4'** was also obtained (149.2 mg, 22%), presumably due to

retro-Michael addition reaction during the thermal amidation. $R_f$ 0.33 (10% MeOH/EtOAc). $^1$H NMR (500 MHz, $CDCl_3$) δ 7.34 – 7.28 (m, 3H), 6.88 (d, J = 30.8 Hz, 3H), 6.28 (dd, J = 3.1, 1.8 Hz, 3H), 6.19 (d, J = 3.2 Hz, 3H), 4.39 (d, J = 5.5 Hz, 6H), 3.57 (dt, J = 23.7, 5.7 Hz, 6H), 3.43 (s, 2H), 3.22 (d, J = 59.5 Hz, 6H), 2.81 (s, 1H), 2.39 (t, J = 5.7 Hz, 6H). $^{13}$C NMR (126 MHz, $CDCl_3$) δ 171.49, 151.70, 151.65, 142.24, 142.21, 110.64, 107.58, 77.48, 77.23, 76.98, 71.03, 70.31, 68.91, 67.48, 67.40, 67.28, 63.91, 63.78, 45.19, 36.72, 36.65, 36.55. ESI-MS: $[C_{29}H_{39}N_3O_{10}+H^+]$ = 590.0

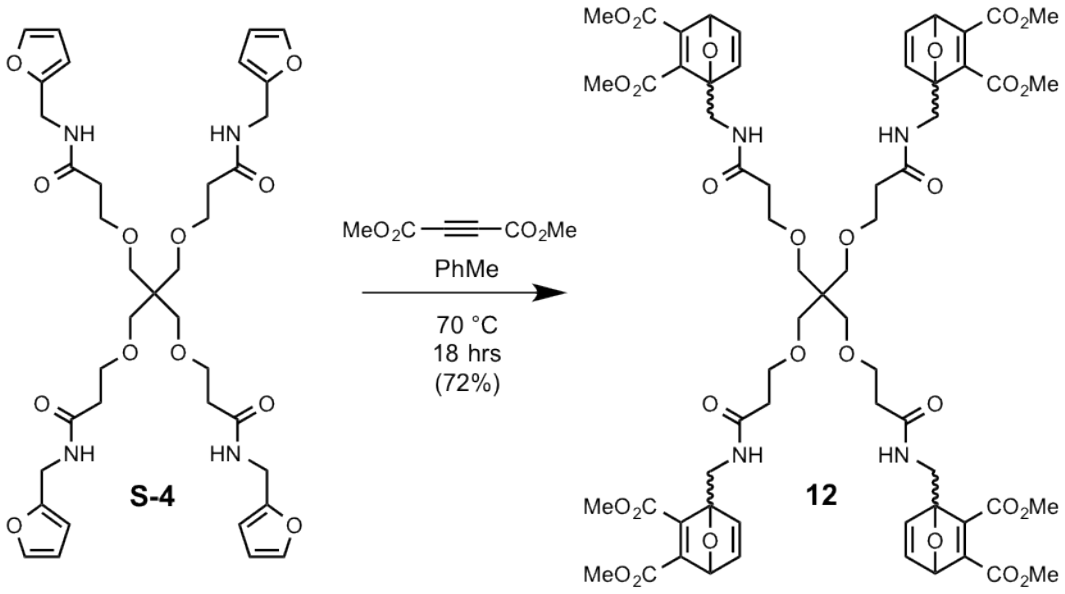


**Tetramethyl 1,1'-(8,8-bis((3-(((2,3-bis(methoxycarbonyl)-7-oxabicyclo[2.2.1]hepta-2,5-dien-1-yl)methyl)amino)-3-oxopropoxy)methyl)-3,13-dioxo-6,10-dioxa-2,14-diazapentadecane-1,15-diyl)bis(7-oxabicyclo[2.2.1]hepta-2,5-diene-2,3-dicarboxylate), 12.** Tetra-furan **S-4** (76.9 mg, 0.104 mmols, 1 equiv) was combined with dimethyl acetylenedicarboxylate (64 µL, 0.519 mmols, 5 equiv.) and 200 µL toluene in a sealed 4 mL vial. The mixture was heated while stirring directly on a hot plate for 18 hours at 70 °C. The crude was then purified by flash chromatography on silica gel, eluting with a gradient from ethyl acetate through 10% MeOH/EtOAc to yield an off-white foaming solid (98.4 mg, 72%). $R_f$ 0.23 (10% MeOH/EtOAc). $^1$H NMR (500 MHz, $CDCl_3$) δ 7.16 (dd, J = 5.2, 1.8 Hz, 4H), 6.98 (d, J = 5.2 Hz, 4H), 6.65 (t, J = 5.8 Hz, 4H), 5.59 (d, J = 1.8 Hz, 4H), 4.15 – 4.03 (m, 4H), 3.99 – 3.94 (m, 4H), 3.76 (two singlets, 24H), 3.56 (t, J = 5.5 Hz, 8H), 3.25 (s,

8H), 2.37 (t, J = 5.8 Hz, 8H). $^{13}$C NMR (126 MHz, $CDCl_3$) δ 171.68, 163.99, 162.71, 153.99, 152.77, 145.36, 143.30, 97.23, 83.73, 77.48, 77.43, 77.23, 76.98, 69.47, 67.38, 52.65, 52.50, 45.26, 37.70, 36.73. FT-IR ($cm^{-1}$): 3365, 2954, 1713, 1652, 1537, 1435, 1264, 1200, 1098, 714. LC-HRMS: [$C_{61}H_{72}N_4O_{28}$+$H^+$] calc: 1309.4406, obs: 1309.4413. rt: 7.147 min (0-90% MeCN/$H_2O$).

**Supplementary Note on Epoxidation Reactions**

Conversion of the OND to the corresponding epoxyoxanorbornene (EONB) is facilitated in high conversion using either dimethyldioxirane (DMDO) or 3-chloroperoxybenzoic acid (mCPBA). Due to challenges with purification, DMDO is the preferred method, as pure epoxide is obtained in near-quantitative yield simply by evaporating the reaction solvent and volatile excess DMDO. In addition to epoxidation of bis-OND **7a** to bis-EONB **8**, test epoxidations were carried out with mono-, tri- and tetra-valent ONDs. Reactions with mono- and tris-ONDs proceeded smoothly. While epoxidation was observed in the case of tetra-OND **12** with DMDO, the reaction was complicated by the presence of ether linkages in the linker core structure, which are easily oxidized by DMDO reagent.3

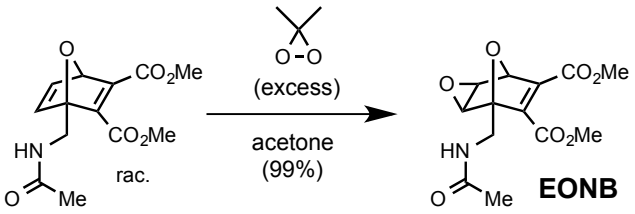


**Dimethyl 1-(acetamidomethyl)-3,8-dioxatricyclo[3.2.1.0$^{2,4}$]oct-6-ene-6,7-dicarboxylate, EONB.** A vial was charged with previously described4-dimethyl 1-(acetamidomethyl)-7-oxabicyclo[2.2.1]hepta-2,5-diene-2,3-dicarboxylate (21.5 mg, 0.076 mmols, 1 equiv), and dissolved in 1.5 mL ~0.07 M solution of DMDO (~1.1 equiv) in acetone at room temperature. The resulting solution was stirred at room temperature for 4 hours, and then condensed under reduced pressure to yield a white solid (22.7 mg, quantitative). $R_f$ 0.28 (EtOAc). $^1$H NMR (500 MHz, $CDCl_3$) δ 5.87 (s, 1H), 5.09 (s, 1H), 4.06

3 Grabovskiy, S.; Timerghazin, Q.; Kabal'nova, N. *Russ. Chem. B+.* **2005**, 54, 2384-2393.
4 Kislukhin, A.; Higginson, C.; Hong, V.; Finn, M *J. Am. Chem. Soc.* **2012**, 134, 6491-6497.

(dd, J = 14.9, 6.3 Hz, 1H), 3.92 (dd, J = 14.9, 5.3 Hz, 1H), 3.84 (s, 3H), 3.80 (s, 3H), 3.78 (d, J = 3.6 Hz, 1H), 3.72 (d, J = 3.6 Hz, 1H), 1.98 (s, 3H). $^{13}$C NMR (126 MHz, $CDCl_3$) δ 170.42, 163.13, 162.02, 149.95, 146.89, 91.35, 78.52, 77.48, 77.23, 76.98, 57.30, 56.55, 53.11, 52.89, 37.31, 23.17. FT-IR ($cm^{-1}$): 3375, 2956, 1717, 1660, 1537, 1435, 1239, 1132, 877. LC-HRMS: [$C_{13}H_{15}NO_7$+$H^+$] calc: 298.0921, obs: 298.0927. rt: 3.803 min (0-90% MeCN/$H_2O$).

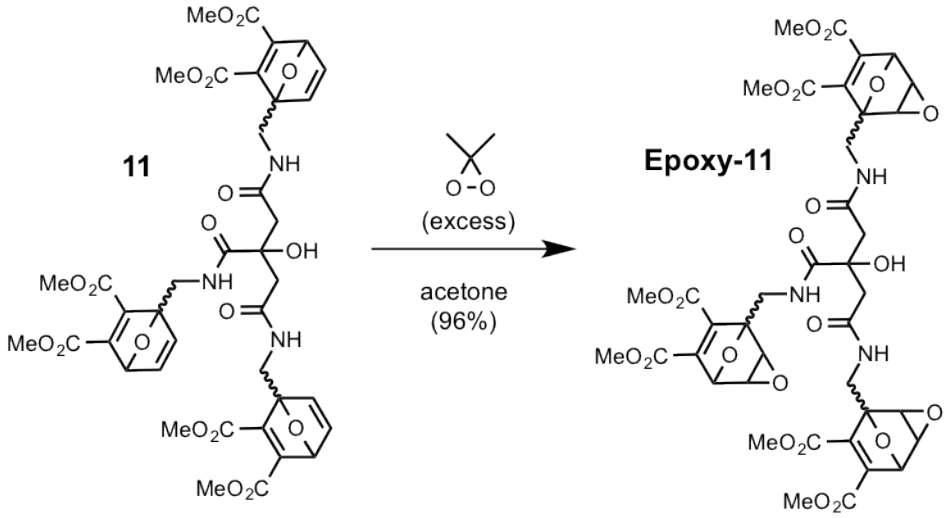


**tetramethyl 1,1'-(((2-(2-(((6,7-bis(methoxycarbonyl)-3,8-dioxatricyclo[3.2.1.0$^{2,4}$]oct-6-en-1-yl)methyl)amino)-2-oxoethyl)-2-hydroxysuccinyl)bis(azanediyl))bis(methylene))bis(3',8'-dioxatricyclo[3.2.1.0$^{2,4}$]oct-6-ene-6,7-dicarboxylate), Epoxy-11**

Tris-OND **11** (30.0 mg, 0.035 mmols, 1 equiv.) was dissolved in 1.95 mL of a ~0.07 M solution of DMDO (~3.9 equiv) in acetone and stirred at room temperature for 19 hours. The reaction mixture was faintly cloudy, and was filtered prior to condensing the filtrate under reduced pressure, and drying the residue on high vacuum to yield a pale foaming solid (30.5 mg, 96%). $R_f$ 0.53 (10% MeOH/EtOAc). $^1$H NMR (500 MHz, $CDCl_3$) δ 7.47 – 7.42 (m, 1H), 7.18 – 6.96 (m, 2H), 6.26 – 5.96 (m, 1H), 5.07 – 5.06 (m, 3H), 4.05 – 3.87 (m, 6H), 3.84 – 3.77 (m, 18H), 3.75 – 3.72 (m, 6H), 2.81 – 2.60 (m, 4H). $^{13}$C NMR (126 MHz, $CDCl_3$) δ 174.17, 174.16, 174.14, 174.12, 171.08, 171.02, 171.00, 170.97, 170.94, 163.14, 163.12, 162.18, 162.17, 162.16, 149.67, 149.63, 149.54, 149.52, 149.48, 149.40, 149.37, 147.51, 147.49, 147.47, 147.44, 147.33, 147.17, 147.14, 91.13, 91.09, 91.07, 91.05, 91.01, 90.98, 80.78, 78.56, 78.54, 75.10, 75.06, 75.05, 57.47, 57.36, 57.34, 56.67, 56.64, 56.60, 56.59, 55.21, 53.05, 52.84, 42.88, 42.76, 42.71, 42.62, 37.16, 37.11, 37.06, 37.02, 36.99, 36.97. FT-

IR ($cm^{-1}$): 3369, 2955, 1716, 1668, 1530, 1238, 1132, 912, 875, 727. ESI-MS: $[C_{39}H_{41}N_3O_{22}+H^+]$ = 904.1.

## III. Preparation of Gels

Trial gelations were performed by premixing a solution of linker **7a** with four-armed thiol-terminated poly(ethylene glycol) (4-PEG-SH. $M_n$ = 10,000) in neutral water containing 17% DMSO by volume. The overall concentration of PEG macromer was varied from 0.4 wt% to 8.3 wt% while maintaining an equimolar ratio of thiol to electrophile. Under these conditions, no gels formed on standing at room temperature for five minutes. Upon addition of stoichiometric triethylamine to the solution and mixing, instantaneous gelation was observed for solutions containing 4-PEG-SH at ≥2.5 wt% (Figure S1).

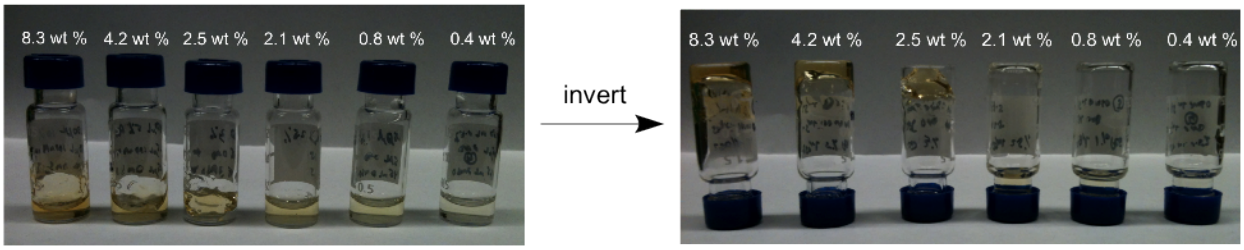


**Figure S1.** (Left) Samples 2 minutes after addition of triethylamine, upright; (Right) Samples shown on left after inversion. Samples at 0.4 – 2.1 wt% are free-flowing solutions.

Based on empirical observations made in these trials, subsequent gels were prepared at room temperature from 3.5 wt% 4-PEG-SH solutions in phosphate buffers containing 7% DMSO at equimolar concentrations of thiol and OND electrophile. Mixtures were mixed briefly with a vortex mixer, and the reaction vial was periodically tilted or inverted. Gelation time was recorded when the sample no longer flowed and was self-supporting. For linkers **7a**, **7b**, **10**-**12**, gels were observed in less than 1.5 minutes at pH 7.2, and approximately 30-45 seconds at pH 7.4. Gels formed with linker **7c** did not form self-supporting gels at pH 7.4, but formed gels at pH 8.0, as described in the main text. Gelation time at 37 °C was determined by pre-warming 4-PEG-SH macromer and OND stock solutions in a 37 °C water bath. Gel components were combined and mixed briefly by

pipetting, and the sample was held in the water bath. Gelation time was determined by the inversion test, as described above.

**IV. Oscillatory Rheology**

We used oscillatory rheology to assess the viscoelastic properties of selected PEG-OND hydrogels. 4-PEG-SH macromer and bis-EONB **8** were combined in a 1:1 thiol:electrophile ratio (1:2 molar ratio) in 100 mM pH 7.2 potassium phosphate buffer containing 7% (v/v) DMSO. The solution was briefly mixed by pipetting and immediately deposited on the center of the rheometer bottom plate, which was maintained at 37 °C. The truncated cone was then brought in contact with the bis-EONB/4-PEG-SH mixture prior to setting of the gel by positioning the tool at the measuring position. The sample was inspected for spillovers and trimmed as required. A preliminary preshearing step consisting of 30 seconds at 0.1% strain and $\omega$ = 0.01 rad/s was performed to ensure good contact with the gel sample. The elastic (storage) and viscous (loss) moduli, G' and G'', respectively, were then measured as a function of time for a constant strain of 1% and an angular frequency of 1 rad/sec. The ability to store energy is described by G', while the amount of energy dissipated is related with G''. We observe that the sample experienced a rapid transformation from an initial state in which G' was not much larger than G'' to a state in which G' was clearly predominant, as shown in Fig. S2; this is consistent with gelation. The observed transformation happened in the first few minutes after preparation, even when the hydrogel continued to rigidify for up to 2-3 hours. At this point, the system reached an essentially time-independent state where G'' was negligible in comparison with G', indicative of the solid-like nature of the material.

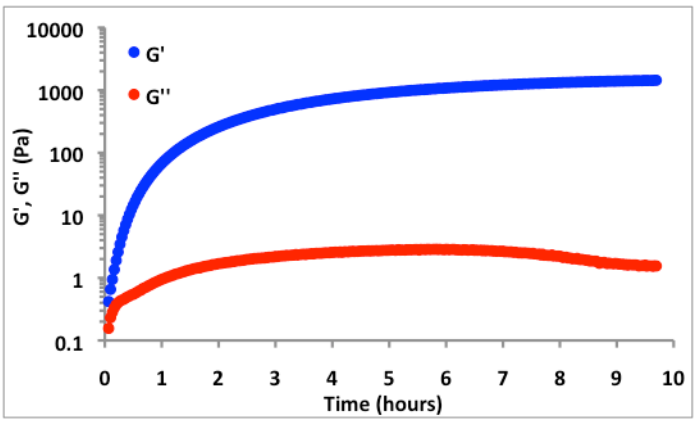


**Figure S2.** Oscillatory time sweep of the gel derived from bis-EONB **8** and 4-PEG-SH (1:1 ratio of reactive groups) at 37 °C.

The linear regime of this sample was determined by performing an oscillatory strain sweep at 37 °C. We found the response to be linear in a wide range of strains, as shown in Fig. S3. Note that G'>>G'', consistent with the time dependence results shown in Fig. S2. The frequency sweep shown in the main text was thus performed in the linear region.

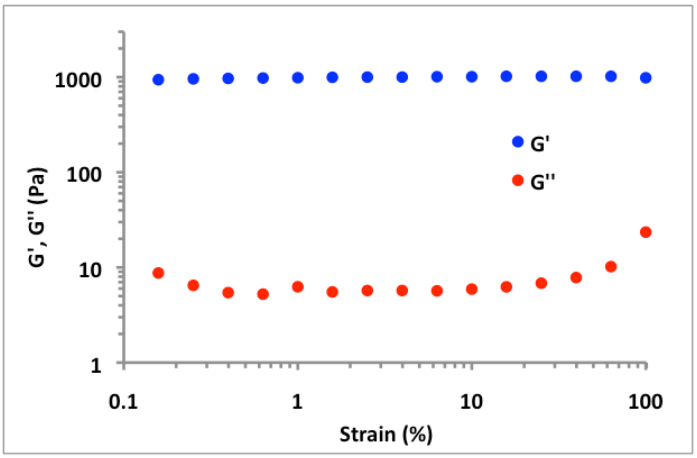


**Figure S3.** Oscillatory strain sweep of gel derived from bis-EONB **8** and 4-PEG-SH (1:1) at 37 °C and $\omega$ = 1 rad/s.

We also have characterized the viscoelasticity of the hydrogel derived from 4-PEG-SH macromer and bis-OND linker **7c**, at pH 8.0 and T = 4 °C, by performing oscillatory strain and frequency sweeps. We find that the response is linear in a wide range of strains, as shown in Fig. S4. Similarly, G' is essentially frequency independent, as shown in Fig. S5. In both experiments, G'>>G''. These results confirm the solid-like nature of this sample in these conditions.

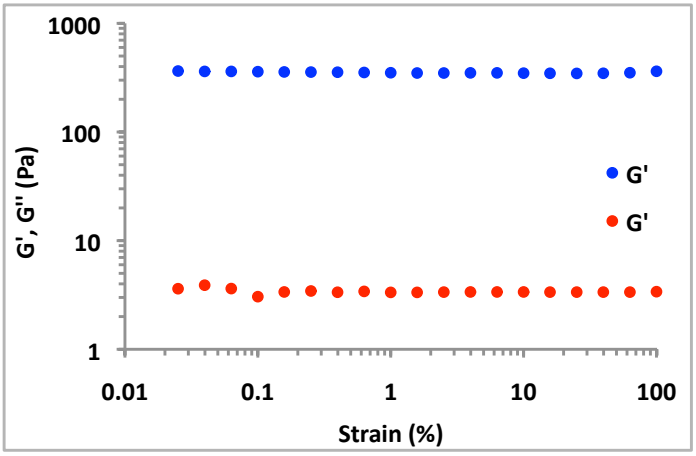


**Figure S4.** Oscillatory strain sweep of the gel derived from bis-OND **7c** and 4-PEG-SH at 4 °C and ω = 1 rad/s.

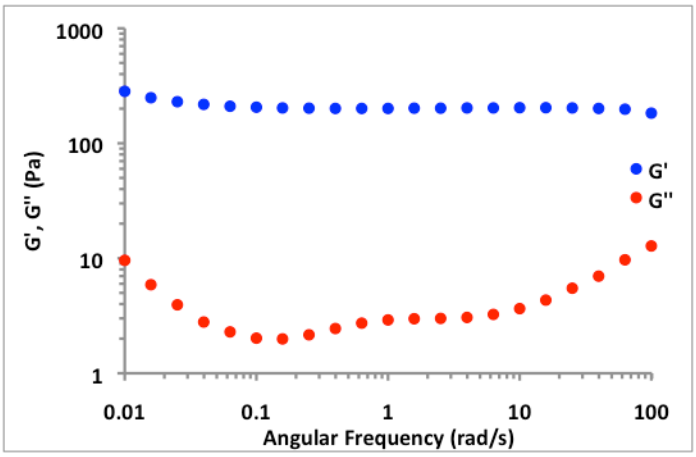


**Figure S5.** Frequency sweep for the gel derived from bis-OND **7c** and 4-PEG-SH macromer (1:1 thiol:OND) at 4 °C and γ = 5%.

## V. Monitoring Degradation of Neat Hydrogels

*V.1. Assessment of gel integrity by the inversion test*

Three 500 µL 3.5 wt% hydrogels were formed with bis-ONDs **7a** and **7b**, and bis-EONB **8**, respectively, in 2 mL vials with caps. The sealed vials were incubated in an oil bath maintained at 50 °C. The samples were periodically removed from heat and the vials were inverted to determine if the gel was still intact, or whether the sample was a free-flowing liquid, as described in the main text. A full time course of the experiment presented in Figure 1 of the main text is shown in Figure S6 below. The gel formed between 4-PEG-SH and bis-EONB **8** in Figure S6 was removed from heat after 5 days, and stored at room temperature in a sealed vial. The hydrogel is still intact at the time of writing (5 days at 50 °C followed by >1 year at room temperature). The inversion test was routinely used in all stability experiments to verify hydrogel integrity during incubation.

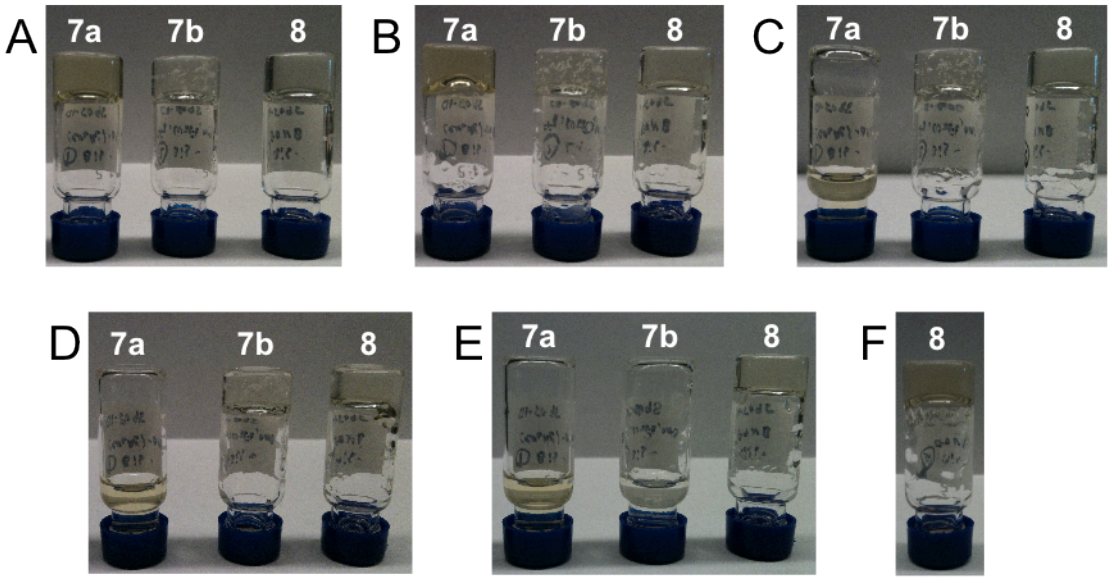


**Figure S6.** Monitoring hydrogel degradation by inversion test. Incubation performed at 50 °C for (A) 0 hours, (B) 2 hours, (C) 3 hours, (D) 8.5 hours, (E) 20.5 hours, (F) 5 days.

*V.2. Time-lapse photography*

In order to observe reverse gelation upon prolonged heating of neat hydrogels, time-lapse photography was carried out. Briefly, 600 µL hydrogels comprised of 3.5 wt% 4-PEG-SH + bis-OND/EONB (**7a**, **7b**, and **8**, respectively) in pH 7.4 100 mM potassium phosphate buffer containing 7% DMSO (v/v) were formed in glass culture tubes and allowed to set for 15 minutes. A glass bead (~160 mg, stained with blue Sharpie-brand marker to improve visibility) was placed carefully on top of each gel, and a drop of silicon oil was added to prevent evaporation at the surface of the gels. The tubes were sealed with lab parafilm and incubated in a 50 °C oil bath. Photos were collected every 2 minutes for ~22 hours using Chronolapse software (v.1.0.4) and a Creative Labs webcam. Photographs were compiled in chronological order using iMovie software, with each photo occupying one 0.1s frame. The resulting video is available as Supporting Movie S1.

## VI. NMR Analysis of Hydrogels

In standard 5mm NMR tubes, a 500 µL 3.5 wt% PEG-OND hydrogel were prepared by mixing 465 µL of 3.76 wt% 4-PEG-SH in pH 7.4 $KDPO_4/K_2PO_4$ buffer and 35 µL 85 mM **7a** in DMSO-$d_6$ and vortexing to mix. $^1$H-NMR spectra were collected on the sample 10 minutes after mixing. Samples were then incubated at 37 °C and $^1$H-NMR were collected periodically. Additionally, spectra were collected as close as possible to the reverse gelation point to determine fractional conversion of OND-thiol adduct to furan. The sample was monitored until complete conversion of thiol adducts to furan was observed (Figure S7, blue highlighted peaks to green highlighted peaks).

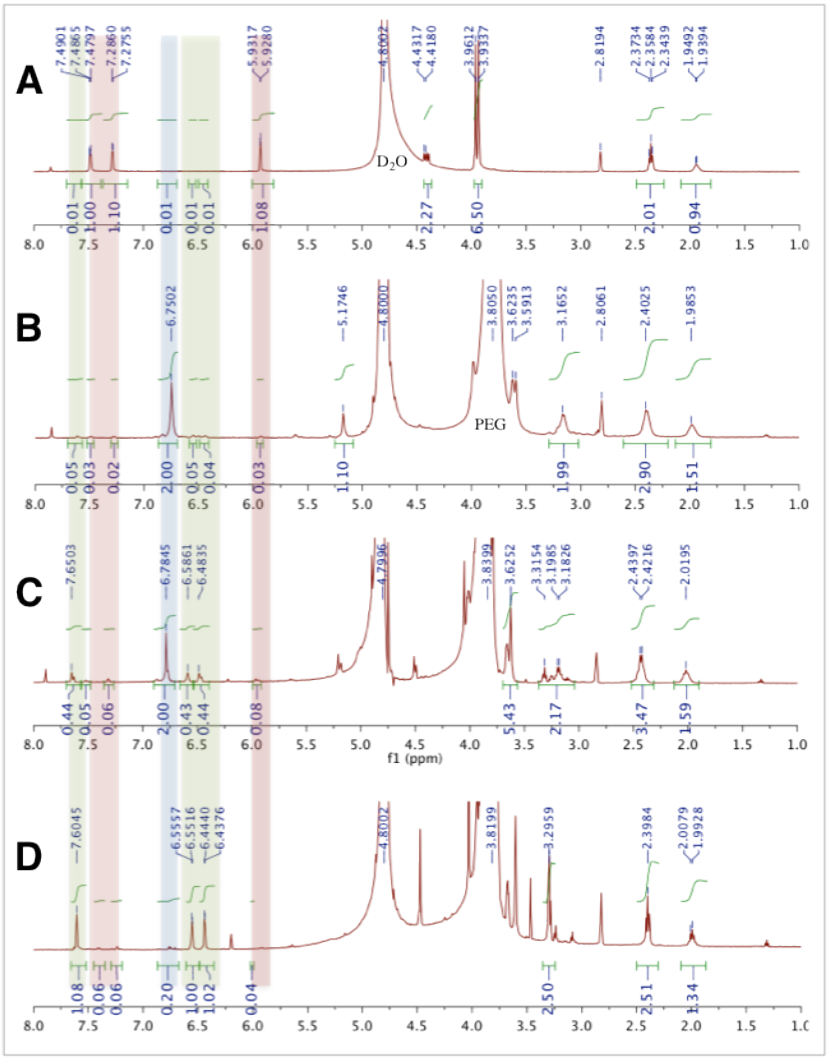


**Figure S7.** $^1$H NMR spectra of PEG-OND Hydrogel formed with 4-PEG-SH macromer and bis-ONDs **7a**. (A) bis-OND **7a** in $KDPO_4/K_2PO_4$ buffer (pH 7.4), (B) PEG-OND hydrogel from 4-PEG-SH and **7a**, 10 mins after mixing at 22 °C, (C) Sample at reverse-gelation point, (D) Sample after complete degradation. Red highlight = distinctive OND peaks, Blue highlight = distinctive OND-thiol adduct peaks, Green highlight = distinctive furan peaks.

A 3.5 wt% hydrogel formed with linker **7b** was prepared in a similar fashion. The sample was a self-supporting gel when the tube was inverted 1 minute after mixing. A $^1$H-NMR spectrum was collected ~15 minutes after mixing the sample. All OND linker was converted to the corresponding thiol adduct. The sample was then placed in a 37 °C incubator and spectra were collected periodically until the gel was no longer intact, as determined by the inversion test (Figure S8).

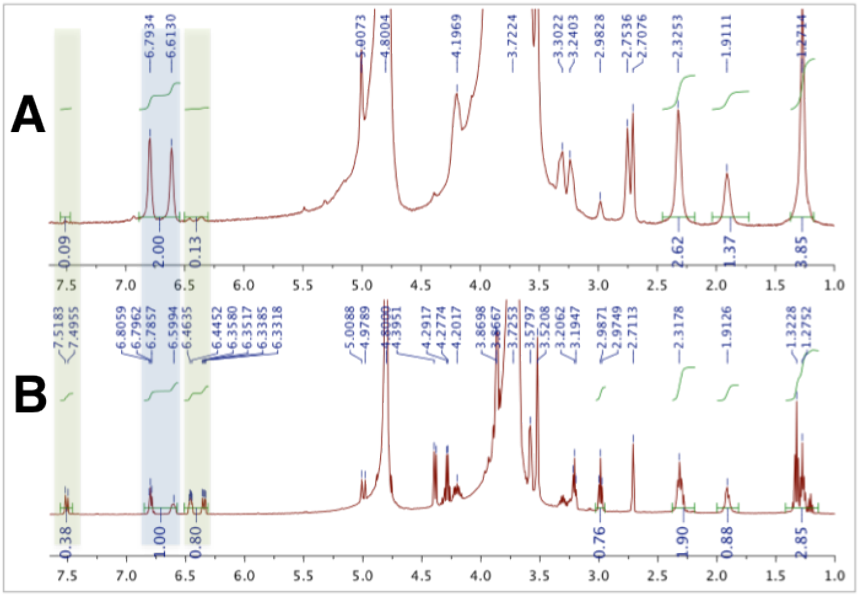


**Figure S8.** $^1$H NMR spectra of PEG-OND Hydrogel formed with 4-PEG-SH macromer and bis-ONDs **7b**. (A) PEG-OND hydrogel from 4-PEG-SH and **7a**, 15 mins after mixing at 22 °C, (B) Sample at reverse-gelation point. Blue highlight = distinctive OND-thiol adduct peaks, Green highlight = distinctive furan peaks.

The degree of conversion of the OND-thiol adducts to furan when sample no longer contained a self-supporting gel was close to the theoretical reverse gelation point for gels formed by step-growth polymerization between tetravalent and divalent components (See section VII.3. for details). To estimate the rate constant for retro-Diels-Alder fragmentation of OND-thiol adducts in the neat hydrogels, the degree of conversion of adduct to furan was determined from integration of the C5 and C6 olefinic protons of thiol adducts (blue highlight, Figures S7 and S8) and the integrals of furan protons (green highlights). For comparison, the same peaks were carefully cut out of printed versions of spectra and weighed. The ratio of the mass of furan peaks to the mass of furan and C5+C6 peaks at each time point provided fractional conversion values similar to those obtained by integration. The degree of conversion was plotted against time and least-squares non-linear curve fitting to the first order integrated rate law was performed using the Solver plug-in in

Microsoft Excel (Figures S9 and S10).[5] Plotting ln(1/1-fraction furan) vs. time yielded linear plots, with slopes providing a rate constant comparable to those obtained in non-linear fitting (Figures S9 and S10, inset).

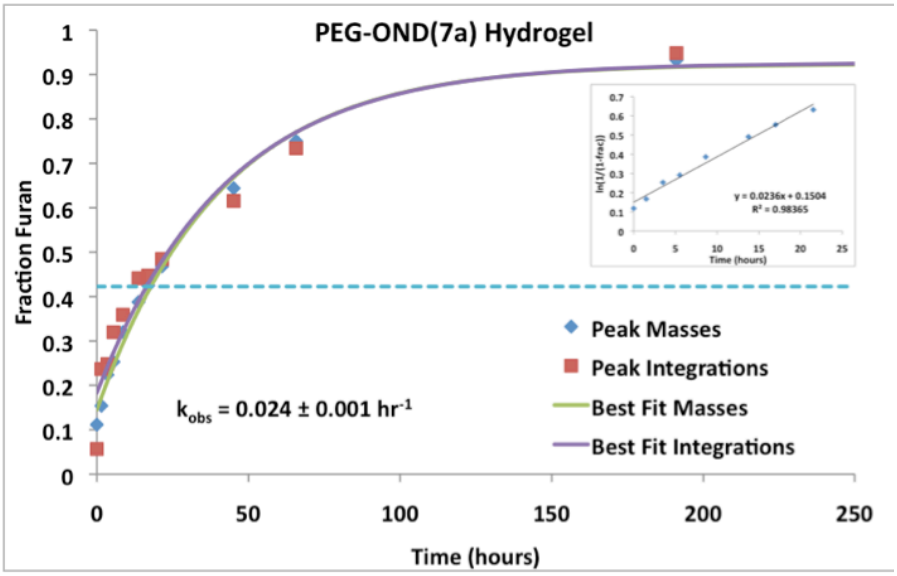


**Figure S9.** Observed conversion of OND-thiol adducts to furan vs. time in a 3.5 wt% PEG-OND hydrogel formed with bis-OND **7a**. The blue dotted line represents the theoretical reverse gelation point.

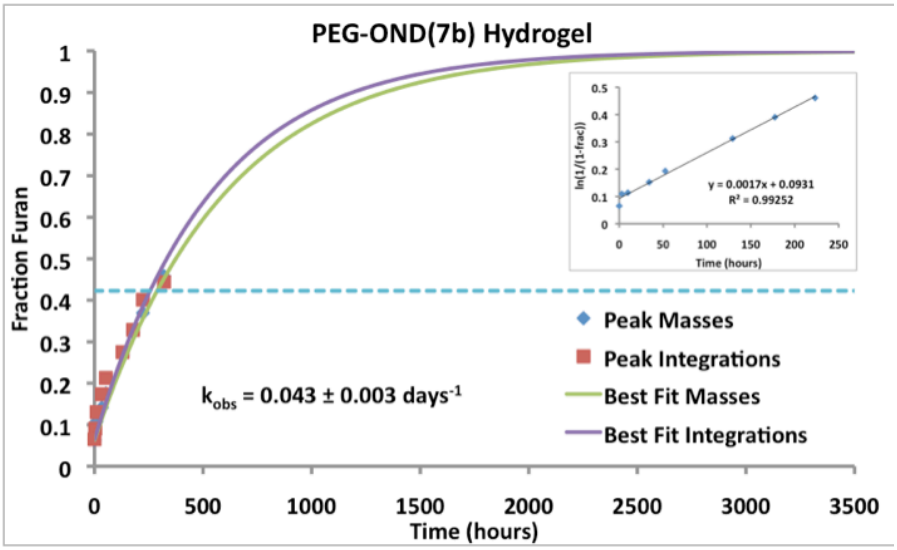


**Figure S10.** Observed conversion of OND-thiol adducts to furan vs. time in a 3.5 wt% PEG-OND hydrogel formed with bis-OND **7b**. The blue dotted line represents the theoretical reverse gelation point.

[5] Kemmer, G.; Keller, S. *Nat. Methods* **2010**, 5, 267-281.

## VII. Equilibrium Swelling and Determination of Gel Fraction

*VII.1. Equilibrium mass swelling ratio determination*

200 μL gels were prepared in pH 7.4 100 mM phosphate buffered saline containing 7% DMSO with 3.5 wt% 4-PEG-SH and the corresponding bis-, tris-, and tetra-ONDs to provide a 1:1 thiol to electrophile ratio, and allowed to cure for 20 minutes at room temperature. The mass of the gels after curing was recorded ($M_{eq}$) prior to suspending in 5.5 mL of water. The hydrogels were stored at 4 °C during swelling to prevent significant degradation of the network during the experiment. The increase in mass of the gels was monitored periodically by decanting and blotting the gel gently with a kimwipe to remove excess water before weighing. After 24 hours swelling, when swelling had stabilized, the mass of the gel was recorded ($M_{eq}$). The equilibrium mass swelling ratio was then determined using the following relationship:

$$\text{Equilibrium Mass Swelling Ratio} = \frac{M_{eq}}{M_0} \qquad \text{(Equation S1)}$$

*VII.2. Gel fraction determination*

After weighing equilibrium-swelled gels to determine equilibrium mass swelling ratio, the gels were freeze-dried and the residual mass was weighed ($M_{res}$). It is expected that buffer salts present in the sample when it was formed were removed by the multiple changes of swelling solvent (pure water). The mass of the remaining residue was compared to the input mass ($M_{in}$) of 4-PEG-SH macromer and OND-based linker. The ratio of the residual mass and the input mass provides the fraction of material by mass incorporated into the hydrogel network (gel fraction), as shown in the following equation:

$$\text{Gel Fraction} = \frac{M_{res}}{M_{in}} \qquad \text{(Equation S2)}$$

*VII.3. Calculations with Flory-Rehner elastic theory*

*Critical Gelation/Reverse Gelation Point:*

During the formation of a homogeneously crosslinked hydrogel network, discrete soluble polymer segments (i.e. macromer monomers or oligomers) become linked as non-

elastic chain ends are chemically stitched together or become physically entangled. This process continues until the critical gelation point is reached, at which point the polymer segments are now part of a macroscopic network. The degradation of a hydrogel formed using labile linkers can be described loosely as the reverse of gel formation. Linkages holding polymer segments together break down, revealing non-elastic chain ends until a critical point at which the gel rapidly disintegrates/dissolves into finite polymer segments. This phase is characterized by a steep "burst" phase of release in the erosion of the hydrogel (see Figure 2, main text). The critical gelation/reverse-gelation point for an ideal network formed by step-growth polymerization between two orthogonally reactive monomers of valence $f_A$ and $f_B$ can be described by adapting the theory first described by Flory and Rehner[6]:

$$P_c^{\text{step-growth}} = \frac{[\text{A} - \text{B linkage}]_t}{[\text{A} - \text{B linkage}]_0} = \frac{1}{\sqrt{r(f_A - 1)(f_B - 1)}} \qquad \text{(Equation S3)}$$

where $P_c^{\text{step-growth}}$ is the fraction of crosslinks between monomers A and B at the critical gelation point (or reverse gelation point), $f_A$ is the valence of monomer A, $f_B$ is the valence of monomer B, and r is the stoichiometric ratio of reactive groups A and B. The value of $P_c^{\text{step-growth}}$ for a network formed from an equimolar mixture of 4-armed PEG-SH ($f_A$ = 4) and divalent OND (or EONB) linkers ($f_B$) is:

$$P_c^{\text{step-growth}} = \frac{1}{\sqrt{1(4-1)(2-1)}} = \frac{1}{\sqrt{3}} \sim 0.5774 \qquad \text{(Calculation S1)}$$

The degree of conversion of OND-Thiol adducts to furan and thiomaleate/thiofumarate in a formed PEG-OND gel network to reach the critical reverse gelation point is $1 - P_c = 0.4226$. Applying Equation S3, the critical reverse gelation point can be calculated for networks formed between 4-PEG-SH and ONDs of higher valence:

[6] (a) Flory, P. J. *Chem. Rev.* **1946**, *39*, 137. (b) Flory, P. J. *J. Chem. Phys.* **1950**, *18*, 108. (c) Flory, P. J.; Rehner, J. *J. Chem. Phys.* **1943**, *11*, 521.

Trivalent OND: $P_c^{step\text{-}growth} = \frac{1}{\sqrt{1(4-1)(3-1)}} = \frac{1}{\sqrt{6}} \sim 0.4082$ (Calculation S2)

Tetravalent OND: $P_c^{step\text{-}growth} = \frac{1}{\sqrt{1(4-1)(4-1)}} = \frac{1}{3} \sim 0.3333$ (Calculation S3)

*Calculation of Theoretical Molecular Weight Between Crosslinks*

Using the masses measured during equilibrium swelling experiments, it is possible to estimate the apparent average molecular weight between crosslinks ($M_c$) present in the hydrogel. For an ideally crosslinked network, this value is determined by the molecular weight and valence of the monomeric/macromeric components, as previously described by Metters and Hubbell[7]:

$$M_{C,\ Initial,\ Ideal} = 2\left(\frac{MW_A}{f_A} + \frac{MW_B}{f_B}\right) \quad \text{(Equation S4)}$$

Since the 4-PEG-SH macromer average molecular weight and valence is kept constant, the $M_{c,\ ideal}$ varies only with the molecular weight and valence of the OND linker used to form the network. However, this formula neglects the formation of physical entanglements or crosslinks, and only accounts for elastically-productive chemical crosslinks. Applying Equation S3, the $M_{c,ideal}$ values for bis-, tris-, and tetra-ONDs/EONBs used in this study are summarized in Table S1.

**Table S1.** Summarized linker molecular weights, valence, and calculated $M_{c,ideal}$.

| Entry | Linker | $MW_B$ *(g/mol)* | Valence, $f_B$ | $M_{c,ideal}$ (g/mol) |
|---|---|---|---|---|
| 1 | **7a** | 574.5 | 2 | 5,575 |
| 2 | **7b** | 622.5 | 2 | 5,623 |
| 3 | **8** | 606.5 | 2 | 5,607 |
| 4 | **10** | 598.5 | 2 | 5,599 |
| 5 | **7a+7b** | 598.5 [a] | 2 | 5,599 |
| 6 | **11** | 855.8 | 3 | 2,785 |
| 7 | **12** | 1,309.2 | 4 | 2,827 |

(a) Average molecular weight for a equimolar mixture of linkers **7a** and **7b**.

[7] Metters, A.; Hubbell, J. *Biomacromolecules* **2005**, 6, 290-301.

*Experimental Determination of Molecular Weight Between Crosslinks by Equilibrium Swelling*

The apparent molecular weight between elastically-productive crosslinks ($M_c$) was determined from equilibrium swelling data, collected as described in section VII.1 and applying a modified form of the Flory-Rehner equation for networks formed under dilute conditions[6]:

$$M_c = \left[ \frac{2}{M_n} - \frac{\frac{\bar{v}}{V_1}\left[\ln(1-\nu_{2,s}) + (\nu_{2,s}) + (\chi(\nu_{2,s})^2\right]}{(\nu_{2,r})\left[\left(\frac{\nu_{2,s}}{\nu_{2,r}}\right)^{1/3} - \frac{\nu_{2,s}}{2\nu_{2,r}}\right]} \right]^{-1} \qquad \text{(Equation S5)}$$

where $M_n$ is the number average molecular weight for the polymeric macromer (10,000 g/mol), $\bar{v}$ is the specific volume of the polymer (0.84 $cm^3/g$ for PEG[8]) $V_1$ is the molar volume of solvent used for swelling (18 $cm^3/g$ for water), $\chi$ is the polymer-interaction parameter (0.43 for PEG-$H_2O$[9] and assumed constant for the described experiments). $\nu_{2,s}$ and $\nu_{2,r}$ are the volume fraction of polymer in the equilibrium swollen gel and the relaxed gel after curing, respectively, and are calculated as follows:

$$\nu_{2,s} = \left[1 + \frac{(q_w - 1)\rho_p}{\rho_{water}}\right]^{-1} \qquad \text{(Equation S6)}$$

$$\nu_{2,r} = \left[1 + \frac{(q_F - 1)\rho_p}{\rho_{cure\ solvent}}\right]^{-1} \qquad \text{(Equation S7)}$$

where $q_w$ is the weight swelling ratio after equilibrium swelling, $q_F$ is the weight swelling ratio after curing, $\rho_p$ is the density of the polymer (1.12 $g/cm^3$ for PEG), $\rho_{water} = \rho_{cure\ solvent}$ is the density of swelling solvent and solvent during gel formation (1.00 $g/cm^3$ for water).

---

[6] (a) Flory, P. J. *Chem. Rev.* **1946**, *39*, 137. (b) Flory, P. J. *J. Chem. Phys.* **1950**, *18*, 108.
[8] Cruise, G.; Scharp, D.; Hubbell, J. *Biomaterials* **1998**, 19, 1287-1294.
[9] Lee, Y.; Kim, D.; Choi, D.; Lee, W.; Park, J.; Koh, W.-G. *Polym. Adv. Technol.* **2008**, 19, 852-858.

The weight swelling ratios $q_w$ and $q_F$ are determined from data gathered in equilibrium swelling experiments using the following relationships:

$$q_w = \frac{m_s}{m_d} \quad \text{(Equation S8)}$$

$$q_F = \frac{m_c}{m_d} \quad \text{(Equation S9)}$$

where $m_s$ is the mass of the gel after equilibrium swelling, $m_c$ is the mass of the gel after curing, and $m_d$ is the mass of the dried gel, or input mass of polymer and crosslinkers.

Using the formulae above, masses of hydrogel samples recorded after equilibrium swelling, curing, and drying were applied to estimate the apparent molecular weight between crosslinks, which are summarized in Table 1 of the main text. The experimentally observed $M_c$ values for gels formed using divalent OND linkers was lower than theoretical ideal value $M_{c,ideal}$. This can be explained by the fact that the $M_{c,ideal}$ values calculated for these gels (entries 1–5 of Table S1) are greater than the entanglement molecular weight for polyethylene glycol (~4,400 g/mol).[10] The experimentally observed $M_c$ values are a combination of chemical and physical crosslinks, while the calculation of $M_{c,ideal}$ only accounts for chemical crosslinks in the network. The experimentally observed $M_c$ values for networks formed with tris- and tetra-OND linkers are greater than the theoretical value $M_{c,ideal}$, but are still a product of both chemical and physical crosslinks.

*Calculation of Hydrogel Mesh Size*

Using the calculated molecular weight between crosslinks, $M_c$, and the method previously described by Canal and Peppas[11], the hydrogel mesh size was calculated. First, the root-mean-square end-to-end distance of the polymer chains in the network, $(\bar{r}_0^2)^{1/2}$, was calculated as follows:

[10] Zdyrko, B; Varshney, S.; Luzinov, I *Langmuir* **2004**, 20, 6727-6735.
[11] Canal, T; Peppas, N. *J. Biomed. Mater. Res.* **1989**, 23, 1183-1193.

$$(\bar{r}_0^2)^{1/2} = l C_n^{1/2} n^{1/2} \quad \text{(Equation S10)}$$

where $l$ is the average bond length in the polymer (0.146 nm for PEG) and $C_n$ is the characteristic ratio of the polymer (4.0 for PEG).[12] The average number of bonds between crosslinks, *n* is calculated using the following equation:

$$n = 2\frac{M_c}{M_r} \quad \text{(Equation S11)}$$

where $M_c$ is the average molecular weight between crosslinks, calculated as described in the previous section, and $M_r$ is the molecular weight of the repeating unit for the PEG macromer (44 g/mol). Finally, the mesh size, $\xi$, is calculated using the following relationship:

$$\xi = \nu_{2,s}^{-1/3}\left(\bar{r}_0^2\right)^{1/2} \quad \text{(Equation S12)}$$

where $\nu_{2,s}$ is the partial volume of polymer in the equilibrium swollen hydrogel, and is calculated using the experimentally determined equilibrium weight swelling ratios. The calculated mesh sizes for the hydrogels studied by equilibrium swelling are shown in Table S2.

**Table S2.** Calculated mesh size for various equilibrium-swollen gels.

| Entry | Linker | ξ (nm)[a] |
|---|---|---|
| 1 | **7a** | 15.2 ± 0.9 |
| 2 | **7b** | 13.1 ± 0.1 |
| 3 | **8** | 14.0 ± 0.9 |
| 4 | **10** | 15.1 ± 1.3 |
| 5 | **7a+7b** | 14.4 ± 0.5 |
| 6 | **11** | 13.7 ± 1.3 |
| 7 | **12** | 13.3 ± 0.9 |

(a) Calculated using Equations S9-S11 using equilibrium swelling data.

[12] (a) Merrill, E; Dennison, K; Sung, C. *Biomaterials* **1993**, 14, 1117-1126. (b) Mellot, M; Searcy, K; Pishko, M. *Biomaterials* **2001**, 22, 929-941.

## VIII. Post-functionalization and Determination of Residual Hydrogel Thiol Content

The thiol content of cured hydrogels was determined by swelling gels in the presence of a small fluorogenic OND **S-6**, which we have previously described in our lab. This probe reacts with thiols to produce a fluorescent adduct (Figure S11, A). The intensity of fluorescence correlates linearly with the concentration of adduct **S-7**; this was demonstrated by incubation increasing concentrations of **S-6** with a large excess of N-acetyl cysteine to produce the standard curve shown in Figure S11, B. Thus, the concentration of reagent **S-6** in solution can be determined by quenching with thiol. Similarly, reagent **S-6** can be used to quantify thiol in solution.

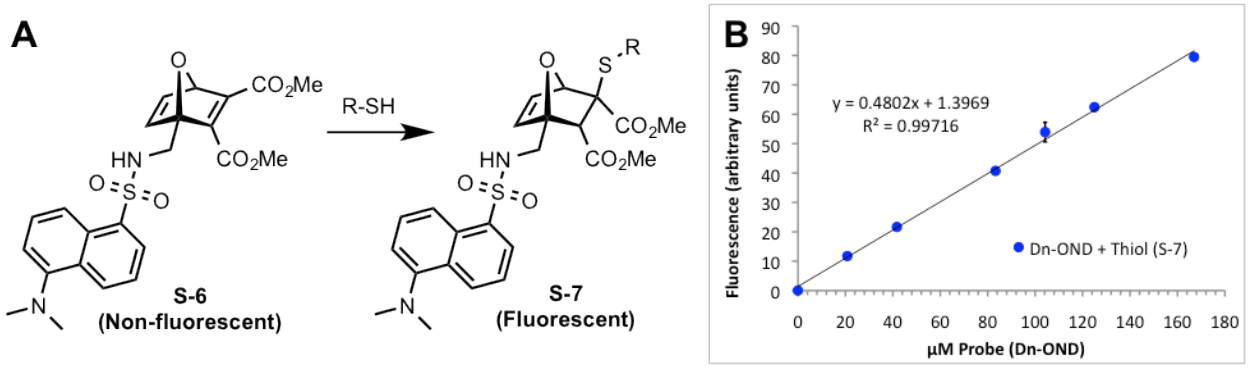


**Figure S11.** Quantitation of fluorogenic OND-thiol adduct concentration as a means of determining thiol concentration. (A) Fluorogenic OND **S-6** reacts with thiols to yield a fluorescent product. (B) A linear correlation with thiol adduct concentration and measured fluorescence is observed.

Based on cargo diffusion studies (*vide infra*, section X of this document), we expected that probe **S-6** should easily permeate the hydrogel network under swelling conditions and react with accessible residual thiols present in the gel network. In order to test this hypothesis, 60 µL hydrogels were freshly prepared from 4-PEG-SH macromer and either linkers **8** or **7a** as described in section III of this document. After curing for 20 minutes at room temperature, 3 mL of pH 7.4 0.1M PBS buffer containing 200 µM probe **S-6** was added, and the gel was swelled at 4 °C for 18 hours. To account for hydrolytic degradation of our thiol probe during incubation, a sample was prepared with **S-6** in buffer alone (lacking 4-PEG-SH and bis-OND linkers). After swelling, the gels were observed under long-wave ultraviolet light to reveal strongly fluorescent gels and weakly fluorescent

supernatants (Figure S12). The control revealed that a small amount of fluorescence was present after incubation in the absence of thiol due to hydrolytic degradation of the linker. Presumably the fluorescence in the supernatant of samples containing gels is due to soluble fraction of 4-PEG-SH macromer and oligomers not incorporated into the gel network.

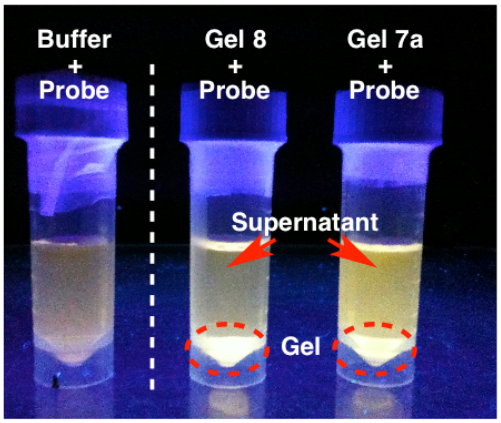


**Figure S12.** Probe **S-6** in pH 7.4 PBS incubated for 18 hours at 4 °C in buffer alone (left), or in the presence of a 60 µL PEG-OND hydrogels formed with linker **8** (middle), and **7a** (right). Fluorescent gel and supernatant indicate residual 4-PEG-SH thiols are accessible post-gelation for further modification.

In order to calculate the amount of residual thiol present in the soluble fraction, aliquots of the supernatant were removed and fluorescence was measured. Thiol content of the soluble fraction was determined by interpolation using the standard curve shown in figure S11 after accounting for fluorescence due to hydrolytic degradation. The concentration of thiol present in the supernatant was found to be 2.1 ± 0.4% and 8.1 ± 3.2% of the input thiol for the gels prepared from linker **8** and **7a** respectively. This amount corresponds well with the soluble fraction (soluble fraction = 1 – gel fraction) determined from swelling experiments (see Table 1 of main text). To determine residual thiol content present in gels, aliquots of the supernatant were quenched with a large excess (10 mM) of N-acetyl cysteine and the increase in fluorescence was measured to determine the amount of unreacted **S-6** remaining in the supernatant. Accounting for the amount of probe already consumed by reaction with soluble fraction thiols and by hydrolytic degradation, the amount of residual thiol accessible for post-modification present in the gel was calculated as 13.4 ± 1.4% and 10.8 ± 2.4% of the initial thiol content of input macromer (average of 11.8 ± 3.3 for both sets of gels prepared from linkers **7a** and **8**).

**Table S3.** Residual Thiol Content of Swelled Hydrogels

| Linker | Sol Fraction % Residual Thiol | Gel Fraction % Residual Thiol |
|---|---|---|
| **7a** | 8.1 ± 3.2 | 10.8 ± 2.4 |
| **8** | 2.1 ± 0.4 | 12.8 ± 2.2 |

These results demonstrate the presence of network defects, and depicted in Scheme 3 of the main text, and demonstrates that thiols are accessible in these networks for post-functionalization purposes. This feature may be useful in potential applications such as 3-D tissue culture.

## IX. Monitoring Erosion of Swollen Hydrogels

*IX.1. Dye labeling of 4-PEG-SH (10K)*

14.8 mg 4-PEG-SH macromer (5.032 μmol thiol) was weighed into a tared vial in a glove box under inert atmosphere (<10 ppm $O_2$) and dissolved in 191 μL dry acetonitrile. Less than 1 μL of $Et_3N$ was added followed by dropwise addition of 202 μL 0.74 mM BODIPY-FL maleimide (0.151 μmol, 3% of thiol content) in acetonitrile over 10 minutes. The resulting neon-green solution was stirred at room temperature wrapped in foil for 2 hours, and then condensed under vacuum to dryness. This residue was redissolved at 3.76 wt% PEG in pH 7.2 100 mM phosphate buffered saline for use in hydrogel formation.

**Scheme S3.** Labeling of 4-PEG-SH macromer with BODIPY-FL maleimide erosion probe.

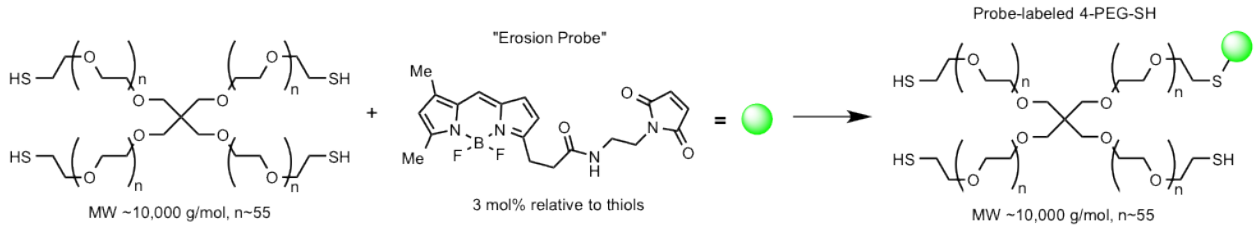


Conjugation of the erosion probe to the 4-PEG-SH macromer was verified by gel permeation chromatography (GPC) analysis with refractive index detector and diode array detector at 504 nm (Figure S13).

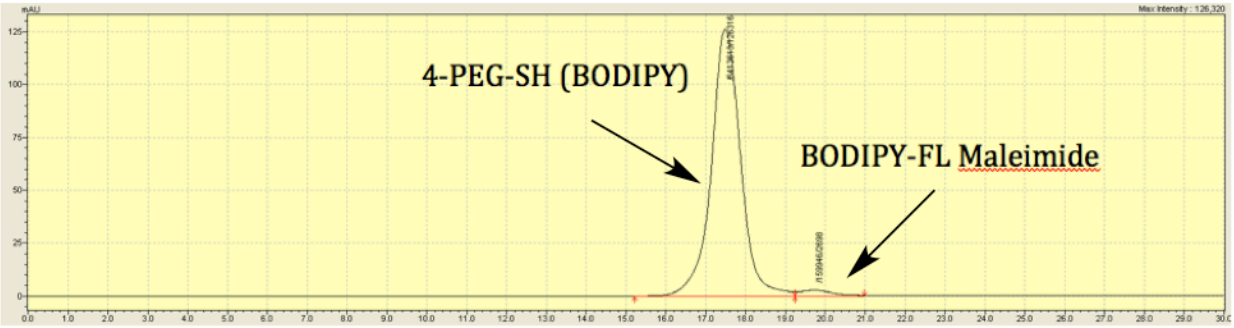


**Figure S13.** GPC analysis of BODIPY FL maleimide-labeled 4-PEG-SH macromer.

Labeling reactions in which a solution of 4-PEG-SH in acetonitrile was added to BODIPY FL maleimide at 25 mM in DMSO were also performed. While complete consumption of BODIPY FL maleimide was observed in these reactions by GPC analysis, this protocol led to poorly controlled labeling, resulting in a large fraction of multiply-labeled 4-PEG-SH macromer. This material yielded gels that release a large fraction of dye within the first 24 hours, and release of up to 50% of dye from non-degradable gels formed with linker **8** and upon storage of degradable gels at 4 °C (in the absence of gel degradation). Controlled addition of the erosion probe to a solution containing a large excess of thiol is necessary in order to obtain clean labeling of the macromer. Finally, attempted labeling reactions in methanol in the presence of catalytic sodium methoxide resulted in poor conversions, most likely due to methanolysis of the maleimide reactive group during the course of the reaction.

*IX.2. Monitoring erosion of hydrogels*

The 3.76 wt% solution of BODIPY-labeled 4-PEG-SH prepared above was used to form hydrogels using a method identical to unlabeled gels. Briefly, BODIPY-labeled 4-PEG-SH was combined with DMSO stocks of multivalent ONDs at equimolar concentration of thiol and electrophile. All reactions yielded self-supporting gels within one minute after mixing the two components at room temperature. These gelations were carried out in an oxygen-free environment and gels were allowed to set for 20 minutes at room temperature prior to dilution with 3 mL of swelling buffer (variable composition, as described in main text). The absorbance of the supernatant at 504 nm was measured immediately to obtain a baseline measurement (t = 0 hours), and the samples were placed into a 37 °C incubator.

The absorbance of the swelling supernatant was monitored periodically by removal of 1 mL of buffer into a cuvette and measuring absorbance of the sample at 504 nm. The supernatant was then returned to the gel sample at 37 °C. This process was repeated for each sample until gel degradation was complete and the absorbance at 504 nm stabilized (100% dye released). In order to estimate the fraction of dye released from the non-degradable gel formed with bis-EONB **8**, a mock endpoint sample consisting of BODIPY-labeled 4-PEG-SH diluted to 3.5 wt% was prepared, and the absorbance at 504 nm was measured. This value was taken as the 100% dye released point. The absorbance values collected over the course of the experiment were divided by the absorbance value measured after gel disintegration to obtain fractional dye release versus time. Each erosion experiment was run with duplicate gel samples for each condition tested, and the experiment was repeated (duplicate of duplicates).

*IX.3. GPC analysis of supernatants*

Additional gel samples formed with linker **7b** were prepared for the purpose of analyzing the contents of the supernatant during erosion. These samples were swelled in Milli-Q ultrapure water and incubated at 37 °C. At various time points during the erosion experiment, the supernatant was removed and dried in vacuum. The residue was taken up in DMF containing 0.1% LiBr and analyzed by gel permeation chromatography. Combinations of monomeric and oligomeric species of PEG macromer were observed. To compare composition of supernatant contents at different stages of erosion, the supernatant was removed and replaced by fresh swelling supernatant. After the desired degree of erosion, this supernatant was also collected for analysis. These supernatant "snapshots" were compared to a sample that did not undergo supernatant changes during erosion (Figure S14).

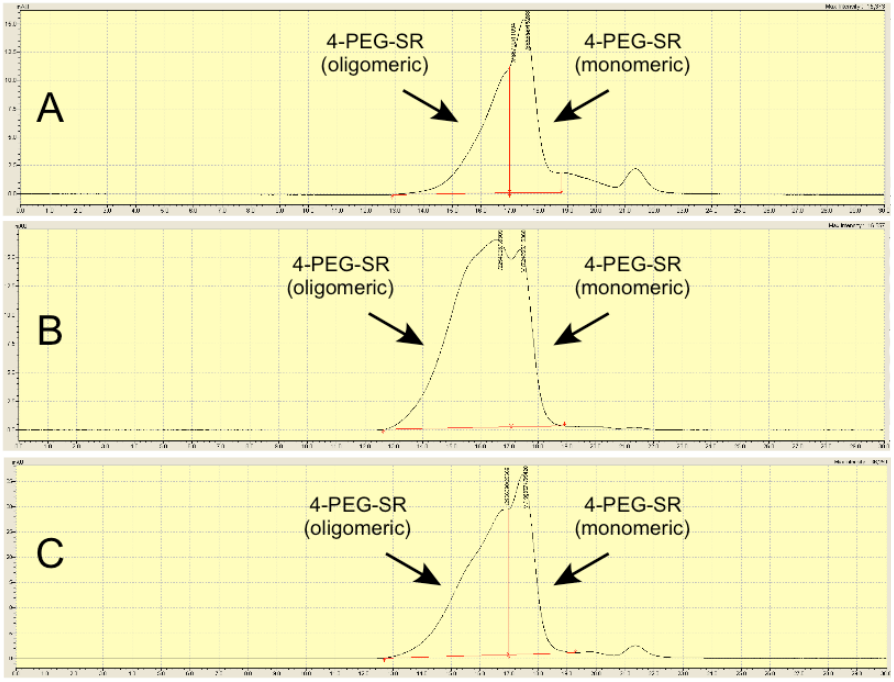


**Figure S14.** GPC analysis of supernatant (swelling buffer) of BODIPY-labeled 3.5 wt% hydrogel formed with linker **7b**. (A) 64 hours of incubation at 37 °C, gel still intact; (B) Sample from A after 180 hours at 37 °C, post-disintegration of gel. (C) Sample after 180 hours at 37 °C, post-disintegration of gel, no buffer exchanges.

GPC analysis was also used to help identify the fragments eluting from non-degradable gels formed with linker **8** (Figure S15).

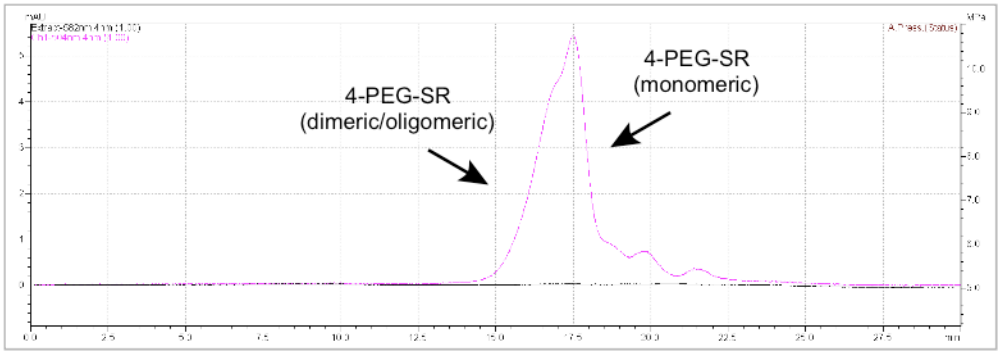


**Figure S15.** GPC analysis of supernatant (swelling buffer) of BODIPY-labeled 3.5 wt% hydrogel formed with linker **8** after 72 hours of incubation at 37 °C.

*IX.4. Monitoring loss of gel mass over time for selected gel compositions*

In order to probe the effect of erosion probe dye labeling on gel erosion rate, hydrogels were prepared with 4-PEG-SH macromer that was unlabeled with BODIPY erosion probe. Briefly, 200 µL gels were prepared by addition of 186 µL 3.76 wt% 4-PEG-SH macromer solution to 14 µL of a solution of bis-ONDs **7a** or **7b** in DMSO to yield a final composition of 3.5 wt% 4-4-PEG-SH macromer with 7% DMSO (v/v) and a 1:1 ratio of thiol:OND electrophile. The samples were mixed briefly with a pipet. Self-supporting gels

were observed by the inversion test within one minute, but were allowed to stand at room temperature for 20 minutes. The mass of the cured gel was measured before suspending the samples in 6 mL of pH 7.4 0.1M PBS buffer and placing in a 37 °C incubator. At various time points, the gels were briefly removed to room temperature, excess buffer was slowly poured off and wicked away with the edge of a Kimwipe delicate task wipe without touching the gel sample. The mass of the gel was measured, and 6 mL fresh buffer (pre-warmed to 37 °C) was added before returning the sample to 37 °C incubation. This process was continued until no gel remained. The mass of the hydrogel remaining at a given time point over the mass of the cured gel was plotted vs. time (Figure S16).

For less stable gel formations, we observe a decrease in stability of hydrogels prepared with erosion probe-labeled 4-PEG-SH macromer (Figure S16, B). This is consistent with the expectation that reducing the number of available thiol end-groups on the 4-PEG-SH macromer will lead to a lower cross-link density in the resulting gels, and produce gels that are expected to degrade sooner at a given temperature. We observe reasonable agreement of degradation times for gels formed with either unlabeled 4-PEG-SH macromer or macromer with 3% of its thiol end-groups labeled with a BODIPY erosion probe, particularly for more stable hydrogel formulations (as shown in Figure S16, A). Even so, the use of the probe-labeled macromer is still valuable for comparing erosion behaviors of gels under physiologically relevant conditions.

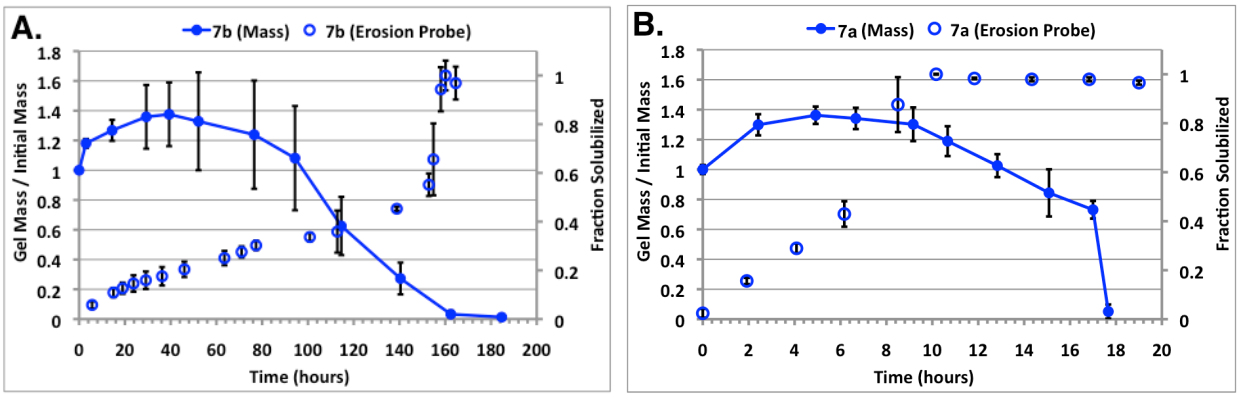


**Figure S16.** Comparison of hydrogel erosion for gels prepared with unmodified 4-PEG-SH macromer, or 4-PEG-SH with 3% of end groups modified with a BODIPY-FL erosion probe and bis-OND linkers **7b** or **7a** (A and B, respectively).

*IX.5. Time-lapse photography*

Time-lapse photography performed to observe reverse gelation upon prolonged heating of hydrogels under swelling conditions at different buffered pH values. Briefly, 4 x 600 µL hydrogels comprised of 3.5 wt% 4-PEG-SH + bis-OND **7a** in pH 7.4 100 mM potassium phosphate buffer containing 7% DMSO (v/v) were formed in glass culture tubes and allowed to set for 20 minutes. A non-degradable control gel from bis-EONB **8** was prepared. A glass bead (~160 mg, stained with blue Sharpie-brand marker to improve visibility) was placed carefully on top of each gel. The remainder of the culture tube was filled with ~7 of buffer at the appropriate pH (pH 1.2 HCl/NaCl with 1 mg/mL pepsin, pH 5.0 acetate, pH 7.4 phosphate buffered saline, and pH 9.0 sodium carbonate buffer). The non-degradable control was diluted with pH 7.4 phosphate buffer. The tubes were sealed with lab parafilm and incubated in a 37 °C oil bath. Photos were collected every 2 minutes for ~22 hours using Chronolapse software (v.1.0.4) and a Creative Labs webcam. Photographs were compiled in chronological order using iMovie software, with each photo occupying one 0.1s frame. The resulting video is available as Supporting Movie S2.

The time at which the glass bead reached the bottom of the tube was recorded. The span of time between when the first and last bead dropped was in reasonable agreement with the time of gel dissolution observed in erosion studies (Figure S17, red highlight).

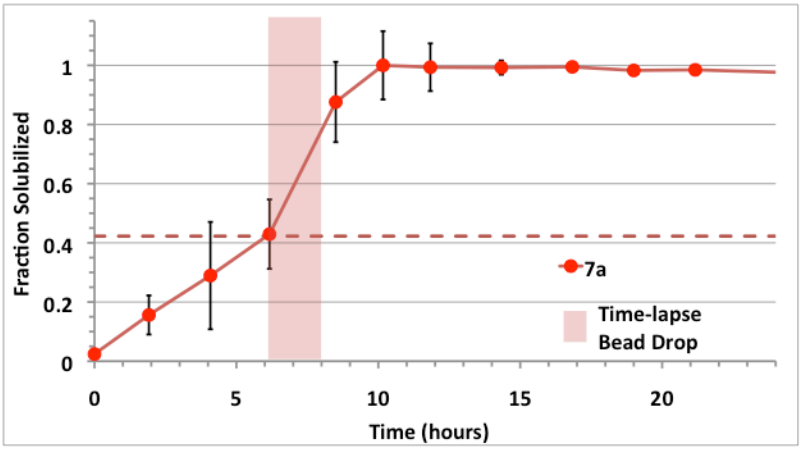


**Figure S17.** Overlay of erosion profile for PEG-OND (**7a**) hydrogel and time frame of gel collapse observed in time-lapse video (Supporting Movie S2).

## X. Comparison of Release of Entrained Cargo

*X.1.a. FITC labeling of bovine serum albumin  WT Qβ virus-like particles*

Bovine serum albumin (BSA) contains a conserved free cysteine (cys-34) that can be oxidized or capped as a mixed disulfide during isolation and storage of the protein. The thiol content of a stock of BSA (Sigma-Aldrich) was determined by the Ellman-Wilson assay[13] and found to be ~0.40 thiols per BSA protein. 500 μL of a 5 mg/mL solution of bovine serum albumin (BSA) in pH 8.5 100 mM sodium borate buffer was added slowly to a solution of fluorescein isothiocyanate (FITC, 2.5 μL 25.7 mM stock in DMSO, 0.07 equiv dye per primary amine on BSA) at room temperature and stirred for one hour (Scheme S4a). The resulting labeled protein was purified by 5 buffer exchanges with pH 7.4 100 mM phosphate buffered saline on Amicon size exclusion filter (MWCO 3 kDa).

*X.1.b. FITC labeling of BSA followed by capping of cysteine-34*

500 μL of a 7 mg/mL BSA solution in pH 8.0 phosphate buffer was added slowly to a solution of fluorescein isothiocyanate (FITC, 10 μL 25.7 mM stock in DMSO, 0.32 equiv dye per primary amine on BSA) at room temperature and rotated for one hour. At this time, 2 equivalents of N-ethylmaleimide were added to cap free cysteine-34, and rotated for an additional 1 hour at room temperature (Scheme S4b) before loading the entire reaction mixture onto a PD-10 desalting column equilibrated in pH 7.4 0.1 M PBS. A bright yellow band was eluted with 3.5 mL of PBS to yield labeled BSA at ~2 mg/mL. This solution was carried on to prepare hydrogels with entrained dye-labeled and thiol-depleted BSA (see section *X.2*).

[13] Wilson, J.M.; Wu, D.; Moth-DeGrood, R.; Hupe, D.J. *J. Am. Chem. Soc.* **1980**, *102*, 359-363.

**Scheme S4.** Labeling of bovine serum albumin with FITC.

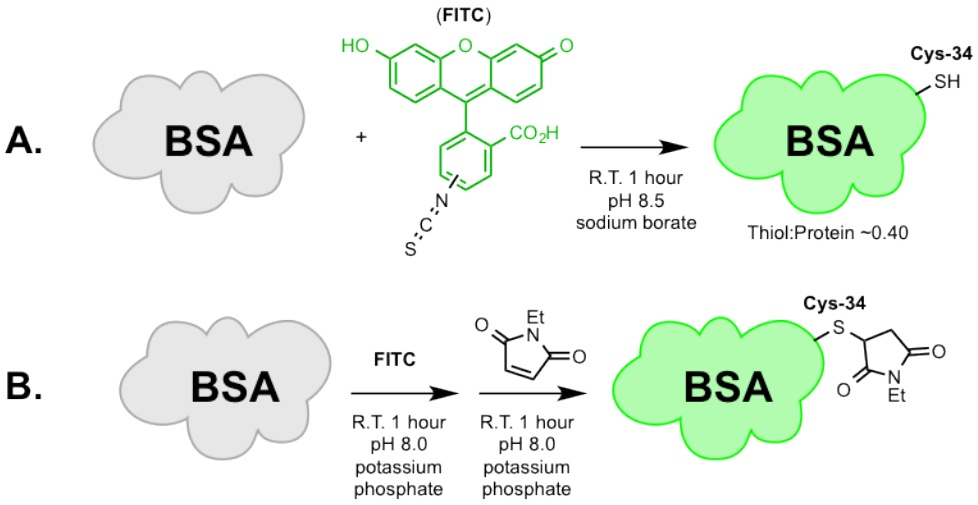


*X.1. FITC labeling WT Qβ virus-like particles*

Wild-type Qβ virus-like particles were obtained by recombinant expression in *E. coli* and purified by sucrose gradient using a previously described protocol.[14] 500 µL of a 4.6 mg/mL solution of wild-type Qβ virus-like particles in pH 8.5 100 mM sodium borate buffer was added slowly to a solution of fluorescein isothiocyanate (FITC, 20 µL 25.7 mM stock in DMSO, 0.19 equiv dye per primary amine on particle) at room temperature and stirred for one hour (Scheme S5). The resulting labeled protein nanoparticle was purified by 12 buffer exchanges with pH 7.4 100 mM phosphate buffered saline on Amicon size exclusion filter (MWCO 3 kDa).

**Scheme S5.** Labeling of Qβ virus-like particle with FITC using standard protocol.

[14] Fiedler, J.D.; Higginson, C.; Hovlid, M.L.; Kislukhin, A.A.; Castillejos, A.; Manzenrieder, F.; Campbell, M.G.; Voss, N.R.; Potter, C.S.; Carragher, B.; Finn, M.G. *Biomacromolecules*, **2012**, 13, 2339-2348.

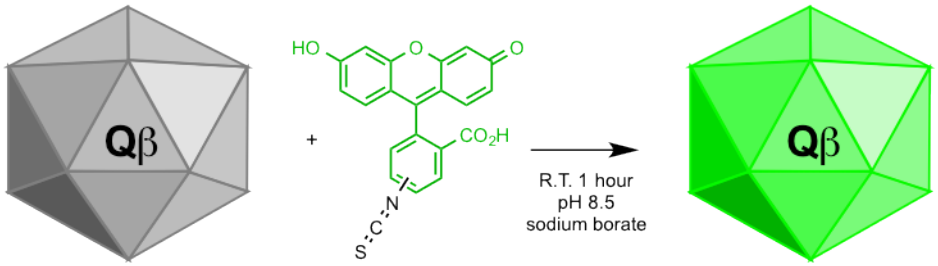


*X.2. Entrainment of cargos and monitoring release*

The labeled protein solutions prepared as described in the previous section were diluted three-fold with pH 7.4 100 mM phosphate buffer and used to dissolve the 4-PEG-SH macromer at 3.76 wt%. This solution was used in an identical manner as pure 4-PEG-SH solution for the purpose of forming PEG-OND hydrogels (Scheme S6). All samples formed self-supporting hydrogels within 1 min after mixing, as determined by the inversion test.

**Scheme S6.** Entrainment of fluorescent cargo in hydrogels for comparison of release rates.

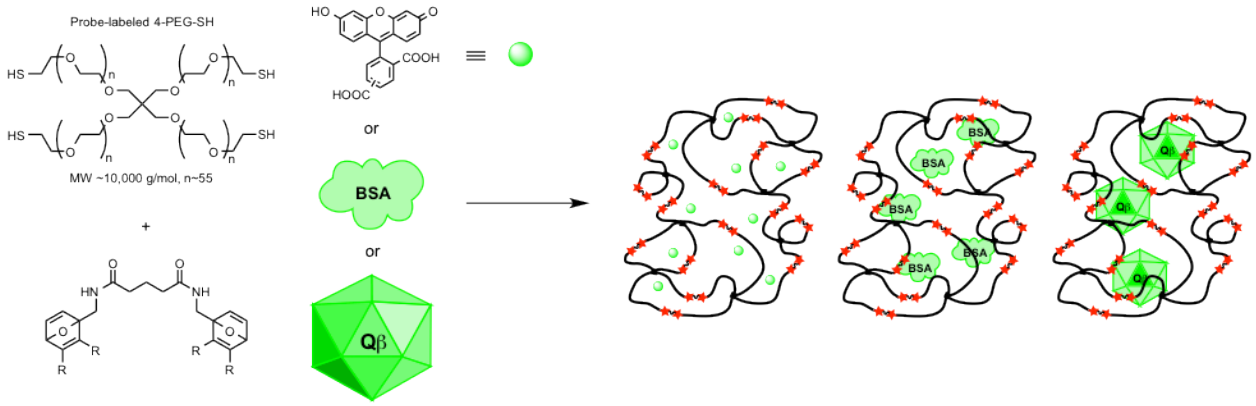


Three sets of three 60 μL gels were prepared using linkers **7a**, **7b**, and **8**, respectively. The first set contained 1 mM small molecule probe 5/6-carboxyfluorescein, while the second and third sets contained FITC labeled BSA and Qβ virus-like particle, respectively. The gels were allowed to set for 30 minutes at room temperature prior to dilution with 3 mL of pH 7.4 100 mM phosphate buffered saline. The samples were incubated at 37 °C and the increase in absorbance of the supernatant at 497 nm was monitored. The fraction of released dye was plotted against incubation time. Least-squares kinetic fitting to a first-order rate law was performed for release profiles obtained for

carboxyfluorescein cargo, and for the release of BSA from non-degradable PEG-EONB(**8**) hydrogel (Solver plug-in, Microsoft Excel).[5]

*X.3. Supplementary Note On Entrained Cargo Release Rates and Hydrogel Mesh Size*

The differences in release rates correlate well with the hydrodynamic radius of the entrained cargo relative to the mesh size of the hydrogels employed in these studies (See Table S2). The mesh size increases during the course of degradation, allowing materials that are otherwise unable to diffuse through the gel network to be released before complete disintegration of the gel. The hydrodynamic radii of encapsulated cargoes are 0.8 nm,[15] 3.48 nm,[16] and 14.5 nm[17] for carboxyfluorescein, bovine serum albumin, and wild-type Qβ virus-like particle, respectively. Smaller cargoes are able to diffuse out of the hydrogel network, with carboxyfluorescein diffusion occurring very rapidly, and BSA experiencing some hindrance. With an average mesh size of 14.0 ± 1.0 nm for equilibrium swelled hydrogels formed using linkers **7a**, **7b**, and **8**, it is clear that release of bacteriophage Qβ protein nanoparticles, with a diameter twice the average mesh size, should be significantly retarded and were observed to be directly dependent on hydrogel degradation.

Bovine serum albumin with ~0.4 thiols per protein present during entrainment/gelation produced hydrogels that released a fraction of protein cargo by diffusion, and the remaining fraction was found to be associated with the gel network. For non-degradable gels derived from bis-OND **8**, approximately 20% of the input BSA did not diffuse from the hydrogel (Figure S18, A). Similarly, roughly 20% of BSA in gels derived from linker **7b** was found be released with a slow rate similar to that observed in experiments with erosion-probe labeled macromers. This behavior may be useful in tuning the release rate of substrates that would otherwise diffuse freely from the network, as is observed in the case of BSA that is capped with N-ethylmaleimide prior to entrainment.

---

[5] Kemmer, G.; Keller, S. *Nat. Methods* **2010**, 5, 267-281.
[15] Banks, D; Fradin, C. *Biophys. J.* **2005**, 89, 2960-2970.
[16] Axelsson, I. *J Chromatogr. A* **1978**, 152, 21-32.
[17] Fiedler, J; Higginson, C; Hovlid, M; Kislukin, A; Castillejos, A; Manzenrieder, F; Campbell, M; Voss, N; Potter, C; Carragher, B; Finn, M. *Biomacromolecules* **2012**, 13, 2339-2348.

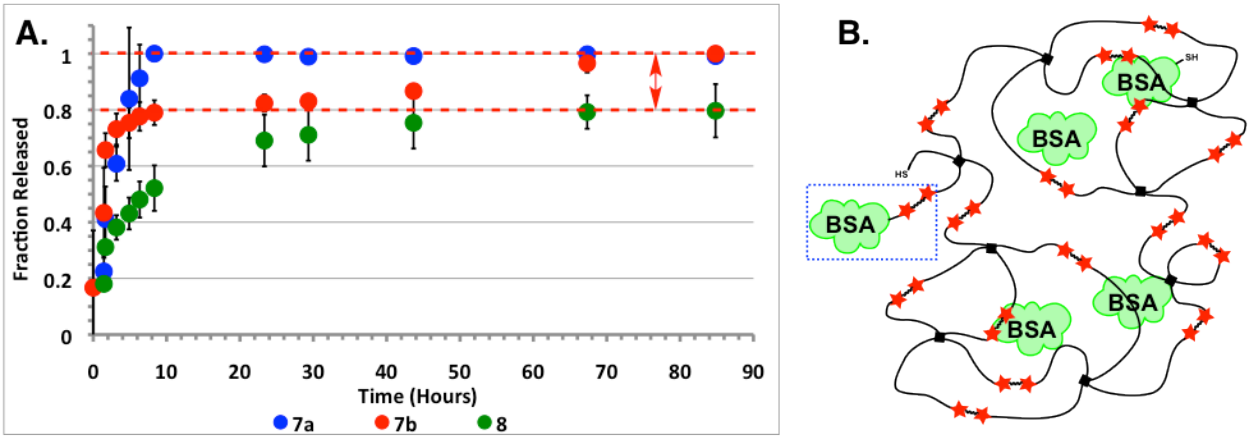


**Figure S18.** (A) Release of entrained FITC-labeled BSA with ~0.4 accessible thiols per protein from bis-OND hydrogels **7a**, **7b**, and **8**. Tracking the fraction of BSA released over time reveals that ~20% of BSA becomes tethered to the network (red dashed lines). (B) Cartoon representation of BSA entrained in bis-OND hydrogels and tethered to the network by reaction with terminal OND electrophiles (blue dotted box).

## XI. $^{1}H$ and $^{13}C$ NMR Spectra

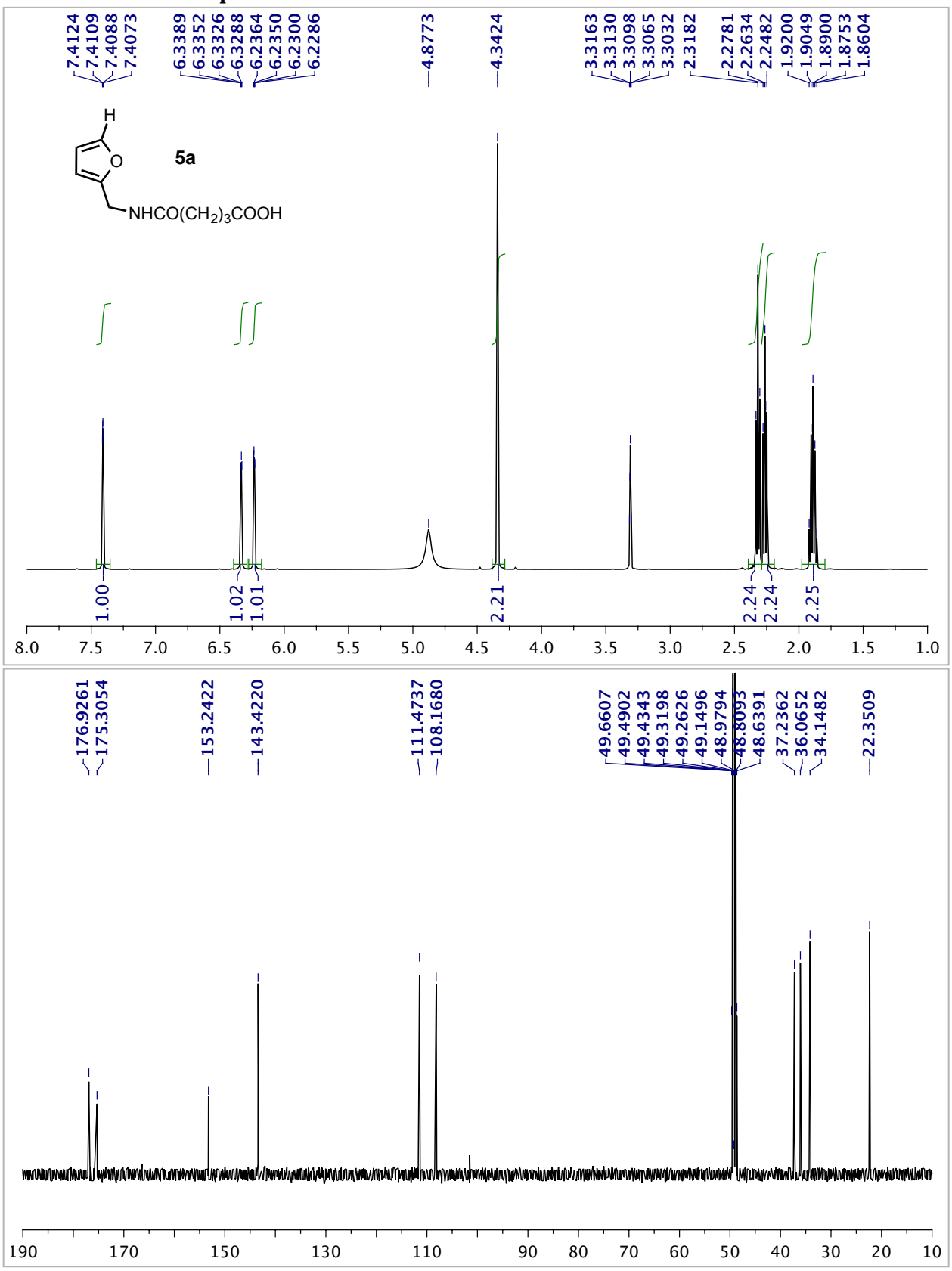

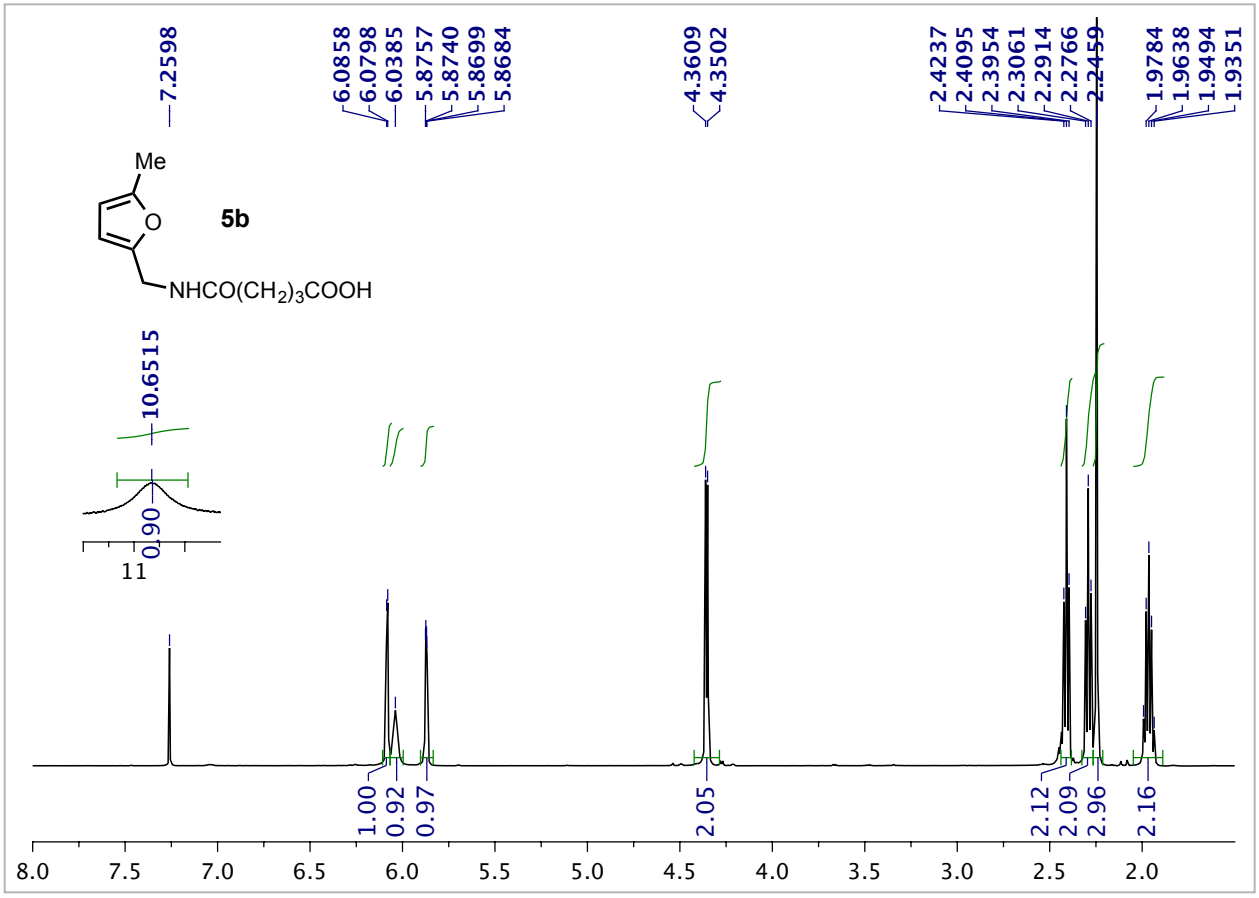
7.2598
6.0858
6.0798
6.0385
5.8757
5.8740
5.8699
5.8684
4.3609
4.3502
2.4237
2.4095
2.3954
2.3061
2.2914
2.2766
2.2459
1.9784
1.9638
1.9494
1.9351
Me
O
5b
NHCO(CH2)3COOH
10.6515
0.90
11
1.00
0.92
0.97
2.05
2.12
2.09
2.96
2.16
8.0
7.5
7.0
6.5
6.0
5.5
5.0
4.5
4.0
3.5
3.0
2.5
2.0

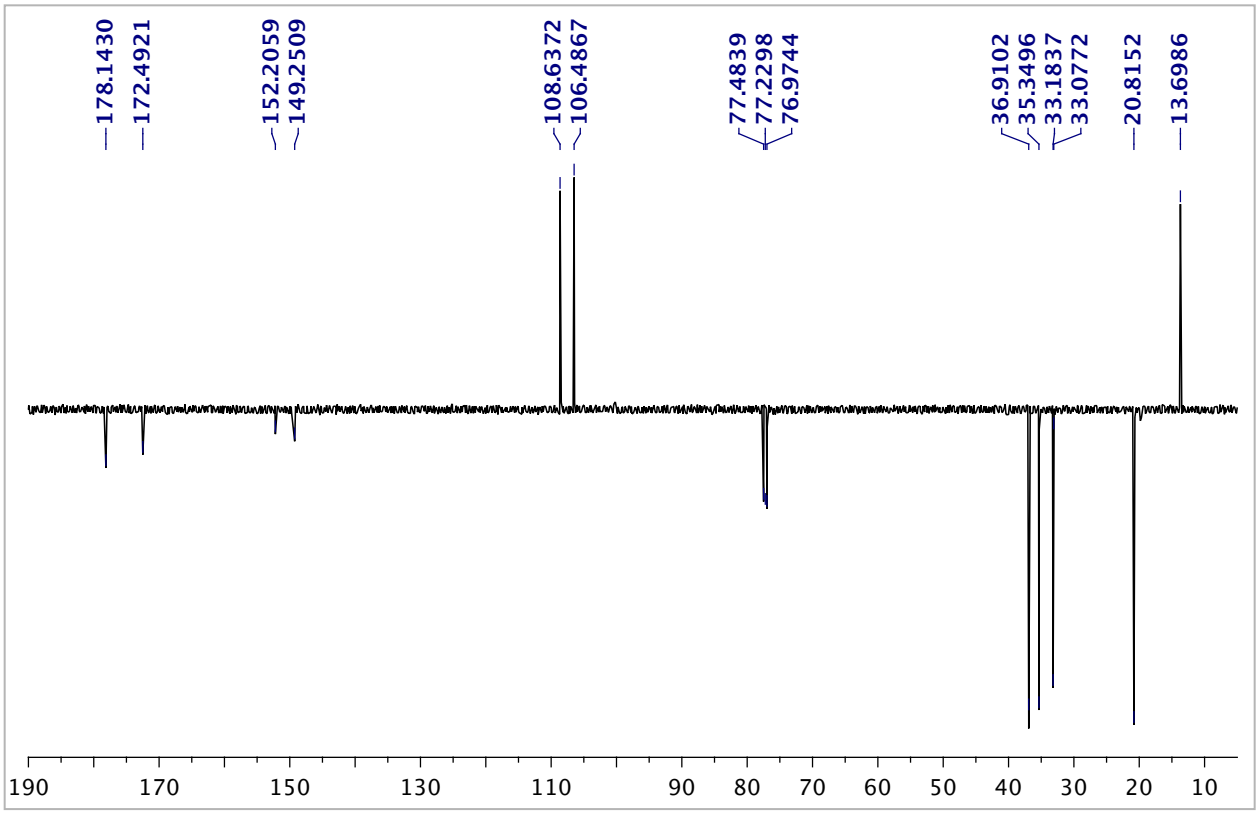
178.1430
172.4921
152.2059
149.2509
108.6372
106.4867
77.4839
77.2298
76.9744
36.9102
35.3496
33.1837
33.0772
20.8152
13.6986
190
170
150
130
110
90
80
70
60
50
40
30
20
10

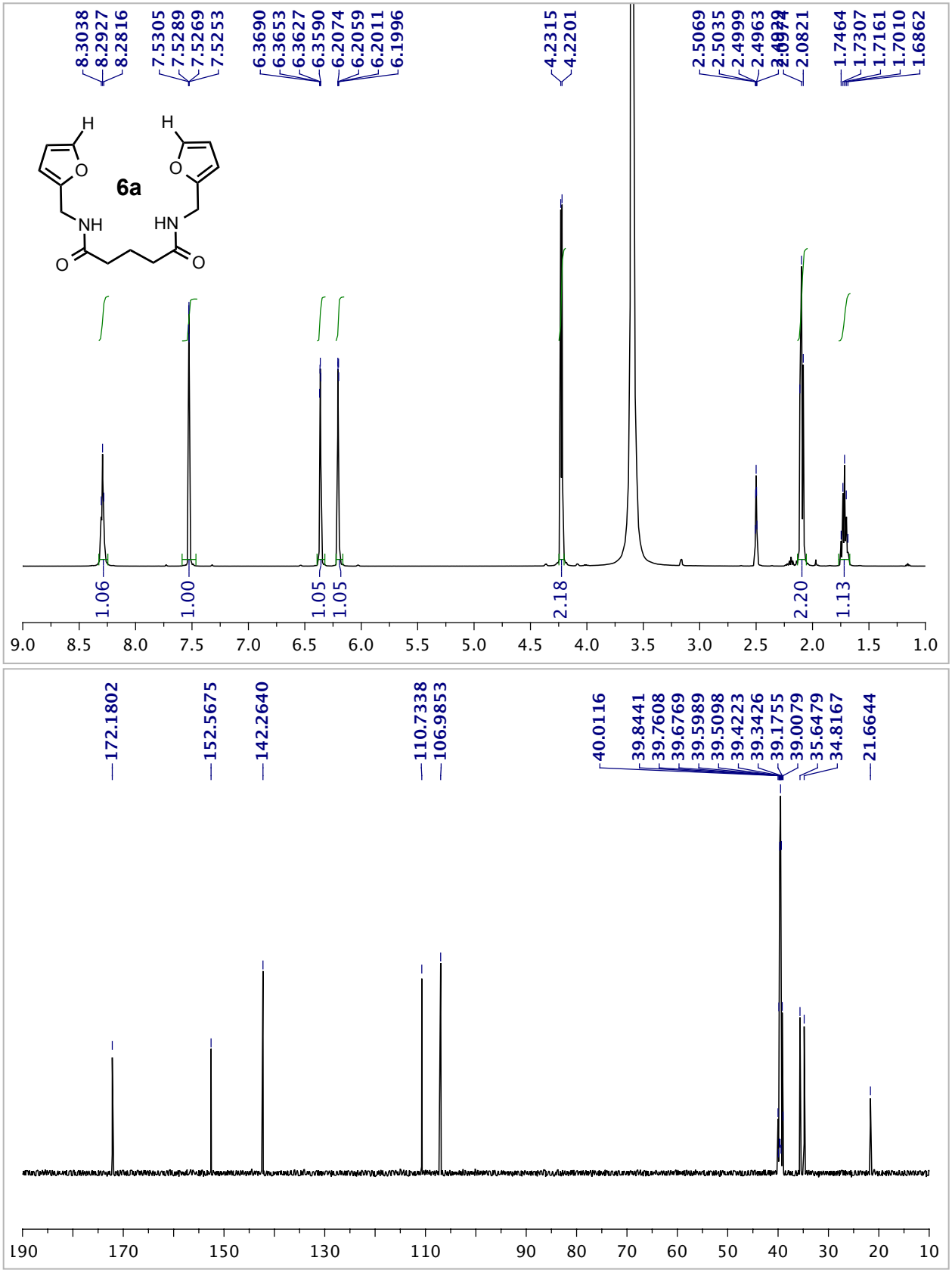
8.3038
8.2927
8.2816
7.5305
7.5289
7.5269
7.5253
6.3690
6.3653
6.3627
6.3590
6.2074
6.2059
6.2011
6.1996
4.2315
4.2201
2.5069
2.5035
2.4999
2.4963
2.0821
1.7464
1.7307
1.7161
1.7010
1.6862
6a
1.06
1.00
1.05
1.05
2.18
2.20
1.13
172.1802
152.5675
142.2640
110.7338
106.9853
40.0116
39.8441
39.7608
39.6769
39.5989
39.5098
39.4223
39.3426
39.1755
39.0079
35.6479
34.8167
21.6644

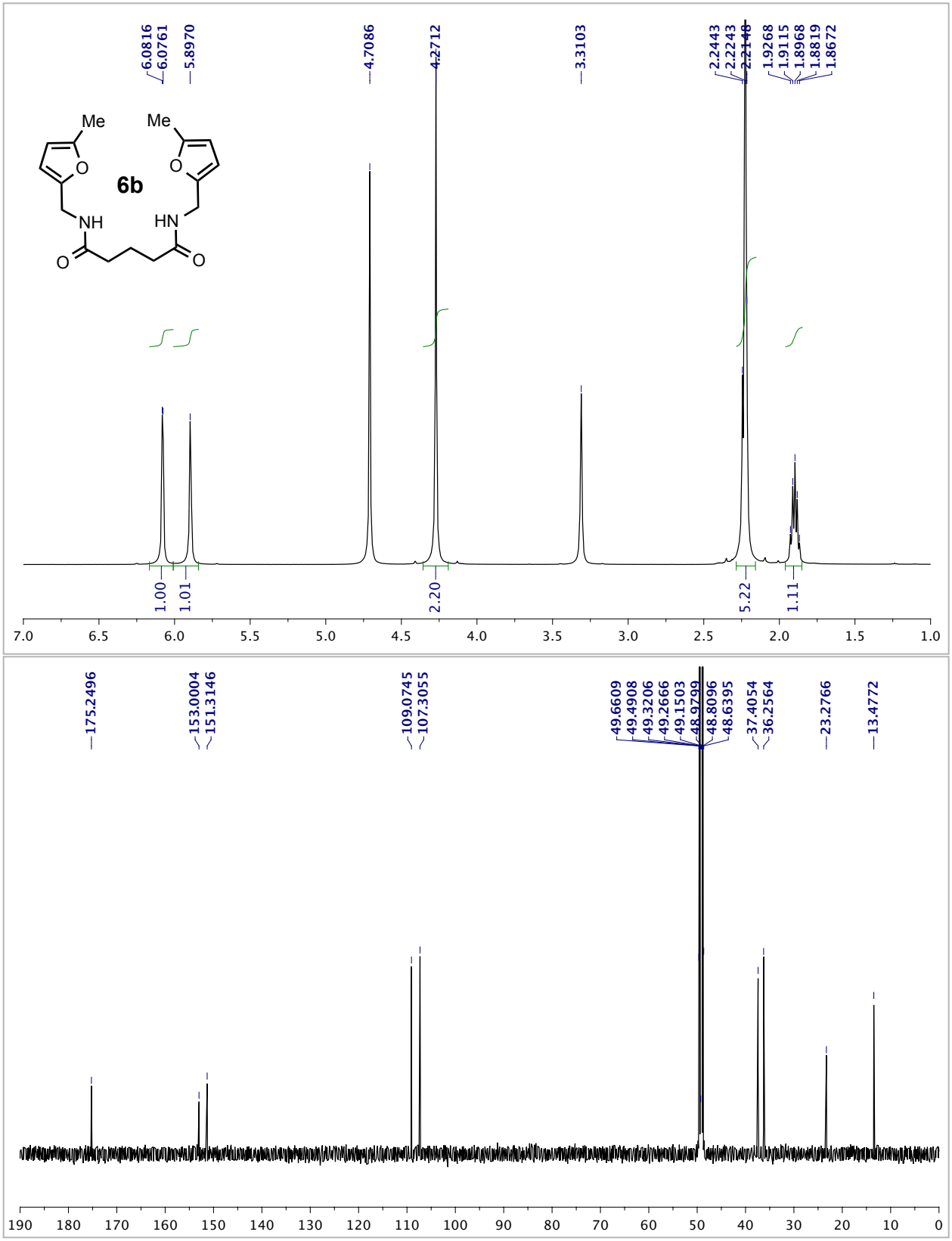
6.0816
6.0761
5.8970
4.7086
4.2712
3.3103
2.2443
2.2243
2.2148
1.9268
1.9115
1.8968
1.8819
1.8672
Me
Me
O
O
6b
NH
HN
O
O
1.00
1.01
2.20
5.22
1.11
7.0
6.5
6.0
5.5
5.0
4.5
4.0
3.5
3.0
2.5
2.0
1.5
1.0
175.2496
153.0004
151.3146
109.0745
107.3055
49.6609
49.4908
49.3206
49.2666
49.1503
48.9799
48.8096
48.6395
37.4054
36.2564
23.2766
13.4772
190
180
170
160
150
140
130
120
110
100
90
80
70
60
50
40
30
20
10
0

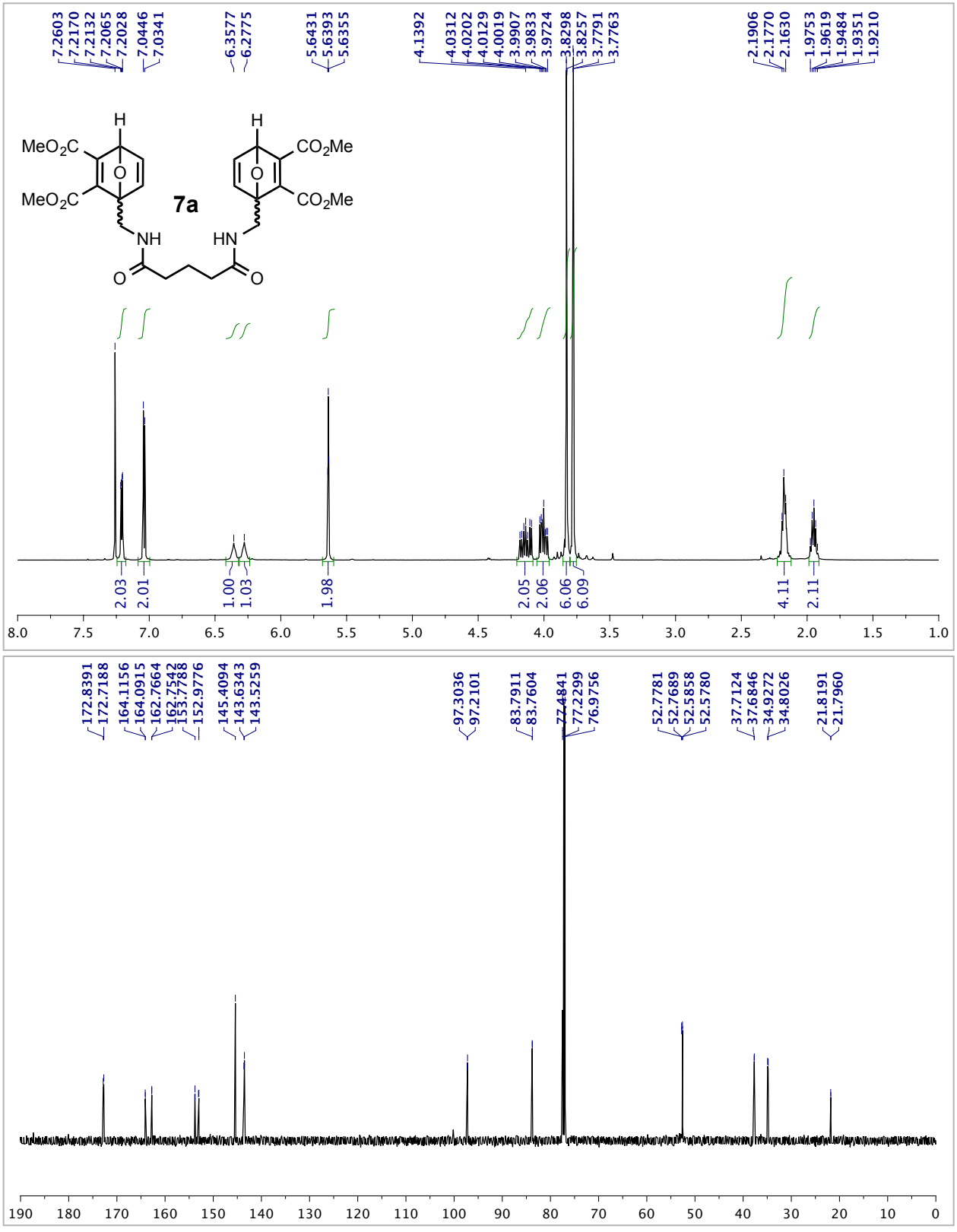
7.2603
7.2170
7.2132
7.2065
7.2028
7.0446
7.0341
6.3577
6.2775
5.6431
5.6393
5.6355
4.1392
4.0312
4.0202
4.0129
4.0019
3.9907
3.9833
3.9724
3.8298
3.8257
3.7791
3.7763
2.1906
2.1770
2.1630
1.9753
1.9619
1.9484
1.9351
1.9210
MeO2C
MeO2C
CO2Me
CO2Me
7a
NH
HN
2.03
2.01
1.00
1.03
1.98
2.05
2.06
6.06
6.09
4.11
2.11
172.8391
172.7188
164.1156
164.0915
162.7664
162.7542
153.7788
152.9776
145.4094
143.6343
143.5259
97.3036
97.2101
83.7911
83.7604
77.4841
77.2299
76.9756
52.7781
52.7689
52.5858
52.5780
37.7124
37.6846
34.9272
34.8026
21.8191
21.7960

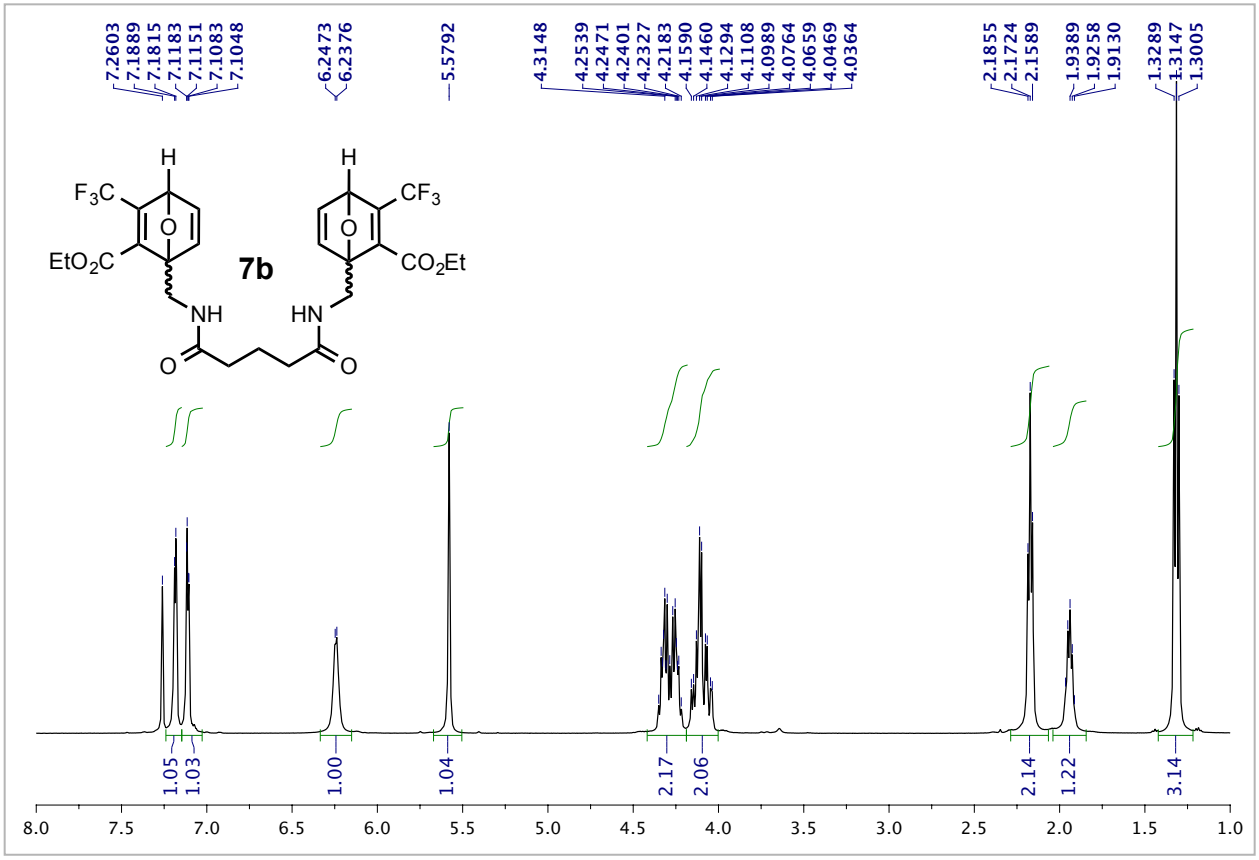
7.2603
7.1889
7.1815
7.1183
7.1151
7.1083
7.1048
6.2473
6.2376
5.5792
4.3148
4.2539
4.2471
4.2401
4.2327
4.2183
4.1590
4.1460
4.1294
4.1108
4.0989
4.0764
4.0659
4.0469
4.0364
2.1855
2.1724
2.1589
1.9389
1.9258
1.9130
1.3289
1.3147
1.3005
H
F3C
O
EtO2C
7b
NH
O
H
CF3
O
CO2Et
HN
O
1.05
1.03
1.00
1.04
2.17
2.06
2.14
1.22
3.14
8.0
7.5
7.0
6.5
6.0
5.5
5.0
4.5
4.0
3.5
3.0
2.5
2.0
1.5
1.0

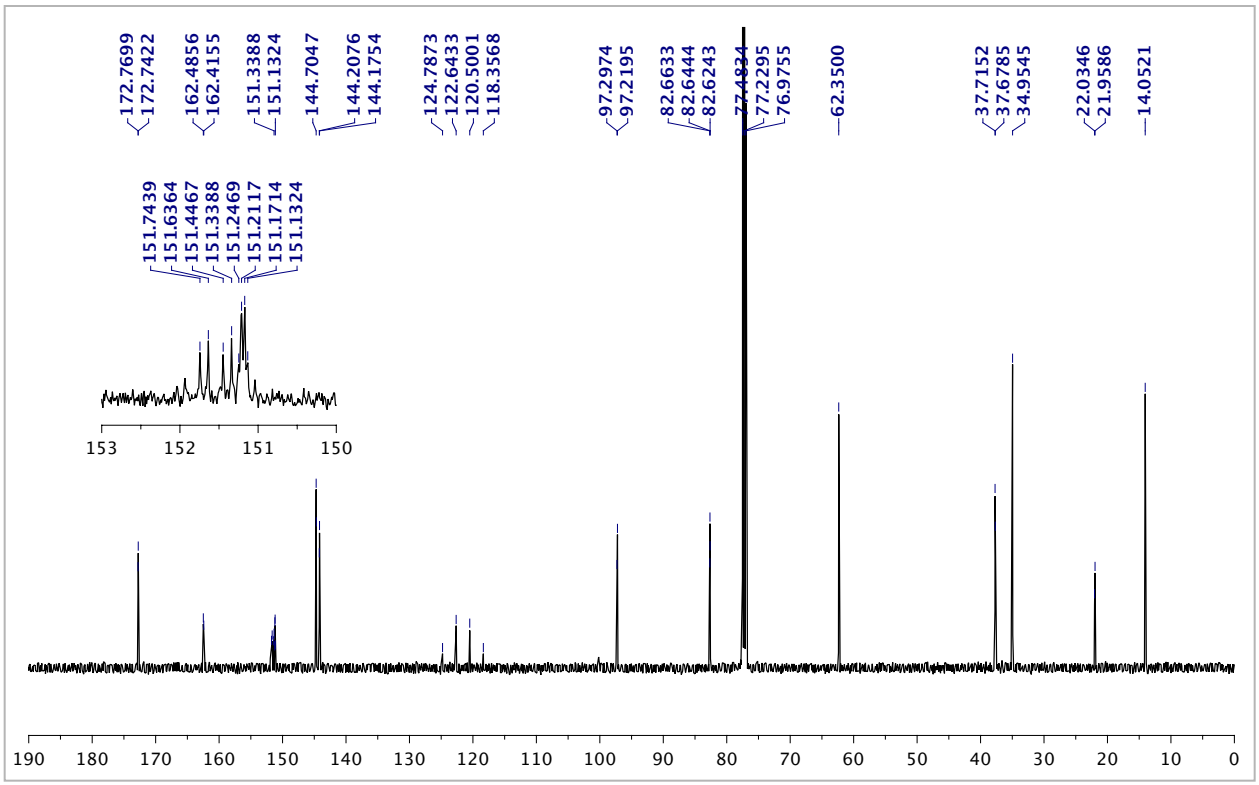
172.7699
172.7422
162.4856
162.4155
151.3388
151.1324
144.7047
144.2076
144.1754
124.7873
122.6433
120.5001
118.3568
97.2974
97.2195
82.6633
82.6444
82.6243
77.4834
77.2295
76.9755
62.3500
37.7152
37.6785
34.9545
22.0346
21.9586
14.0521
151.7439
151.6364
151.4467
151.3388
151.2469
151.2117
151.1714
151.1324
153
152
151
150
190
180
170
160
150
140
130
120
110
100
90
80
70
60
50
40
30
20
10
0

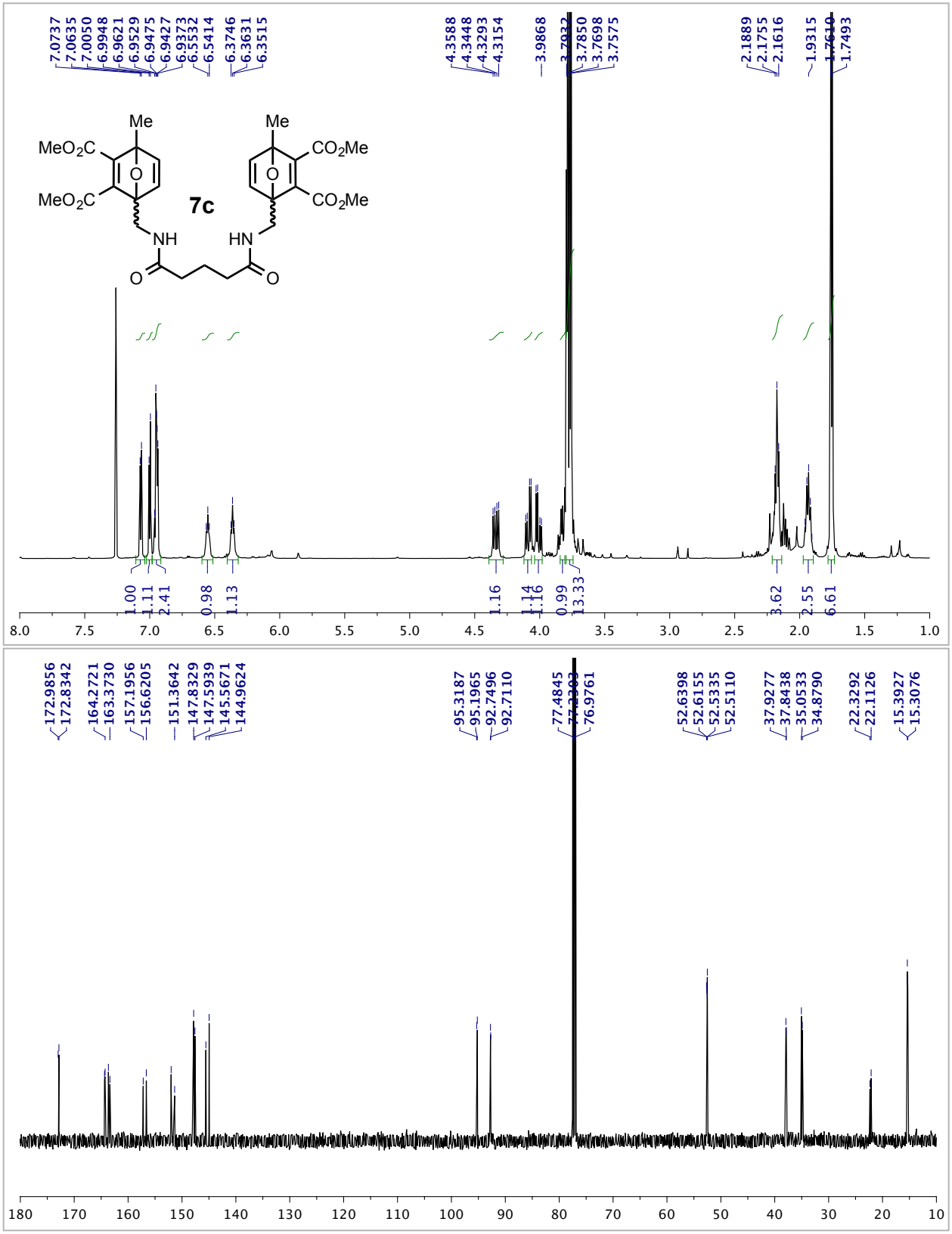
7.0737
7.0635
7.0050
6.9948
6.9621
6.9529
6.9475
6.9427
6.9373
6.5532
6.5414
6.3746
6.3631
6.3515
4.3588
4.3448
4.3293
4.3154
3.9868
3.7932
3.7850
3.7698
3.7575
2.1889
2.1755
2.1616
1.9315
1.7610
1.7493
Me
MeO2C
MeO2C
O
NH
O
7c
Me
CO2Me
CO2Me
O
HN
O
1.00
1.11
2.41
0.98
1.13
1.16
1.14
1.16
0.99
13.33
3.62
2.55
6.61
8.0
7.5
7.0
6.5
6.0
5.5
5.0
4.5
4.0
3.5
3.0
2.5
2.0
1.5
1.0
172.9856
172.8342
164.2721
163.3730
157.1956
156.6205
151.3642
147.8329
147.5939
145.5671
144.9624
95.3187
95.1965
92.7496
92.7110
77.4845
77.3303
76.9761
52.6398
52.6155
52.5335
52.5110
37.9277
37.8438
35.0533
34.8790
22.3292
22.1126
15.3927
15.3076
180
170
160
150
140
130
120
110
100
90
80
70
60
50
40
30
20
10

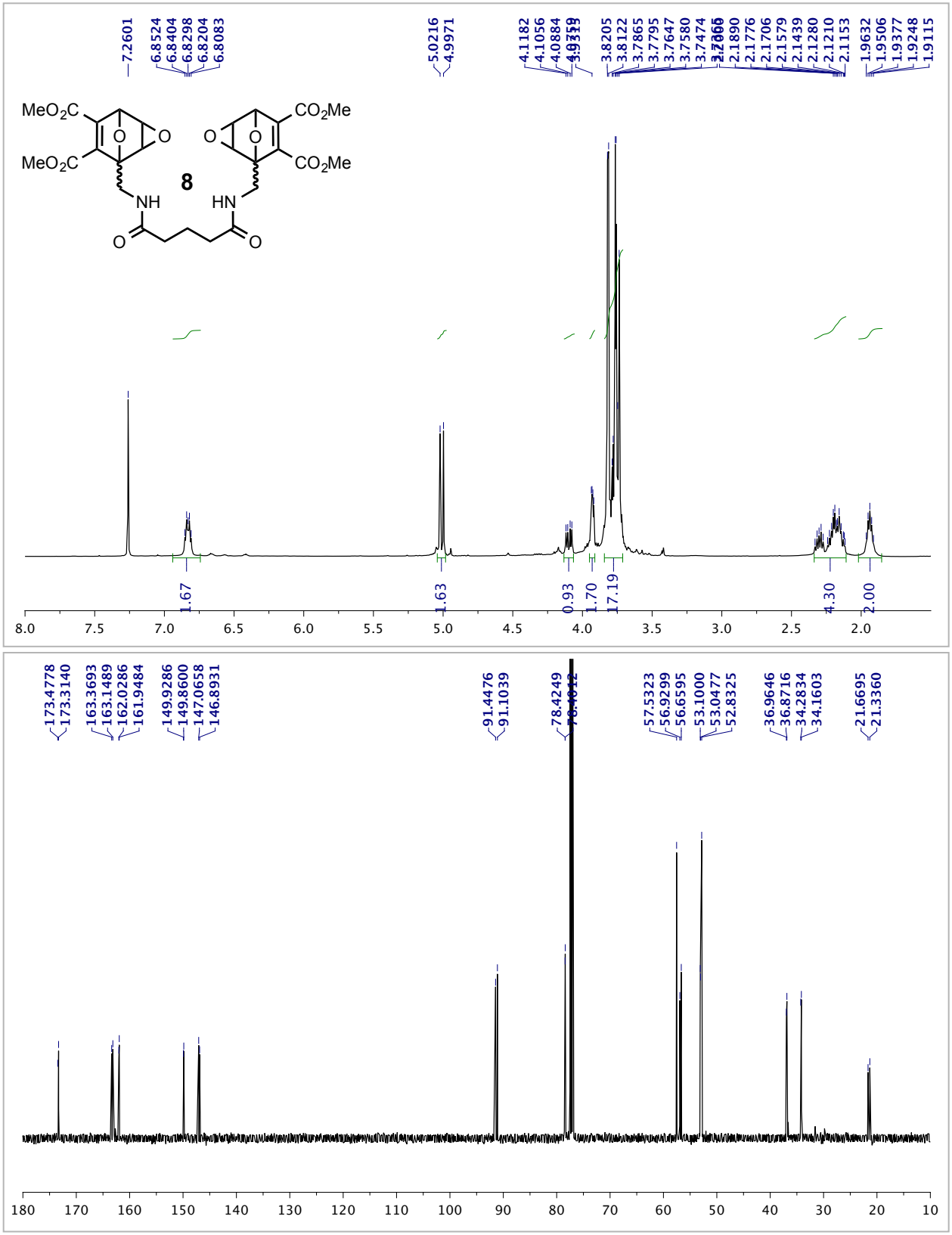
MeO2C
MeO2C
CO2Me
CO2Me
O
O
O
O
NH
HN
O
O
8
7.2601
6.8524
6.8404
6.8298
6.8204
6.8083
5.0216
4.9971
4.1182
4.1056
4.0884
3.8205
3.8122
3.7865
3.7795
3.7647
3.7580
3.7474
2.1890
2.1776
2.1706
2.1579
2.1439
2.1280
2.1210
2.1153
1.9632
1.9506
1.9377
1.9248
1.9115
1.67
1.63
0.93
1.70
17.19
4.30
2.00
8.0
7.5
7.0
6.5
6.0
5.5
5.0
4.5
4.0
3.5
3.0
2.5
2.0
173.4778
173.3140
163.3693
163.1489
162.0286
161.9484
149.9286
149.8600
147.0658
146.8931
91.4476
91.1039
78.4249
78.1612
57.5323
56.9299
56.6595
53.1000
53.0477
52.8325
36.9646
36.8716
34.2834
34.1603
21.6695
21.3360
180
170
160
150
140
130
120
110
100
90
80
70
60
50
40
30
20
10

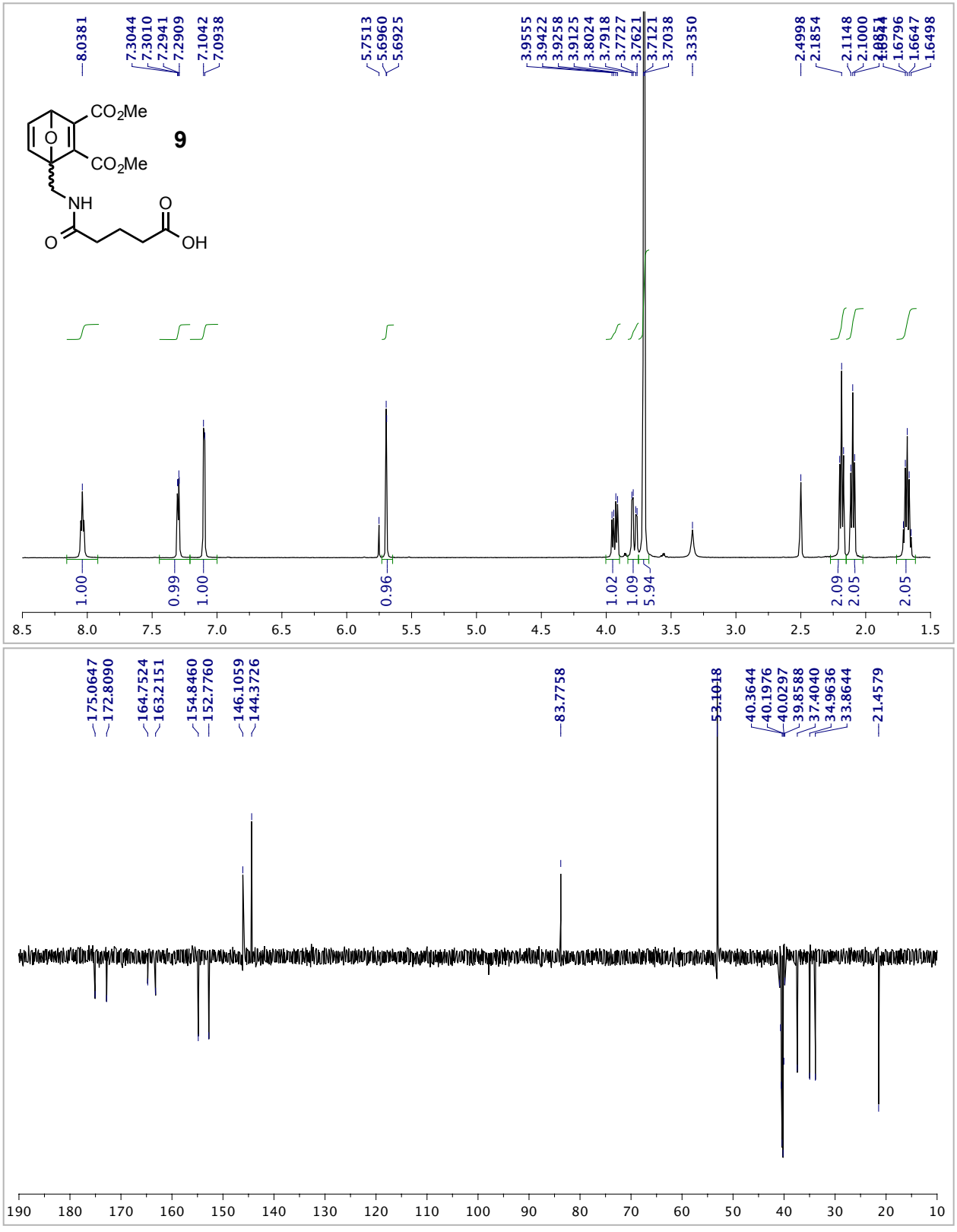
8.0381
7.3044
7.3010
7.2941
7.2909
7.1042
7.0938
5.7513
5.6960
5.6925
3.9555
3.9422
3.9258
3.9125
3.8024
3.7918
3.7727
3.7621
3.7121
3.7038
3.3350
2.4998
2.1854
2.1148
2.1000
1.6796
1.6647
1.6498
CO2Me
CO2Me
9
NH
O
O
OH
1.00
0.99
1.00
0.96
1.02
1.09
5.94
2.09
2.05
2.05
175.0647
172.8090
164.7524
163.2151
154.8460
152.7760
146.1059
144.3726
83.7758
53.1018
40.3644
40.1976
40.0297
39.8588
37.4040
34.9636
33.8644
21.4579

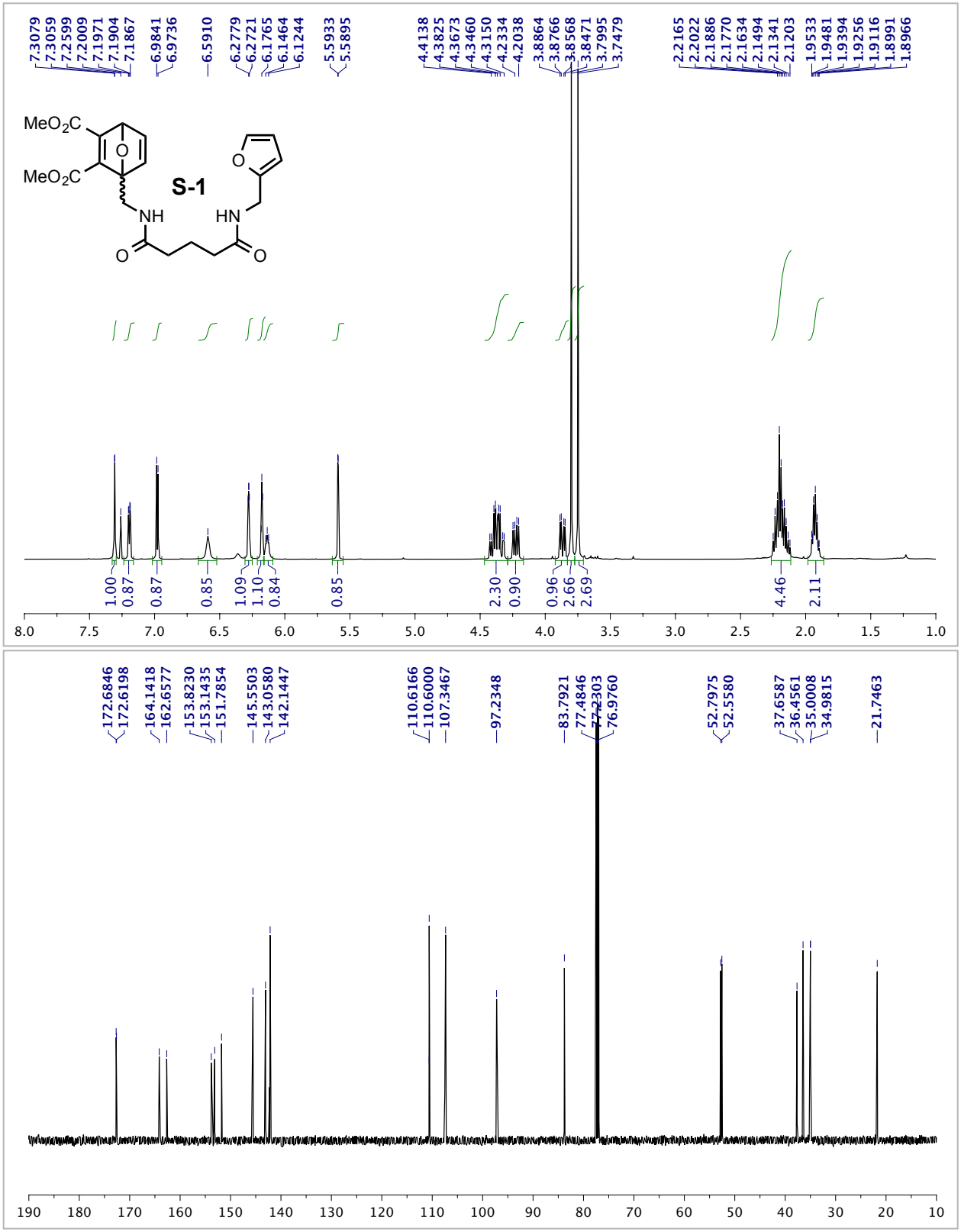
MeO2C
MeO2C
O
NH
HN
O
O
O
O
S-1
7.3079
7.3059
7.2599
7.2009
7.1971
7.1904
7.1867
6.9841
6.9736
6.5910
6.2779
6.2721
6.1765
6.1464
6.1244
5.5933
5.5895
4.4138
4.3825
4.3673
4.3460
4.3150
4.2334
4.2038
3.8864
3.8766
3.8568
3.8471
3.7995
3.7479
2.2165
2.2022
2.1886
2.1770
2.1634
2.1494
2.1341
2.1203
1.9533
1.9481
1.9394
1.9256
1.9116
1.8991
1.8966
1.00
0.87
0.87
0.85
1.09
1.10
0.84
0.85
2.30
0.90
0.96
2.66
2.69
4.46
2.11
8.0
7.5
7.0
6.5
6.0
5.5
5.0
4.5
4.0
3.5
3.0
2.5
2.0
1.5
1.0
172.6846
172.6198
164.1418
162.6577
153.8230
153.1435
151.7854
145.5503
143.0580
142.1447
110.6166
110.6000
107.3467
97.2348
83.7921
77.4846
77.2303
76.9760
52.7975
52.5580
37.6587
36.4561
35.0008
34.9815
21.7463
190
180
170
160
150
140
130
120
110
100
90
80
70
60
50
40
30
20
10

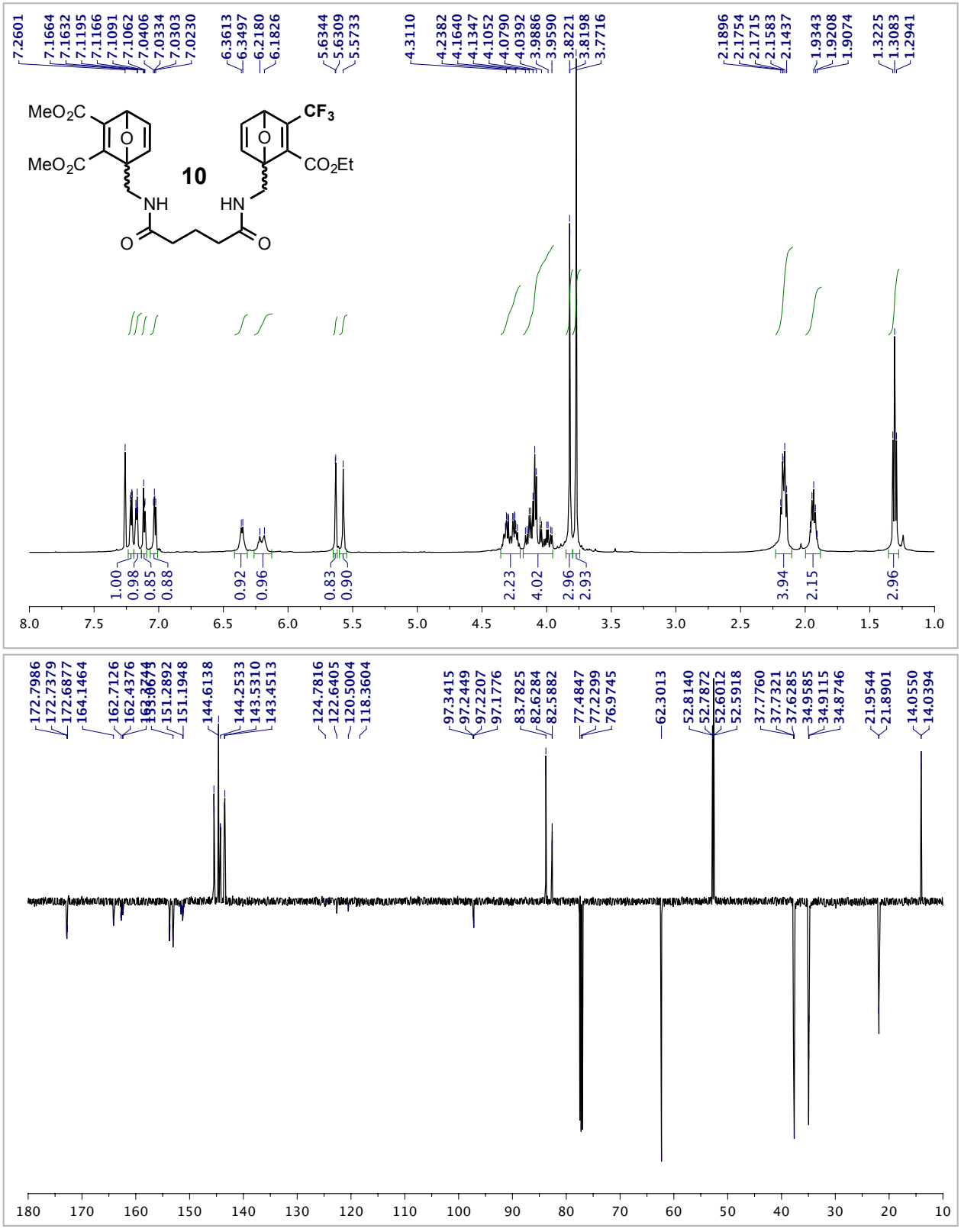
MeO2C
MeO2C
CF3
CO2Et
10
NH
HN
O
O
O
O
7.2601
7.1664
7.1632
7.1195
7.1166
7.1091
7.1062
7.0406
7.0334
7.0303
7.0230
6.3613
6.3497
6.2180
6.1826
5.6344
5.6309
5.5733
4.3110
4.2382
4.1640
4.1347
4.1052
4.0790
4.0392
3.9886
3.9590
3.8221
3.8198
3.7716
2.1896
2.1754
2.1715
2.1583
2.1437
1.9343
1.9208
1.9074
1.3225
1.3083
1.2941
1.00
0.98
0.85
0.88
0.92
0.96
0.83
0.90
2.23
4.02
2.96
2.93
3.94
2.15
2.96
8.0
7.5
7.0
6.5
6.0
5.5
5.0
4.5
4.0
3.5
3.0
2.5
2.0
1.5
1.0
172.7986
172.7379
172.6877
164.1464
162.7126
162.4376
151.2892
151.1948
144.6138
144.2533
143.5310
143.4513
124.7816
122.6405
120.5004
118.3604
97.3415
97.2449
97.2207
97.1776
83.7825
82.6284
82.5882
77.4847
77.2299
76.9745
62.3013
52.8140
52.7872
52.6012
52.5918
37.7760
37.7321
37.6285
34.9585
34.9115
34.8746
21.9544
21.8901
14.0550
14.0394
180
170
160
150
140
130
120
110
100
90
80
70
60
50
40
30
20
10

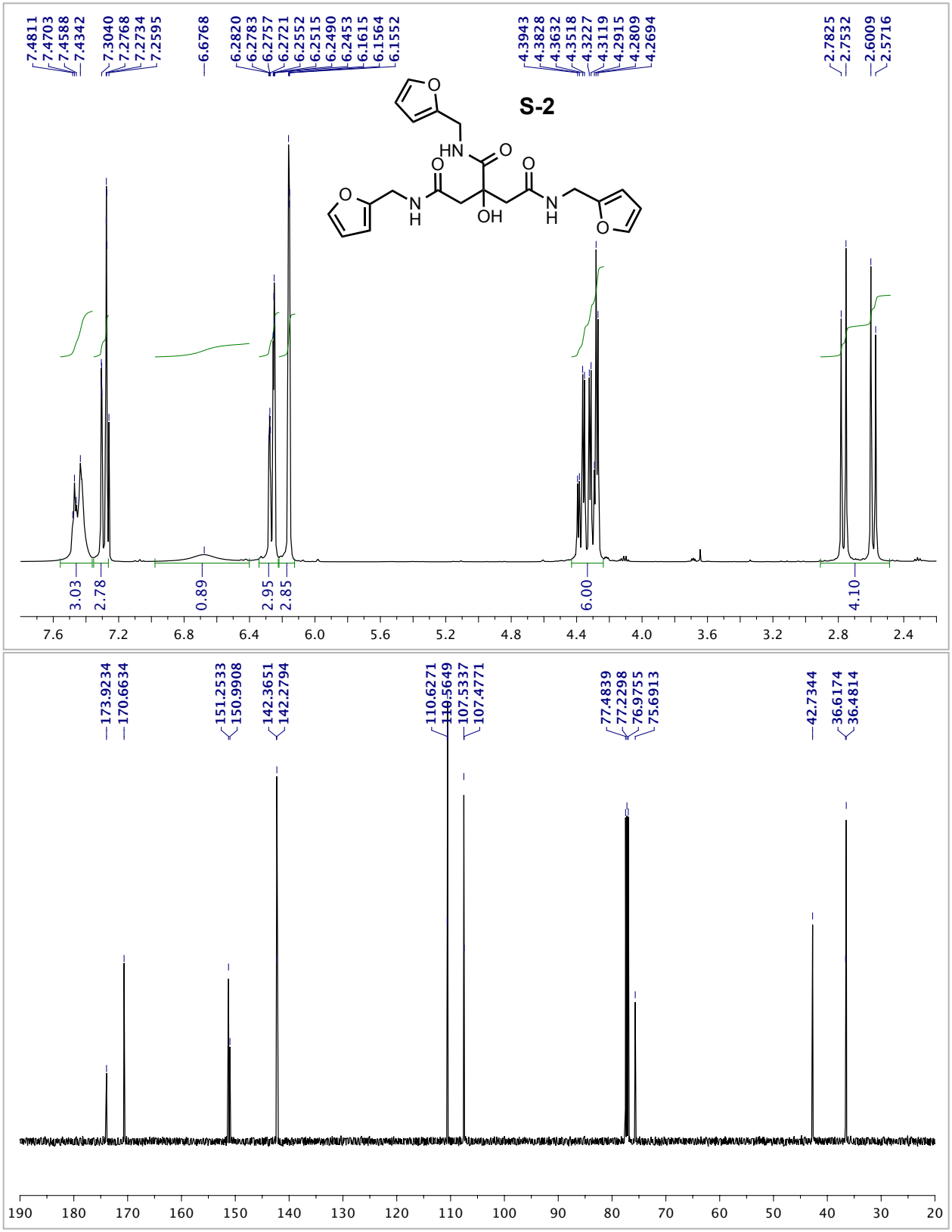
S-2
7.4811
7.4703
7.4588
7.4342
7.3040
7.2768
7.2734
7.2595
6.6768
6.2820
6.2783
6.2757
6.2721
6.2552
6.2515
6.2490
6.2453
6.1615
6.1564
6.1552
4.3943
4.3828
4.3632
4.3518
4.3227
4.3119
4.2915
4.2809
4.2694
2.7825
2.7532
2.6009
2.5716
3.03
2.78
0.89
2.95
2.85
6.00
4.10
173.9234
170.6634
151.2533
150.9908
142.3651
142.2794
110.6271
110.5649
107.5337
107.4771
77.4839
77.2298
76.9755
75.6913
42.7344
36.6174
36.4814

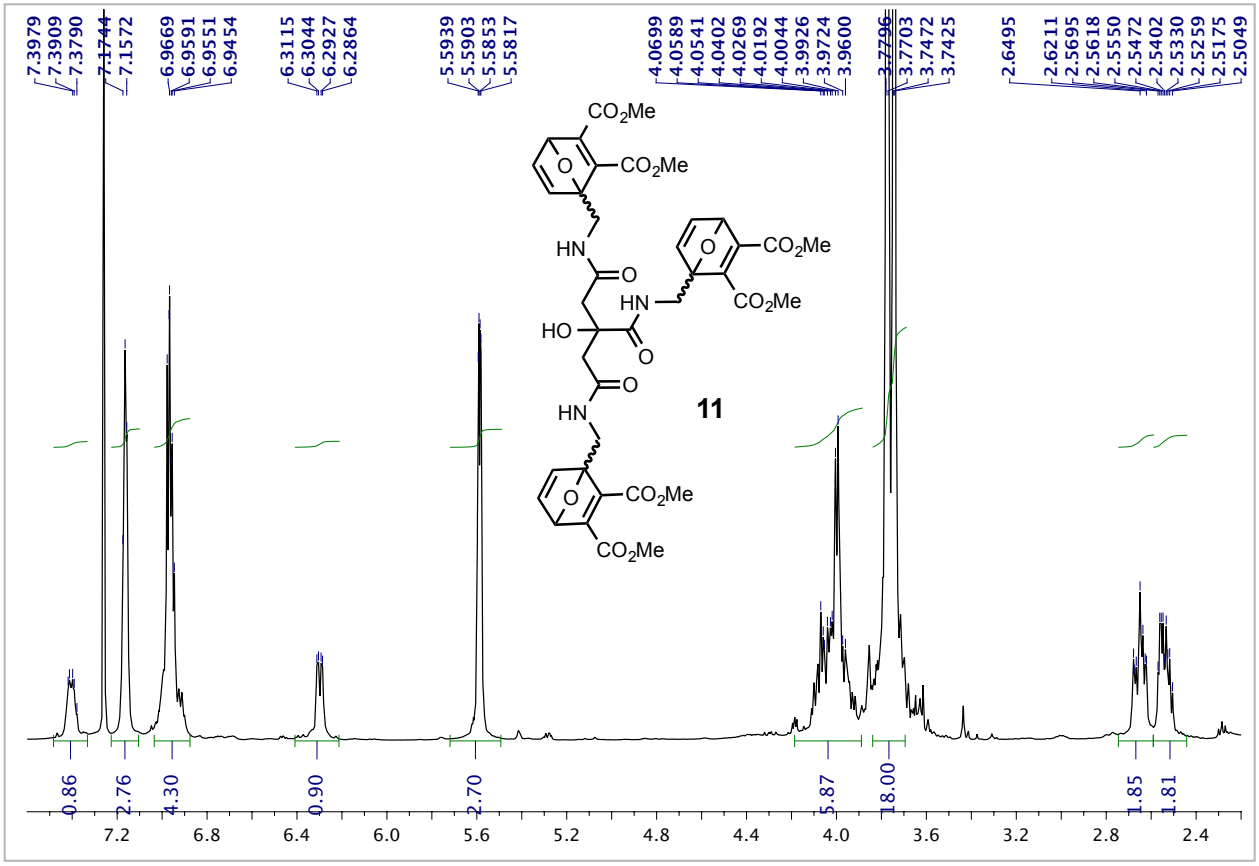
11

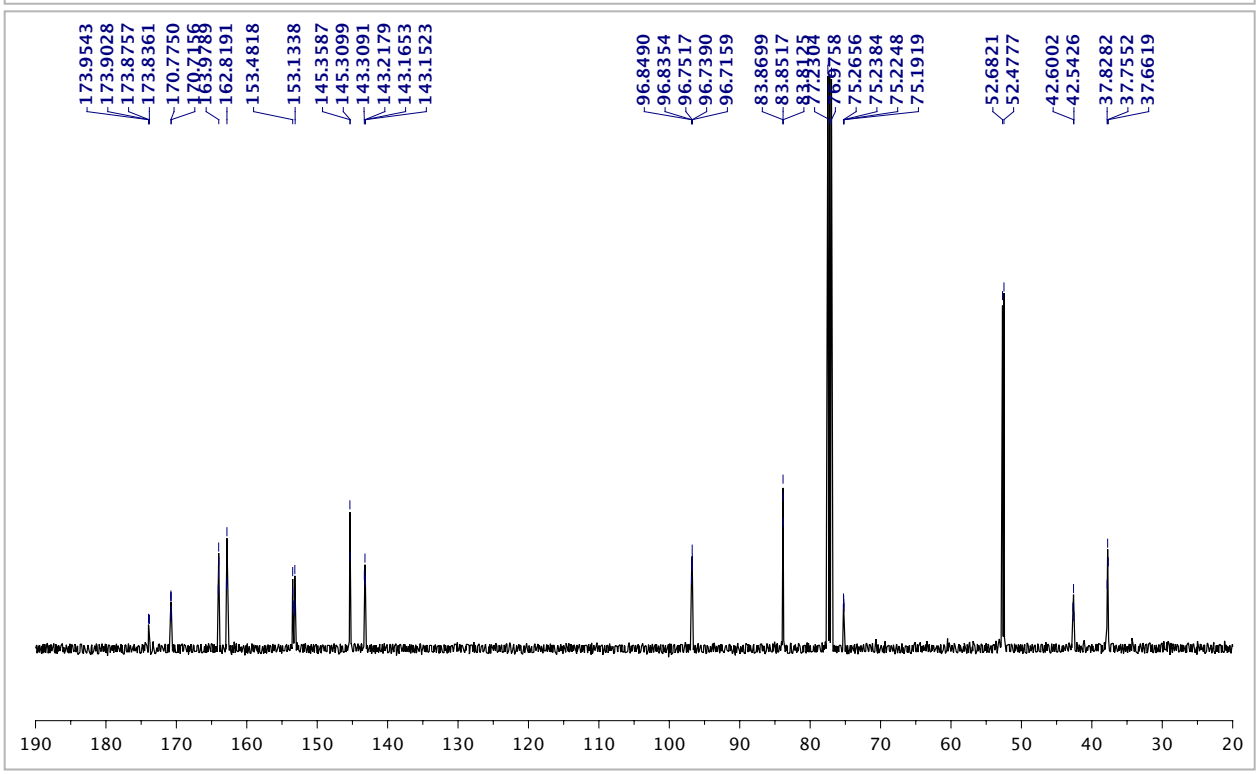

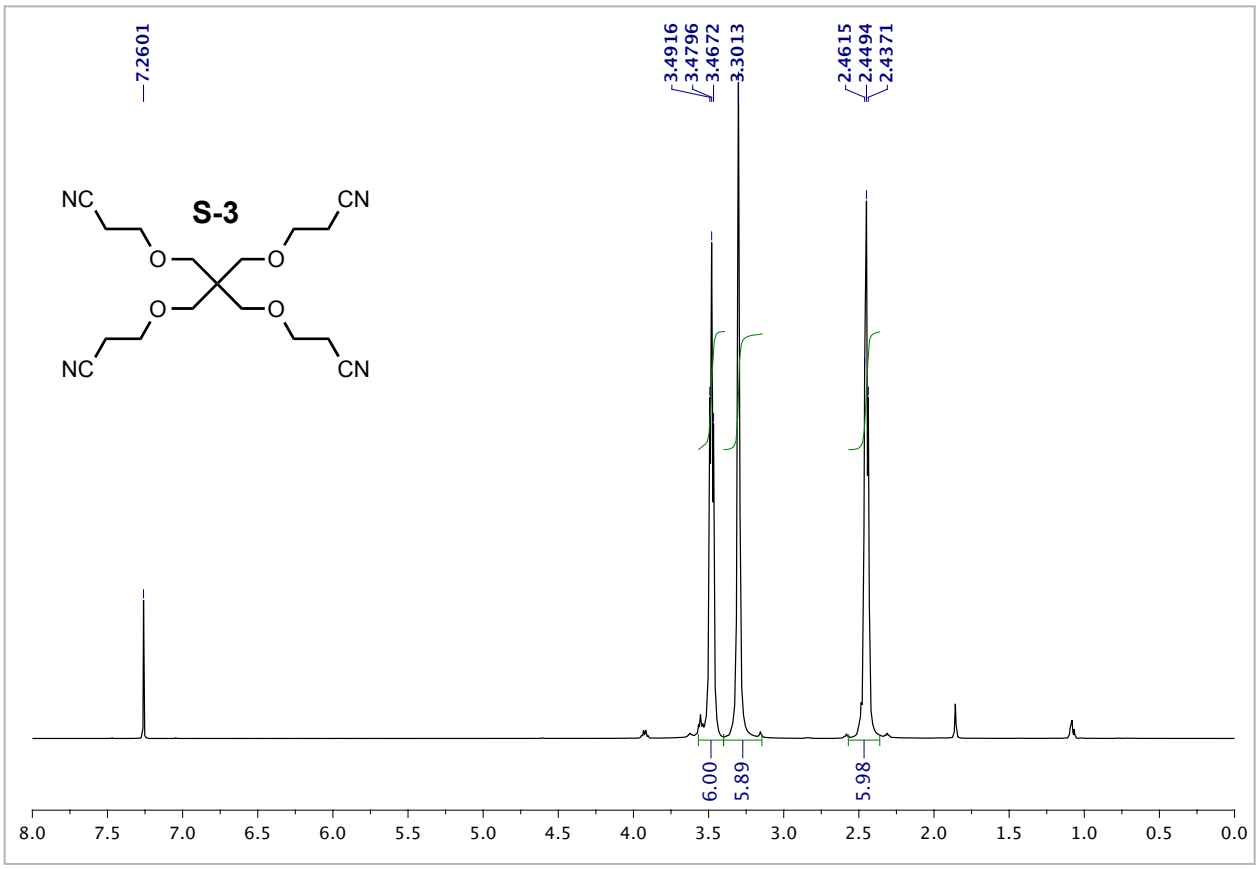
7.2601
3.4916
3.4796
3.4672
3.3013
2.4615
2.4494
2.4371
S-3
NC
CN
O
6.00
5.89
5.98
8.0
7.5
7.0
6.5
6.0
5.5
5.0
4.5
4.0
3.5
3.0
2.5
2.0
1.5
1.0
0.5
0.0

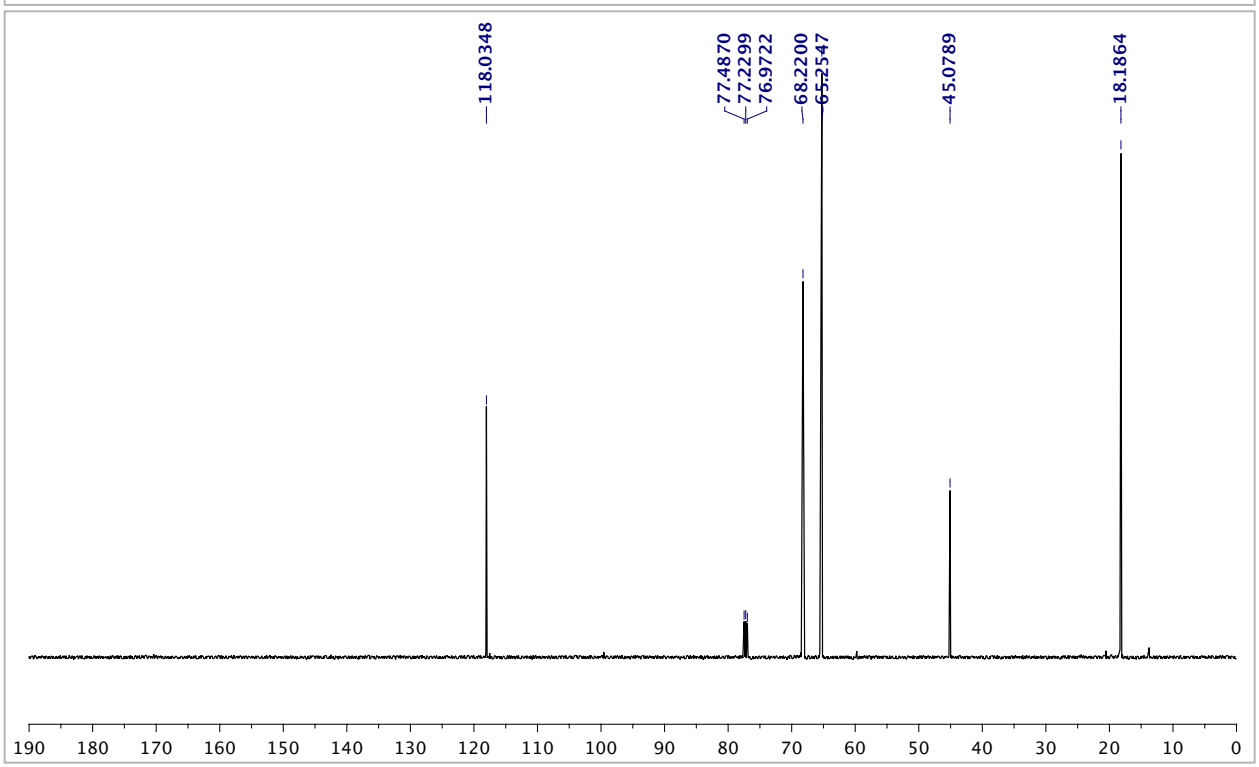
118.0348
77.4870
77.2299
76.9722
68.2200
65.2547
45.0789
18.1864
190
180
170
160
150
140
130
120
110
100
90
80
70
60
50
40
30
20
10
0

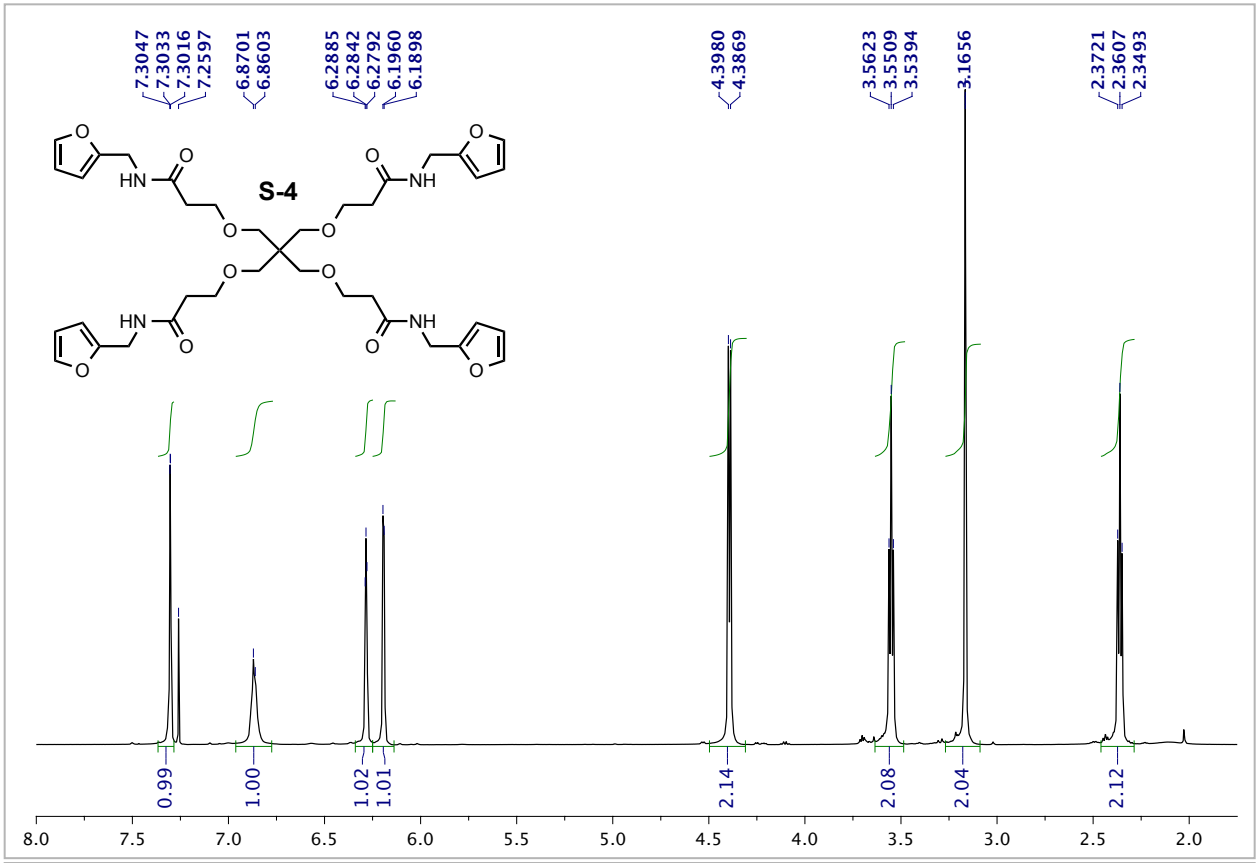
7.3047
7.3033
7.3016
7.2597
6.8701
6.8603
6.2885
6.2842
6.2792
6.1960
6.1898
4.3980
4.3869
3.5623
3.5509
3.5394
3.1656
2.3721
2.3607
2.3493
S-4
HN
NH
0.99
1.00
1.02
1.01
2.14
2.08
2.04
2.12
8.0
7.5
7.0
6.5
6.0
5.5
5.0
4.5
4.0
3.5
3.0
2.5
2.0

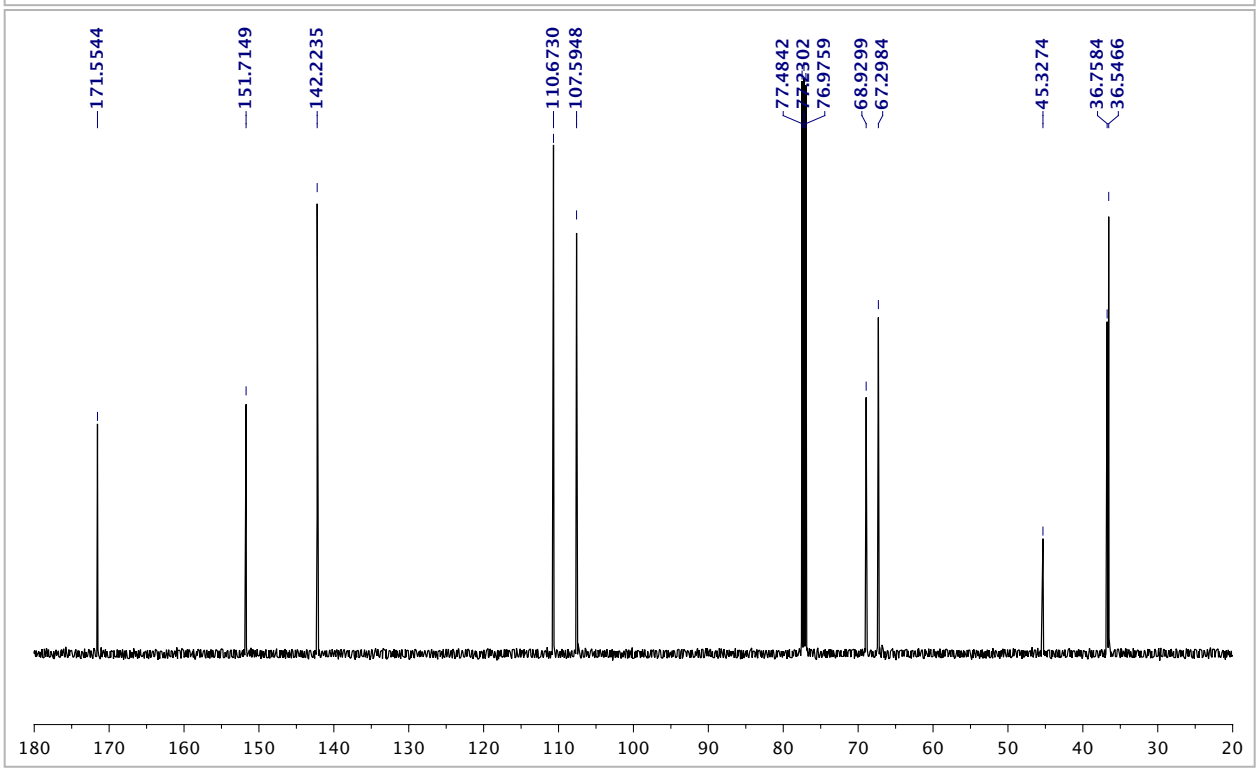
171.5544
151.7149
142.2235
110.6730
107.5948
77.4842
77.2302
76.9759
68.9299
67.2984
45.3274
36.7584
36.5466
180
170
160
150
140
130
120
110
100
90
80
70
60
50
40
30
20

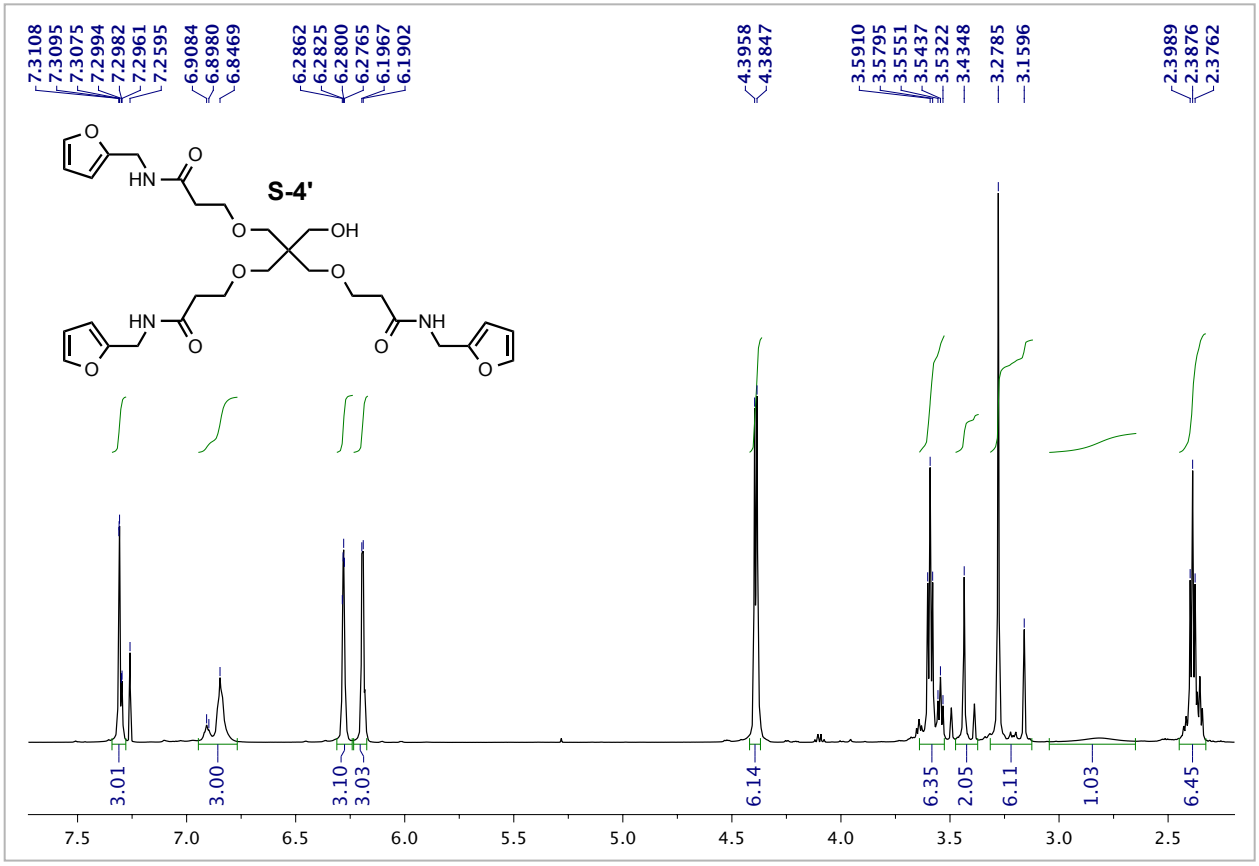
7.3108
7.3095
7.3075
7.2994
7.2982
7.2961
7.2595
6.9084
6.8980
6.8469
6.2862
6.2825
6.2800
6.2765
6.1967
6.1902
4.3958
4.3847
3.5910
3.5795
3.5551
3.5437
3.5322
3.4348
3.2785
3.1596
2.3989
2.3876
2.3762
S-4'
3.01
3.00
3.10
3.03
6.14
6.35
2.05
6.11
1.03
6.45

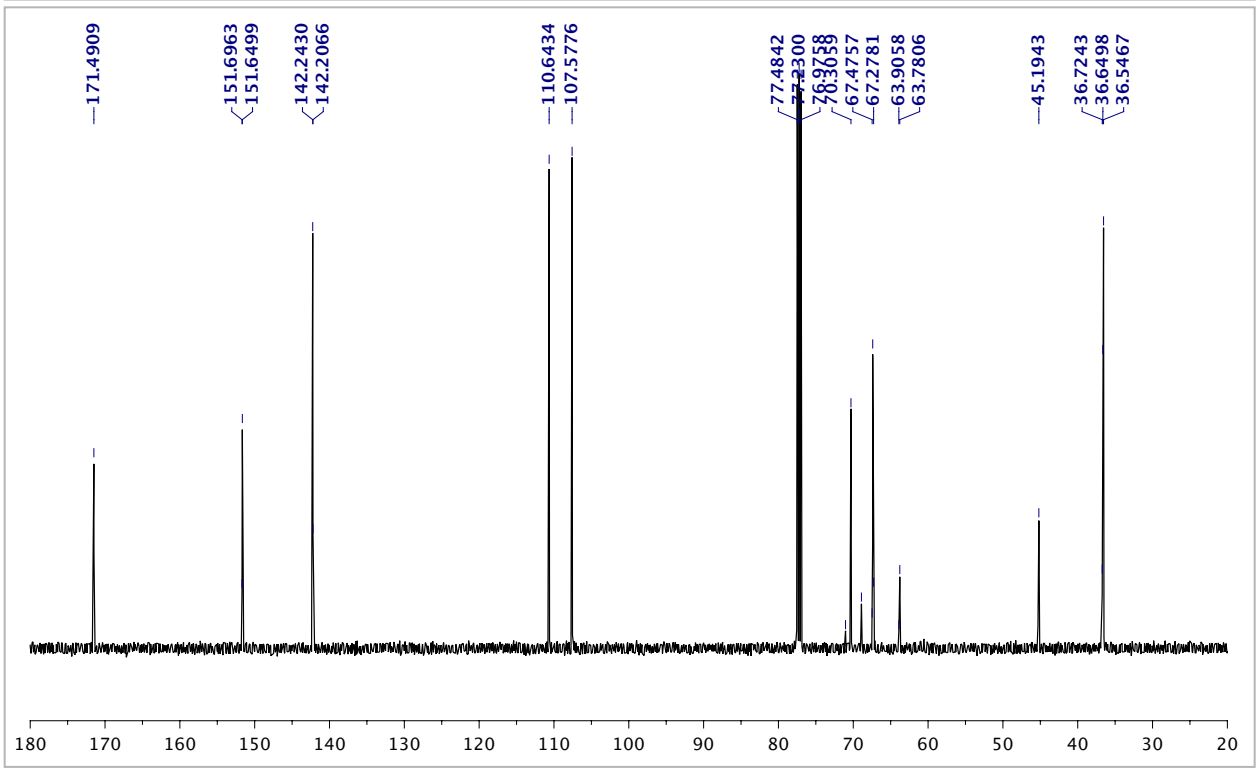
171.4909
151.6963
151.6499
142.2430
142.2066
110.6434
107.5776
77.4842
77.2300
76.9758
70.3059
67.4757
67.2781
63.9058
63.7806
45.1943
36.7243
36.6498
36.5467

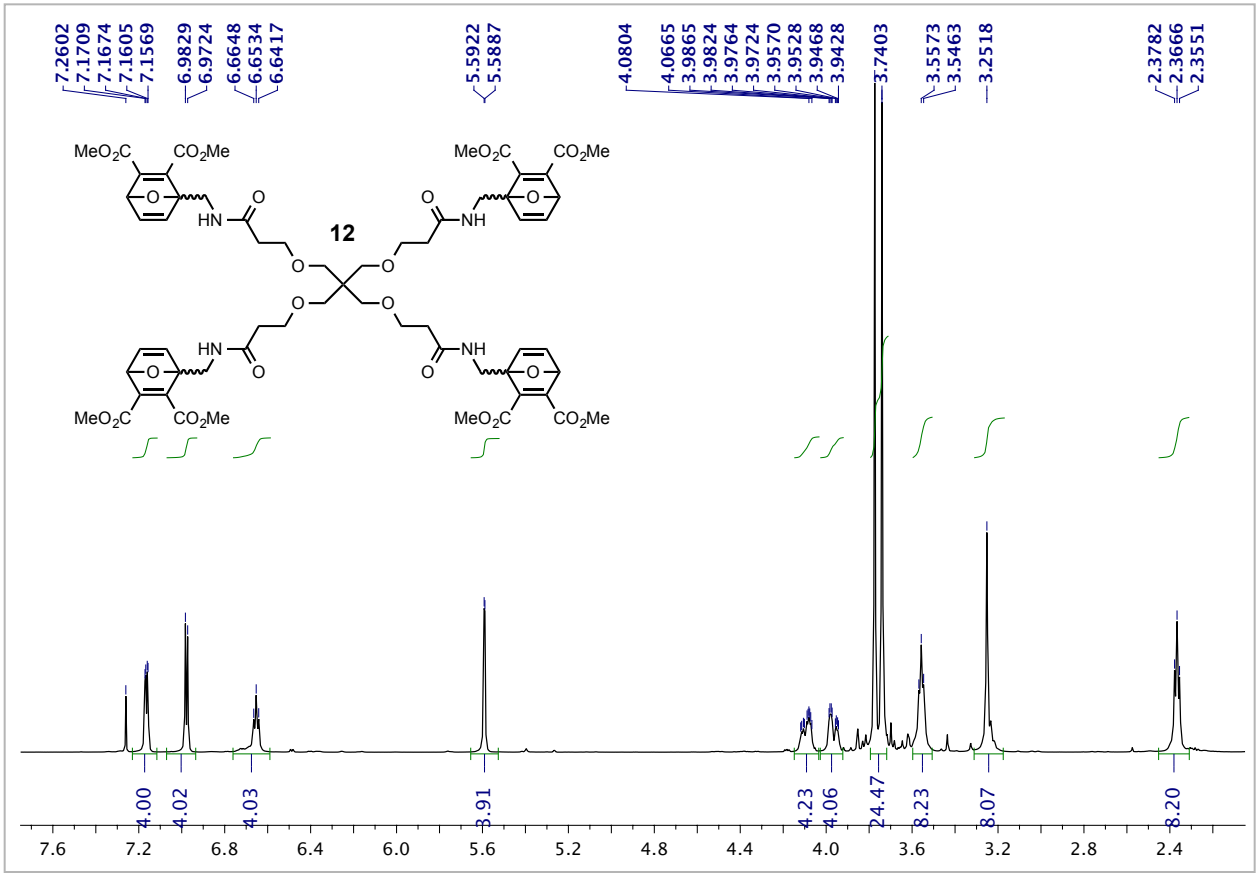
12

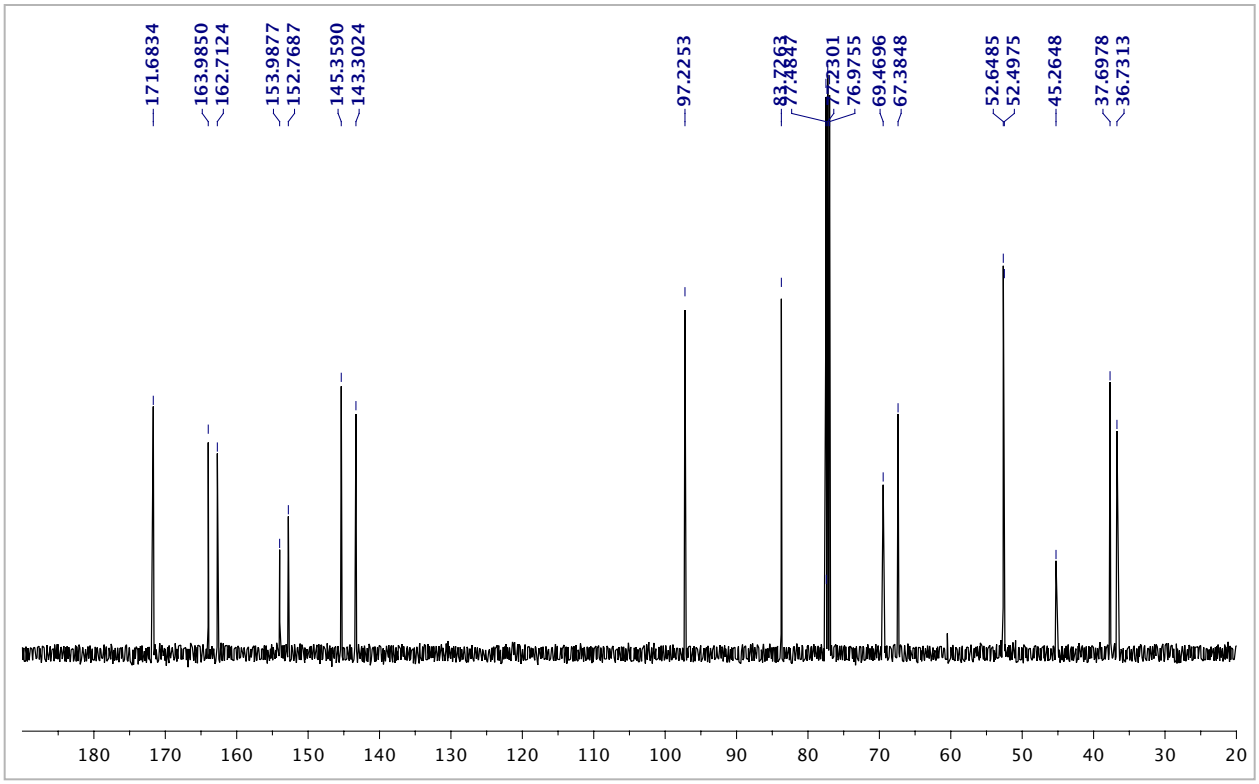

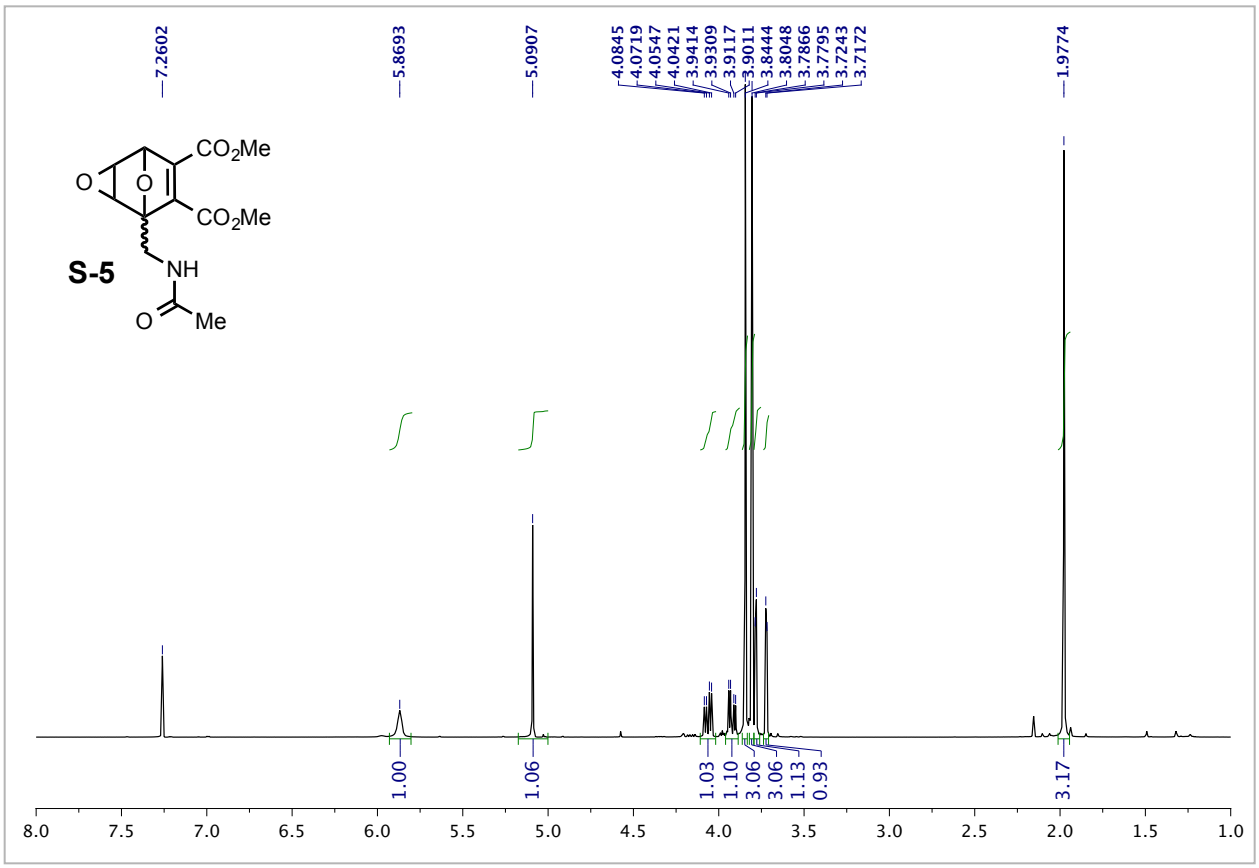
7.2602
5.8693
5.0907
4.0845
4.0719
4.0547
4.0421
3.9414
3.9309
3.9117
3.9011
3.8444
3.8048
3.7866
3.7795
3.7243
3.7172
1.9774
CO2Me
CO2Me
O
O
NH
O
Me
S-5
1.00
1.06
1.03
1.10
3.06
3.06
1.13
0.93
3.17
8.0
7.5
7.0
6.5
6.0
5.5
5.0
4.5
4.0
3.5
3.0
2.5
2.0
1.5
1.0

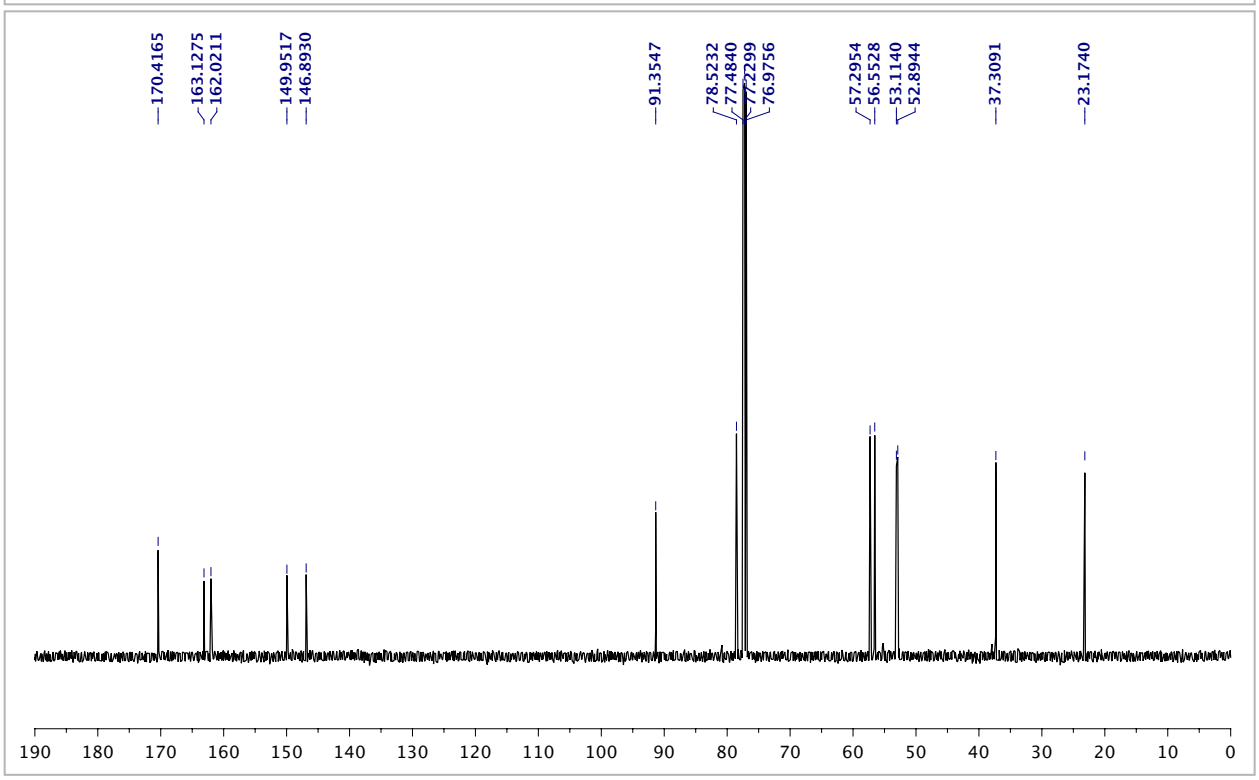
170.4165
163.1275
162.0211
149.9517
146.8930
91.3547
78.5232
77.4840
77.2299
76.9756
57.2954
56.5528
53.1140
52.8944
37.3091
23.1740
190
180
170
160
150
140
130
120
110
100
90
80
70
60
50
40
30
20
10
0

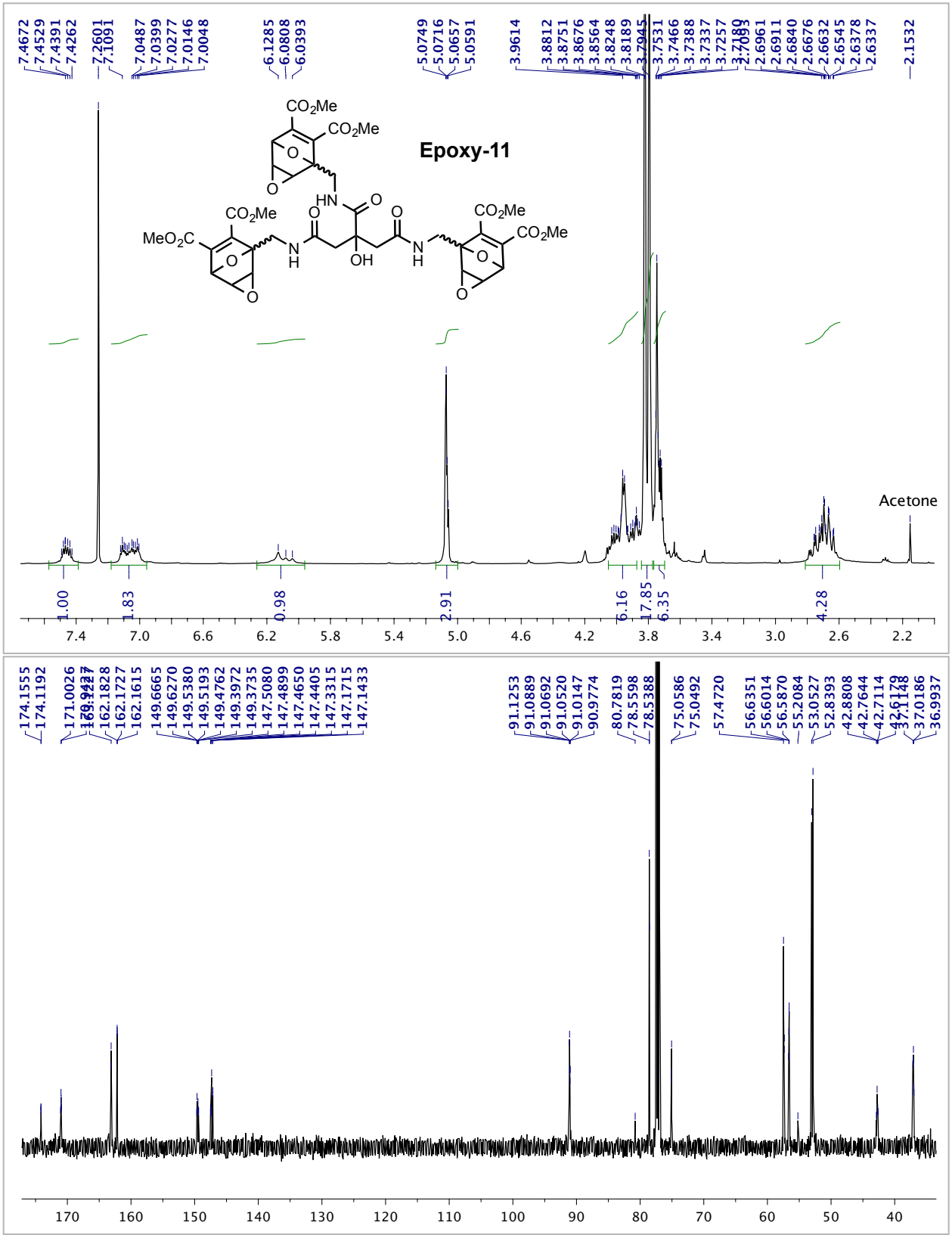
Epoxy-11
Acetone